BORON INCORPORATION INTO SYNTHETIC ARAGONITE

BORON INCORPORATION INTO SYNTHETIC ARAGONITE: REFINING THE BORON ISOTOPE-pH PROXY

By CHRISTA KLEIN GEBBINCK, B.Sc.

A Thesis Submitted to the School of Graduate Studies in Partial Fulfillment of the Requirements for the Degree Master of Science

McMaster University

MASTER OF SCIENCE (2013) McMaster University

(Earth and Environmental Science – Geochemistry) Hamilton, Ontario

TITLE: Boron Incorporation into Synthetic Aragonite: Refining the Boron Isotope-pH Proxy

AUTHOR: Christa Klein Gebbinck, B.Sc. (McMaster University)

SUPERVISOR: Dr. Sang-Tae Kim

NUMBER OF PAGES: viii, 122

PRELIMINARIES

ABSTRACT

By studying the boron isotope composition of marine carbonates, the effectiveness of the tracer to reconstruct the ancient seawater pH and, in turn, atmospheric pCO_2 can be assessed. The boron isotope-pH proxy relies on the hypothesis that only $B(OH)_4^-$, which has a known boron isotope composition with respect to pH, is incorporated into the carbonate crystal lattice. This research synthesized inorganic aragonite from a range of stable pH values to quantify the dependence of aragonite $\delta^{11}B$ on the pH of the precipitating solution. The increasing boron isotope composition of aragonite with increasing pH is consistent with sole incorporation of $B(OH)_4^-$ into the carbonate. The sensitivity of the acid dissociation and isotope equilibrium constants make it difficult to confirm whether or not $B(OH)_4^-$ is the only species contributing to the boron isotope composition of aragonite. The relationship between the boron isotope composition of marine carbonates and ocean pH has wide appeal and, if properly understood, could provide tremendous insight into the history of Earth's climate.

This research also evaluated carbon isotope fractionation between aragonite and dissolved inorganic carbon (DIC) in high ionic strength systems at 25 °C and found it to be consistent with carbon isotope fractionation in low ionic strength environments. The analysis of various isotopic compositions within this study led to the development of new methodology to simultaneously measure the oxygen isotopes of water and carbon isotopes of DIC from small solution samples using continuous flow isotope ratio mass spectrometry (CF-IRMS).

ACKNOWLEDGEMENTS

First and foremost, I would like to thank my supervisor, Dr. Sang-Tae Kim, for his support and guidance throughout my graduate work, as well as providing a research position throughout my undergraduate studies. With this opportunity, I developed a great interest in research and particularly in isotope geochemistry. Your advice and enthusiasm was influential and a key factor in the completion of this project.

Thank you also to all of the members of the McMaster Research Group for Stable Isotopologues, both past and present. Specifically, I would like to thank Martin Knyf for his assistance throughout this research. Thank you for always being willing to help with equipment, listening to my ideas, and assisting during running of many trials!

I am thankful for funding provided to me by the School of Geography and Earth Sciences (SGES) at McMaster University. And also to funding support for this research provided by the Donors of the American Chemical Society – Petroleum Research Fund (ACS-PRF), Natural Science and Engineering Research Council (NSERC) Discovery Grant, Ontario Ministry of Research and Innovation – Ontario Research Fund (MRI-ORF), Canada Foundation for Innovation – Leaders Opportunity Fund (CFI-LOF), and also McMaster University, through Dr. Sang-Tae Kim.

To my friends, in particular Jason Kusters and Taylor Goldup, thank you for being there for me and for always having an open ear when I discuss my research with you – and for trying to make sense of it all! I couldn't have done it without you. And finally, to my family: Dad, Mom, Bryan, Mark, and of course, Brady. Thank you for your constant support, for always making me smile, always believing in me, and for always encouraging me to do the best that I can.

Table of Contents

LIST OF TABLES

LIST OF FIGURES

Chapter 1: Introduction to Research: Literature Review

In 1896, propositions initially made by Arrhenius (1896) suggested that high levels of atmospheric carbon dioxide (expressed as partial pressure: pCO_2) were causing early Cenozoic warmth. Since then, arguments have been made with regards to the potential controls of pCO_2 over long timescales (e.g. Chamberlin, 1899; Owen and Rea, 1985; Raymo and Ruddiman, 1992; Kerrick and Caldeira, 1998). In order to quantify the impact of climate change as a response to current increases in pCO_2, it is important to identify relationships between fluctuations over the course of Earth's history and potential causal effects.

Calcium carbonate is ubiquitous in the oceanic system and is a useful tool in paleoclimate studies due to influences from surrounding water and carbon dioxide on isotopic compositions. Understanding the carbonate-CO_2-water system and the controls on stable isotope fractionations within the systems can lead to greater knowledge of the history of the Earth. When interpreting changes in the Earth over time, direct measurement of various properties (i.e. ancient ocean temperature) is often impossible and therefore proxies have been explored to establish connections. Stable isotopes have been implemented into many different paleo proxies including paleothermometry (e.g. McCrea, 1950; Grossman and Ku, 1986), reconstructing ocean circulation patterns (e.g. Duplessy et al., 1984; Oppo and Fairbanks, 1987), and paleoproductivity (e.g. Meyer et al., 2011).

The pH of the surface ocean is a function of the ratio of alkalinity to total inorganic carbon concentration and these parameters together control dissolved PCO_2.

Dissolved PCO_2 has two degrees of freedom and therefore, the calculation requires knowledge of two of the three properties listed. Dissolved PCO_2 is in equilibrium with atmospheric pCO_2 and reconstructions can infer ancient atmospheric carbon dioxide concentrations. The boron isotope composition of marine carbonates has been investigated as a tool to reconstruct seawater pH, termed the boron isotope-pH proxy. The application of pH reconstructions for estimations of pCO_2 relies on the fact that an increase in atmospheric carbon dioxide concentration results in more CO_2 dissolved in the oceans, and reduces overall pH. If both pH of seawater and either alkalinity or the dissolved inorganic carbon concentrations are known, atmospheric pCO_2 can be calculated.

1.1 Boron Isotopes in Marine Carbonates

Boron has a relatively long residence time in seawater (~3.5 Myr) (Taylor and McLennan, 1985; Lemarchand et al., 2000; Lemarchand et al., 2002) and the boron isotope composition of seawater has not experienced significant variation over the past 21 million years (Spivack et al., 1993; Hemming and Hönisch, 2007; Rollion-Bard et al., 2011) from 39.61‰ (Foster et al., 2010). The boron concentration in modern marine carbonates has been measured to be in the range of 1-100 ppm (Milliman, 1974; Furst et al., 1976; Vengosh et al., 1991) and the incorporation of boron into carbonates has been hypothesized to occur as a function of pH. Therefore, variations in the boron isotope composition of foraminifera can be used to interpret past variations in the pH of the ocean.

1.1.1 Dissociation constant of boric acid

The two dominant aqueous species of boron in seawater are trigonal boric acid, $B(OH)_3$, and tetrahedral borate, $B(OH)_4^-$ (Figure 1.1) (Hershey et al., 1986). The chemical potential of polynuclear boron species (i.e. $B_3O_3(OH)_4^-$, $B_4O_5(OH)_4^{2-}$, $B_5O_6(OH)_4^-$) is negligible at concentrations smaller than 25 mmol kg^{-1} (Su and Suarez, 1995; Klochko et al., 2006) and thus, the aforementioned species can be ignored at typical seawater concentrations of boron, approximately 0.4 mmol kg^{-1}.

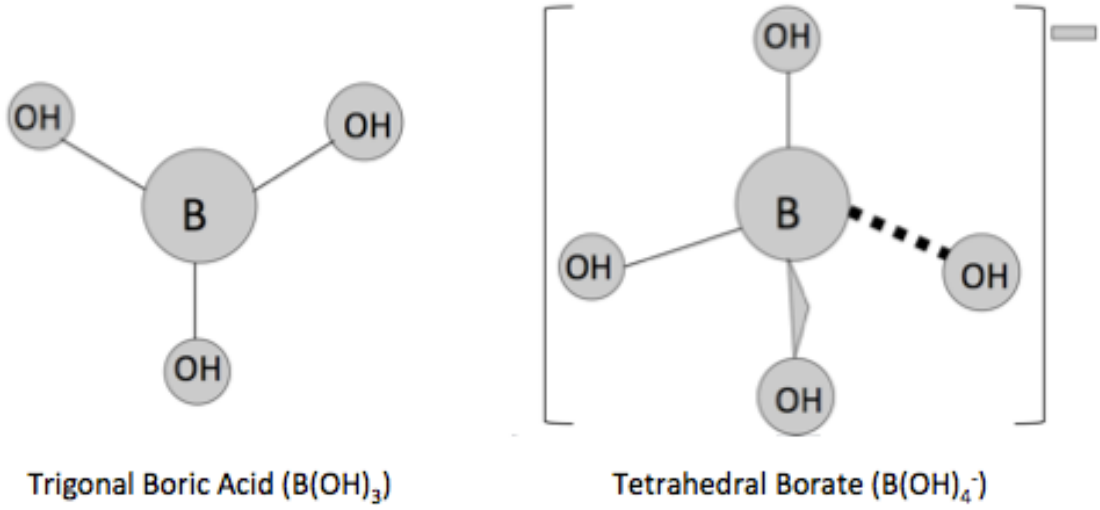

Figure 1.1: Configurations of the dominant aqueous boron species in seawater, trigonal boric acid and tetrahedral borate.

The speciation of the two most abundant aqueous boron species in seawater is strongly affected by seawater pH (Hershey et al., 1986). Equilibration is rapid (Zeebe et al., 2001) and is described by the following dissociation reaction

$$B(OH)_3 + H_2O \leftrightarrow H^+ + B(OH)_4^- \quad (1.1)$$

The acid dissociation constant for the reaction can be described by

$$K_B^* = \frac{[B(OH)_4^-]\cdot[H^+]}{[B(OH)_3]} \quad (1.2)$$

With an accurate acid dissociation constant (expressed as pK_B^*) of $B(OH)_3$, the concentration of each species can be determined as a function of pH (Dickson, 1990; Pagani et al., 2005). To apply the correct pK_B^* value, the experimental conditions used to quantify the constant and the experimental conditions to which it is applied must be similar. Varying temperatures and chemical constituents in the solution can lead to different reaction mechanisms and has the potential to generate erroneous results.

It is important to identify the pH scale applied when the pK_B^* value was determined because in order to estimate the pCO_2 from pH, the dissociation constants for CO_2 equilibra (i.e. K_1, K_2, See Appendix) must also be determined on the same pH scale. The different pH scales include the NBS scale (pH_{NBS}), total scale (pH_T), free scale (pH_F), and the seawater scale (pH_{SWS}). The pH_{NBS} scale is defined by standard buffer solutions, with assigned pH values, that are typically a low ionic strength (I = ~0.1 mol kg^{-1}). In a high ionic strength solution, methods employed to define the pH are not compatible with those that define low ionic strength media (Dickson, 1993). For example, when working with seawater, which has a high ionic strength (I = ~0.7 mol kg^{-1}), the large differences in the ionic strengths cause significant differences, several millivolts (Hansson, 1973), in the liquid junction potential. It is inaccurate to assume that direct pH recordings are sufficient due to this difference in electrical potential that arises due to a charge difference between solution and electrode (Hickman, 1970). Hansson (1973) resolved this issue by introducing the pH_T scale, with synthetic seawater

containing sulfate ions (SO_4^{2-}) as the standard state and generated standard buffers of high ionic strengths with assigned pH values. In the pH_T scale, protonation of SO_4^{2-} occurs and is taken into consideration. The pH_F scale omits the protonation of SO_4^{2-} and focuses solely on the hydrogen ion concentration. While this scale is seemingly the most straightforward, it estimates the concentration of SO_4^{2-} and also the stability constant of HSO_4^-, K_S^*. This scale assumes sulphate concentration is constant, and it is also difficult to obtain an accurate value for the stability constant due to uncertainties in estimating the activity coefficients needed, as a result the use of the scale is limited. The pH_{SWS} scale takes into account the protonation of SO_4^{2-} as well as fluoride (HF) ions. This scale, however, is only significant in systems where fluoride is abundant, for instance, in seawater the concentration of SO_4^{2-} is much greater than HF and as a result the differences seen between calculated values on total and seawater scale are very small.

The use of the boron isotope-pH proxy to reconstruct seawater pH relies mainly on marine foraminifera originating in natural seawater. In order to best simulate boron incorporation into carbonates in the natural environment, ionic strengths are considered for inorganic experiments. In order to maintain a consistent pH scale, the measurements taken directly from the experimental solutions on the pH_{NBS} scale must be properly converted to the pH_T scale, as suggested by Dickson (1993).

To correct the pH measurements obtained using the pH_{NBS} scale, a pH buffer with ionic concentrations similar to that of the experimental solutions can be utilized. The buffers based on 2-amino-2-hydroxymethyl-1,3-propanediol, also known as Tris, in synthetic seawater are now used as primary buffers to define seawater pH scales (Hansson, 1973; Ramette et al., 1977; DelValls and Dickson, 1998). This approach

incorporates buffer solutions of similar ionic strength to the experimental solution so that the residual liquid junction potential is equal to zero (Dickson, 1993). For this research, high ionic strength Tris buffer solutions were prepared. The values of pH measured using the total hydrogen scale will be consistent with recent measurements for the dissociation of boric acid in seawater.

The pK_B^* of boric acid has been determined under a range of temperatures, chemical compositions, and salinities (Table 1.1). Hansson (1973) determined the stoichiometric dissociation constant of boric acid in synthetic seawater through a series of titrations, however the data was limited in terms of temperature range and salinities tested. The dissociation constants calculated by Dickson (1990), which utilizes the pH_T scale, is currently considered the most accurate determination of pK_B^* and is in agreement with values determined by Hansson (1973). Both Hansson (1973) and Dickson (1990) performed experiments using synthetic seawater, consisting of the major constituents in seawater (Na^+, Mg^{2+}, Ca^{2+}, Cl^- SO_4^{2-}, and Dickson (1990) also included K^+). Hershey et al. (1986) determined a pK_B^* of 8.830 in 0.68 mol kg^{-1} NaCl solution at 25 °C. Figure 1.2 demonstrates that, in seawater, virtually all boron species exists as $B(OH)_3$ at pH < 8.6, whereas $B(OH)_4^-$ is dominant when pH > 8.6 (Dickson, 1990; Hemming and Hanson, 1992; Klochko et al., 2006), using the pK_B^* value of 8.597 for seawater at 25 °C.

Table 1.1: Acid dissociation constants for $B(OH)_3$ at 25°C

Author(s)	pH scale	Ionic Strength (mol kg^{-1})	Media	pK_B^*
Buch (1933)	uncertain	(34.4)[a]	Na^+, Ca^{2+}, Cl^-	8.74
Owen and King (1943)	pH_{NBS}	0.725	Na^+, Cl^-	8.831
Lyman (1958)	pH_{NBS}	(33)[a]	seawater	8.54[b]
Dyrssen and Hansson, (1973)	uncertain	0	pure water	9.237
		0.7	Na^+, Cl^-	8.85
		0.7	synthetic seawater (Na^+, Cl^-, Ca^{2+}, Mg^{2+}, SO_4^{2-})	8.61
Hansson (1973)	pH_T	0.7	Na^+, Mg^{2+}, Ca^{2+}, Cl^-, SO_4^{2-}	8.61
Bryne and Kester (1974)	pH_{NBS}	0.7	Na^+, Ca^{2+}, Cl^-	8.774[c]
			Na^+, Mg^{2+}, Cl^-	8.715[c]
Hershey et al. (1986)	pH_T	0.68	Na^+, Cl^-	8.83
			Na^+, Mg^{2+}, Cl^-	8.725
			Na^+, Ca^{2+}, Cl^-	8.675
Dickson (1990)	pH_T	0.7	Na^+, Mg^{2+}, Ca^{2+}, Cl^-, K^+,SO_4^{2-}	8.597
Tossell (2005)	n/a	n/a	computational	9.2
Bryne et al. (2006)	pH_T	0.6	K^+, Cl^-	8.64

[a]In salinity (psu)
[b]calculated from Pitzer interaction parameters in Hershey et al. (1986)
[c]corrected by Millero (1982)

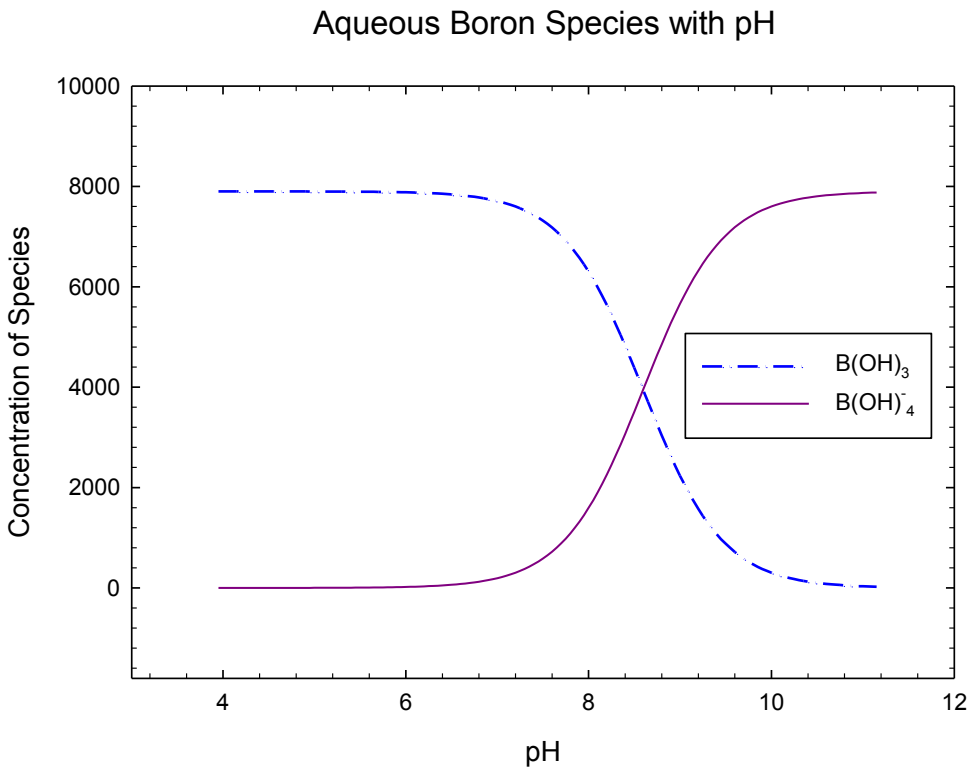

Figure 1.2: Distribution of aqueous boron species as a function of pH (pK_B = 8.597 at 25 °C and an ionic strength of 0.7 mol/kg).

1.1.2 Boron isotope equilibrium constant

The equilibrium isotope exchange reaction between the two most abundant aqueous boron species, $B(OH)_3$ and $B(OH)_4^-$, is described as

$$^{10}B(OH)_3 + {}^{11}B(OH)_4^- \leftrightarrow {}^{11}B(OH)_3 + {}^{10}B(OH)_4^- \quad (1.2)$$

The equilibrium constant of equation 1.2 is defined by

$$^{11\text{–}10}K_B = \frac{[{}^{11}B(OH)_3][{}^{10}B(OH)_4^-]}{[{}^{10}B(OH)_3][{}^{11}B(OH)_4^-]} \quad (1.3)$$

There are two ways to determine the isotope equilibrium constant, theoretically or experimentally. The equilibrium constant can be determined theoretically by using calculations on the basis of the different vibrational energies of the two boron coordinations, $B(OH)_3$ and $B(OH)_4^-$, trigonal and tetrahedral respectively (e.g. Kakihana et al., 1977). However, disadvantages to this method exist because of the sensitivity surrounding experimentally-obtained vibrational energy values as well as to the theoretical methods that are applied to calculate molecular forces (Klochko et al., 2006; Rustad and Bylaska, 2007).

A theoretically calculated boron isotope equilibrium constant ($^{11\text{-}10}K_B$) of 1.0194 by Kakihana et al. (1977), using reduced function partition ratios, has been widely cited in the literature, however, this value has been reevaluated and a critical sensitivity in the calculation of the molecular forces using $LaBO_3$ instead of $B(OH)_3$ and Fadini's "Verfahren der Nächsten Lösung" for $B(OH)_4^-$ was identified (Zeebe, 2005). Furthermore, more recent studies have reported larger $^{11\text{-}10}K_B$ values than that of Kakihana et al. (1977) (Table 1.2).

Table 1.2: Boron isotope fractionation factors cited within literature

Author(s)	Treatments/Methods	Isotope Equilibrium Constant ($^{11\text{-}10}K_B$)
Kakihana et al., (1977)	Ion-exchange separation based on reduced partition function ratios and using spectroscopic data for molecular vibrations	1.0194
Palmer et al., (1987)	Adsorption of B from seawater onto marine clay	1.033
Oi, (2000)	*Ab initio* molecular orbital theory calculating vibrational frequency at the optimized structure	1.026
Pagani et al., (2005)	Best fit with inorganic carbonate precipitation experiments conducted in artificial seawater	1.0267
Zeebe, (2005)	*Ab initio* molecular orbital theory and spectroscopic data for molecular vibrations	≥1.030
Liu and Tossell, (2005)	*Ab initio* molecular orbital theory using the "water droplet" method	1.027
Tossell, (2005)	Quantum mechanical calculations considering vibrational, rotational, and translational contributions to the free energy	1.0322
Bryne et al., (2006)	Experimental observations of chemical equilibrium in 0.6 mol kg^{-1} H_2O KCl	1.0285
Klochko et al., (2006)	Experimental observations of chemical equilibrium in "pure water", 0.6 mol kg^{-1} H_2O KCl, and 0.7 mol kg^{-1} synthetic seawater, at 25 and 40°C, with 0.01-0.05 mol kg^{-1} total boron concentrations	1.0308, 1.0250, and 1.0272, respectively
Rustad and Bylaska, (2007)	*Ab initio* molecular dynamics using Fourier transformation of the velocity autocorrelation function to obtain vibrational densities	1.028

Bryne et al. (2006) reported the first experimentally determined $^{11\text{-}10}K_B$ value of 1.0285 in 0.63 mol kg^{-1} H_2O KCl solution at 25 °C. Klochko et al. (2006) proposed a new boron isotope equilibrium constant of 1.0272 based upon spectrophotometric measurements using a range in total boron concentrations, which is currently considered the most accurate value as it is purely experimental with no reliance on theoretical deductions and it is in agreement with more recent *ab initio* calculations. The experiments performed by Klochko et al., (2006) simulated a range of conditions including "pure water" solutions, 0.6 mol kg^{-1} H_2O KCl, which resulted in an ionic strength close to that of natural seawater, and synthetic seawater prepared with seawater constituent salts (NaCl, KCl, Na_2SO_4, $CaCl_2$, $MgCl_2$), at 25 and 40 °C.

Due to variation in molecular coordination and vibrational frequencies between the aqueous species of boron, $B(OH)_3$ is enriched in ^{11}B relative to $B(OH)_4^-$ (Kakihana et al., 1977; Nomura et al., 1982; Oi et al., 1989; Vengosh et al., 1991; Hemming and Hönisch, 2007; Honisch et al., 2007) by ~27 ‰ (Klochko et al., 2006). The relationship between the boron isotope composition of carbonate ($\delta^{11}B_{carb}$) in seawater and pH can be summarized as

$$pH = pK_B^* - \log\left(\frac{\delta^{11}B_{SW} - \delta^{11}B_{carb}}{\delta^{11}B_{SW} - {}^{11\text{–}10}K_B\delta^{11}B_{carb} - 1000\cdot({}^{11\text{–}10}K_B - 1)}\right) \quad (1.4)$$

Figure 1.3 shows the $\delta^{11}B$ of the aqueous boron species vs. seawater pH, which was generated by combining the equation outlining the distribution of aqueous boron species (1.1) and the equilibrium boron isotope exchange reaction (1.2) (Hemming and Hanson, 1992).

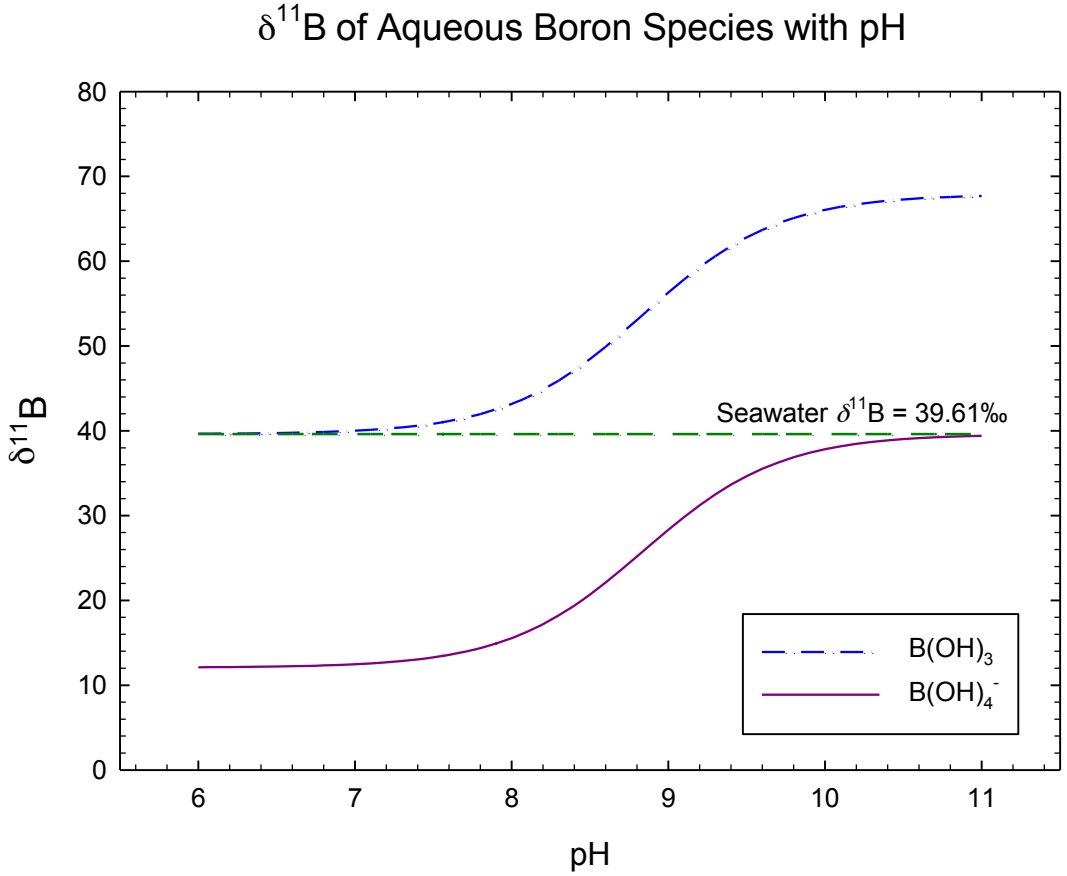

Figure 1.3: $\delta^{11}B$ of $B(OH)_3$ and $B(OH)_4^-$ in seawater as a function of pH ($^{11\text{-}10}K_B$ = 1.0272 at 25 °C and an ionic strength of 0.7 mol/kg).

1.1.3 $B(OH)_4^-$ incorporation into carbonate minerals

The boron isotope-pH proxy relies on the hypothesis that only the $B(OH)_4^-$ ion is incorporated into the crystal lattice. This idea was initially proposed after the observation that boron in clay was isotopically lighter than seawater, which was interpreted to result from the uptake of a charged, isotopically lighter $B(OH)_4^-$ ion into clays (Schwarcz et al., 1969). A similar fractionation is seen with marine carbonates (Vengosh et al., 1991; Hemming and Hanson, 1992). Since then, attempts to understand the possible mechanisms causing the preferential incorporation of $B(OH)_4^-$ into calcite and aragonite

have been investigated (e.g. Kitano et al., 1978; Hemming and Hanson, 1992; Hemming et al., 1995; Tossell, 2006).

There is a higher content of boron observed in marine biogenic aragonite (15 ppm) relative to calcite (9 ppm) (Furst et al., 1976; Vengosh et al., 1991; Hemming et al., 1995). Boron is located within the inorganic constituents of the shells and not the organic matrix (Furst et al., 1976), and therefore, this observation may be attributed to the larger amount of organic matter presented in calcite versus aragonite. Differences in boron concentrations among the different polymorphs of calcium carbonate may potentially be related to biogenic effects of controlling incorporation (e.g., corals) or exclusion (e.g., gastropods) of aqueous boron species (Vengosh et al., 1991).

A dominant influence on boron uptake into calcium carbonate appears to be processes at the crystal surface (Hemming et al., 1995). Hemming and Hanson (1992) theorized that because $B(OH)_4^-$ is charged, it is more likely to be attracted to the positively charged sites on the calcium carbonate surface than boric acid. The coordination of boron in carbonates may have implications as to the mechanism of boron incorporation. A study by Sen et al. (1994) used ^{11}B magic angle spinning nuclear magnetic resonance (MAS NMR) techniques to study the local coordination of boron in natural calcite and aragonite, synthetic calcite and aragonite, and a phase changed calcite. Sen et al. (1994) concluded that natural and synthetic calcite contained 90% BO_3 and 10% BO_4. The natural and synthetic aragonite contained only BO_4. Interestingly, calcite that had been altered from aragonite by being finely crushed and heated contained only BO_3. This suggested that a potential change in coordination during the incorporation of boron into calcite might be required, generating an energy barrier. This energy barrier

may have a greater impact on the boron inclusion than that of size or charge (Sen et al., 1994). Kitano et al. (1978) proposed that both calcium carbonate polymorphs uptake $B(OH)_4^-$, however the presence of tetrahedral boron is dominant in aragonite, while trigonal boron is more abundant in calcite. When considering ionic size with this observation, understanding the inclusion of boron into calcium carbonate is complicated. This implies that the larger, tetrahedral anion, $B(OH)_4^-$, appears to be substituted into the smaller lattice sites in aragonite, whereas the smaller, trigonal $B(OH)_3$ is substituted into the larger lattice sites in calcite.

Studies have found the boron isotope composition of both calcite and aragonite to be similar to the boron isotope composition of $B(OH)_4^-$ (Hemming and Hanson, 1992) and these observations imply that despite containing different coordinations of boron within the crystal structures, $B(OH)_4^-$ is adsorbed onto the crystal surface of both polymorphs and structurally incorporated. The $B(OH)_4^-$ maintains coordination when incorporated into aragonite, however a change in the coordination is required for calcite, which does not appear to cause significant isotope fractionation. Hemming et al. (1995) confirm that $B(OH)_4^-$ is present in aragonite and are in agreement that a change in coordination may be required during incorporation of $B(OH)_4^-$ into calcite. It is also hypothesized that $B(OH)_4^-$ may be adsorbed onto the calcite crystal lattice and then transformed to another ion, potentially HBO_3^- (Hemming and Hanson, 1992).

Contrasting the results of Sen et al. (1994), Klochko et al. (2009) observed equal abundances of trigonal and tetrahedral boron in biogenic calcite and aragonite samples using MAS NMR studies and did not discern a strict dependency of boron coordination into carbonate crystal structures. However, the $\delta^{11}B$ data available for both natural and

synthesized carbonates suggest that changes in coordination of boron species occurs during carbonate precipitation (Hemming and Hanson, 1992; Sen et al., 1994; Klochko et al., 2009). These complications suggest that the boron isotope-pH proxy may not be as straightforward as previously speculated.

The considerations that there may be changes in coordination through intermediate phases of incorporation, suggest that boron inclusion does not occur by basic adsorption onto the carbonate surface (Tossell, 2006). Instead, chemical reactions between HCO_3^- and either $B(OH)_3$ or $B(OH)_4^-$ take place on carbonate surfaces during early growth stages, referred to as "chemosorption" (Tossell, 2006). During this stage, $B(OH)_2CO_3^-$ isomers of either trigonal or tetrahedral coordination form on the surface (Figure 1.4). These reconstructive processes that occur at the crystal surface may involve boron isotope fractionation.

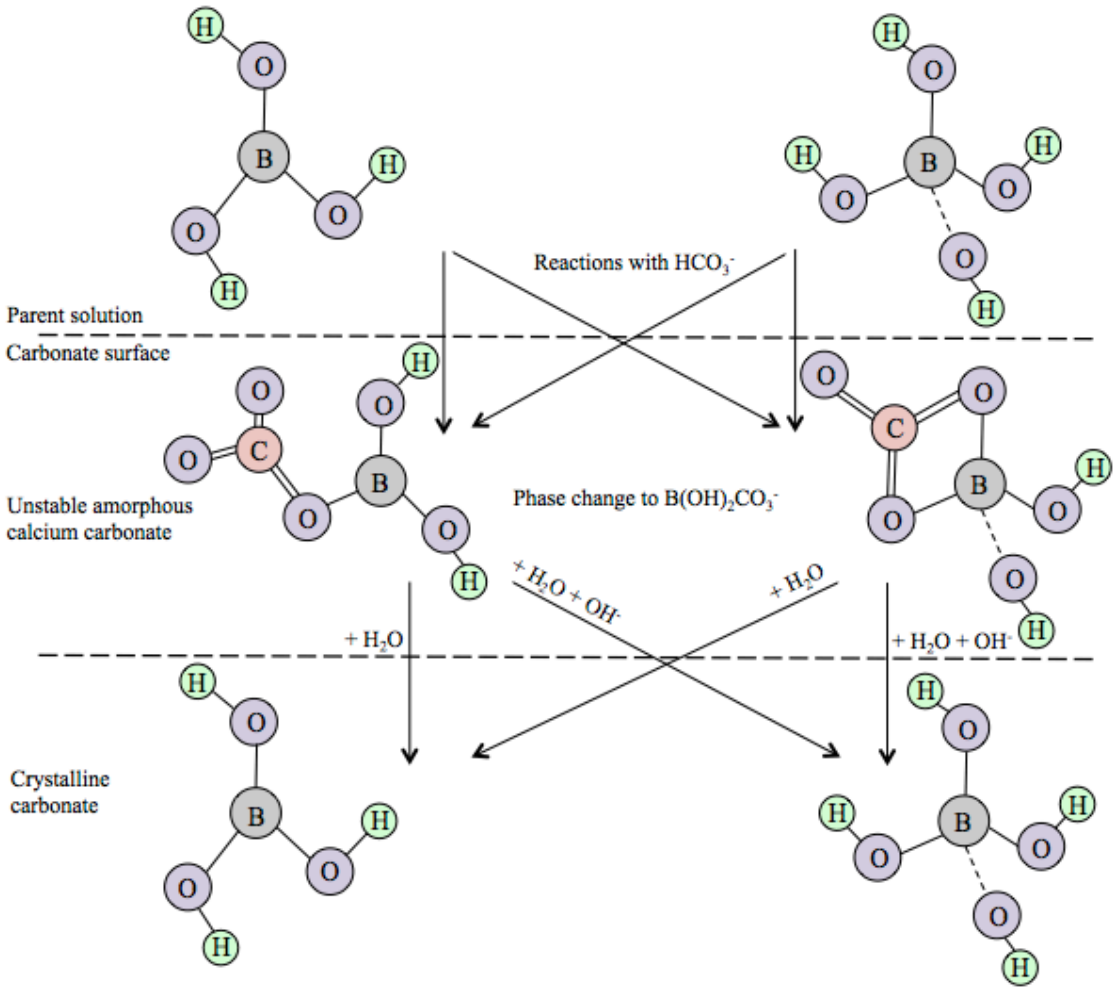

Figure 1.4: Potential model of boron incorporation into calcium carbonate. Modified from Tossell, (2006) and Klochko et al. (2009).

Regardless of mineral dynamics, it is assumed that boron incorporation into a carbonate mineral is an equilibrium process between the precipitating carbonate and the parent solution (Vengosh et al., 1991). The hypothesis that only $B(OH)_4^-$ is incorporated into the carbonate lattice without significant fractionation further suggests that the $\delta^{11}B_{carb}$ should be equal to the boron isotope composition of $B(OH)_4^-$, $\delta^{11}B_{B(OH)4-}$. The boron concentration in both calcite and aragonite increases as the boron concentration in parent solution increases (Vengosh et al., 1991; Hemming et al., 1995). When the pH of a parent solution increases, a higher concentration of boron was measured in carbonates

(Kitano et al., 1978; Hemming et al., 1995; Hobbs and Reardon, 1999). If boric acid, which is more abundant at lower pH (see Figure 1.2), were being incorporated into the carbonate structure, a higher boron concentration in carbonates should be seen at a lower pH. Consequently, this experimental observation supports the hypothesis that only the borate ion is contributing to the boron isotope composition of the precipitating calcium carbonate.

1.1.4 Boron paleo-pH proxy and previous research

The application of the boron isotope composition of marine carbonates to seawater pH reconstruction has been investigated, as previously discussed, on the postulation that only $B(OH)_4^-$ ions are incorporated into carbonate crystal structures. As discussed in Section 1.1.1., based on the dissociation of $B(OH)_3$ in seawater, the relative proportions of $B(OH)_3$ and $B(OH)_4^-$ in seawater are present as a function of pH, with trigonal $B(OH)_3$ being enriched in ^{11}B relative to $B(OH)_4^-$. If only $B(OH)_4^-$ ions are incorporated into carbonate lattice during calcification, the $\delta^{11}B_{carb}$ should be equal to $\delta^{11}B_{B(OH)4-}$, calculated at the given pH value. By analyzing marine carbonates for their boron isotope composition, the pH of the ocean at the time of the carbonate formation can be estimated as long as the boron isotope-pH proxy has been properly calibrated. The effects of dissolution of calcium carbonate on applying the boron isotope-pH proxy can be minimized by incorporating samples from areas of low productivity and large shell size fractions (Honisch et al., 2007). Utilization of the boron isotope-pH proxy can potentially address how increases in atmospheric carbon dioxide concentrations due to human perturbations may have altered the oceanic-CO_2 system.

It is challenging to develop a geochemical proxy based on natural samples because of the ambiguity in tracing environments from which the samples were formed (e.g., pH, temperature, and salinity). The application of culture studies (e.g. Sanyal et al., 1996) allow more control of the external environment, however, are subject to being influenced by unknown biogenic effects during calcium carbonate precipitation. The application of culture studies is beneficial in terms of identifying species-specific vital effects that must be taken into consideration once the principles of the boron isotope-pH proxy have been better understood. Therefore, conducting laboratory studies, where all components can be controlled, are essential to better understand the boron isotope systematics of marine carbonates. Previous studies have used boron isotope compositions of synthetic carbonates and analyzed the boron inclusion with regards to boron isotopic composition and/or total boron concentration in calcium carbonate (Hemming et al., 1995; Sanyal et al., 2000).

Hemming et al. (1995) grew calcite and aragonite under uniform conditions using a "free-drift technique" without using any seed material. The calcium carbonate was synthesized in solutions of seawater-like ionic strength, 0.5 mol kg^{-1}, with a range of boron concentrations from 0.45 to 500 ppm. The results of the study indicate that the boron isotope compositions of the synthesized carbonate were equal to that for the borate ion at a given pH value. However, the carbonate samples were only synthesized from a single pH value and no stirrer was used in the experimental setup, which would not guarantee uniform conditions throughout the precipitating solution. The study combined the use of total boron concentration and the boron isotopic composition of calcium carbonate to infer a probable aqueous boron species interacting at the carbonate surface.

The pH of the experiments conducted by Hemming et al. (1995) increased from 5.6 to 8.0 over the first two days. During the pH fluctuations in the beginning of the synthesis experiment it is unclear how Hemming et al. (1995) confirmed that no crystals had precipitated during the pH fluctuations, they only acknowledge no crystals were visible. Any crystals that may have been formed while pH was fluctuating would not reflect the intended pH range. It is also of importance to acknowledge that in studies utilizing similar methodology (e.g. Paquette and Reeder, 1995), pH gradients have been observed. The pH must not change over the course of carbonate synthesis when trying to determine if the $\delta^{11}B$ of the carbonate is equal to that for the $B(OH)_4^-$ ion at the same pH value the incorporation of boron would occur over a range of pH values and cannot be precisely compared.

Sanyal et al. (2000) synthesized calcium carbonates using seed material from a small range of pH conditions (pH 7.9-8.6) in Mg free artificial seawater with an ionic strength of 0.7 mol kg^{-1}. This study was performed to establish whether or not a relationship exists between the pH of the parent solution and the boron isotope composition of the synthetic carbonates, as well as to evaluate the potential influence that biogenic effects could have on boron isotope composition. The $\delta^{11}B_{carb}$ synthesized in their study were slightly lighter than that of $\delta^{11}B_{B(OH)4-}$ in seawater at the same pH when applying a $^{11\text{-}10}K_B$ of 1.0194. There was no temperature control used within this study, the experiments were simply carried out in ambient laboratory conditions. The calcite growth rate was not consistent between the experiments for the three different pH values, and Sanyal et al. (2000) only assume that no potential kinetic effects were at play because the resulting $\delta^{11}B_{carb}$ of their samples parallels the $\delta^{11}B_{B(OH)4-}$ versus pH curve generated by

Kakihana et al. (1977). Sanyal et al. (2000) did not confirm whether or not the experimental system was in isotopic equilibrium, which would have more accurately depicted whether or not kinetic effects played a role in the synthesis of calcium carbonate.

Hemming et al. (1995) showed good agreement between the boron isotope composition of borate in the solution and that of the synthetic calcium carbonate. In contrast, Sanyal et al. (2000)'s inorganic calcite experiments found $\delta^{11}B_{carb}$ to be lighter than $\delta^{11}B_{B(OH)4-}$ and also suggested that the proxy may not be applicable for all marine calcite as a small biogenically induced isotope fractionation was observed in some foraminiferal shells. As a result, studies are necessary to confirm potential effects in other species. There is an offset in $\delta^{11}B_{carb}$ compared to the predicted equilibrium $\delta^{11}B_{B(OH)4-}$ between Hemming et al. (1995) and Sanyal et al. (2000) for reasons unknown. The experimental method and ionic strength applied in each study was different, initiating potential disagreement between the studies. Both studies adjusted pH manually to obtain a particular range; Hemming et al. (1995) adjusted pCO_2 in the reaction chamber in order to adjust pH, whereas Sanyal et al. (2000) added acids and bases (HCl and NaOH) in order to obtain the desired pH, and added Na_2CO_3 in order to maintain the constant pH throughout synthesis.

In general, neither study synthesized calcium carbonate samples from a wide enough pH range to reliably depict boron isotope incorporation into carbonates. Both studies were successful in showing correlation between boron isotope composition of calcium carbonate and solution pH; however, the disagreement implies that more studies

with better-constrained variables are required to gain a better understanding of the boron isotope-pH proxy.

1.1.5 δ^{11}B analysis: reliability

Boron is a light element with only two stable isotopes (^{10}B and ^{11}B). They have a relatively large difference in mass, which may generate potential instrumental mass fractionation, and to correct for this, mass fractionation must be identical between samples and normalizing standards (Foster et al., 2006; Rae et al., 2011). In order to apply the boron isotope-pH proxy to natural samples, it is necessary to have an analytical method that can accurately analyze the boron isotope composition from modern marine carbonates, where the boron concentration can range from 1 to 100 ppm. One of the most reliable geological archives for paleoclimate research utilizes foraminiferal shells; however, these samples only contain approximately 10-15 ppm of boron (Hemming and Hönisch, 2007), therefore, analyzing techniques must be efficient and potential laboratory contamination must be carefully controlled (Rae et al., 2011).

There are six different techniques available for the analysis of boron isotope compositions of foraminifera (Table 1.3). It is difficult to judge the accuracy of boron isotope analysis through interlaboratory comparisons because many analytical techniques are utilized (Aggarwal et al., 2009). While there is an international standard for boron isotope analysis, NIST SRM 951, the disagreement between interlaboratory measurements may arise from sample preparation, potential sample contamination, or due to the instrumental techniques utilized to analyze the samples (Gonfiantini et al., 2003;

Aggarwal et al., 2009). Efforts have been made in order to better constrain the sample preparation techniques and provide more reliable results (e.g. Aggarwal et al., 2009).

Early measurements of boron isotope analysis used positive ion thermal mass spectrometry (PTIMS), where sample sizes were typically ~ 5 μg B. These requirements were not sufficient for the measurement of boron isotope compositions of foraminiferal carbonate. While PTIMS has since been somewhat refined, and offers significant signal stability, it still requires larger sample sizes that must be chemically pure. A major advancement in boron isotope analysis, in terms of applications to paleoceanography, was the introduction of negative ion thermal mass spectrometry (NTIMS). NTIMS achieves greater ionization efficiencies and as a result, allows for the analysis of small sample sizes (~ 1 ng) (Hemming and Hanson, 1994). However, there are numerous problems with boron isotope measurements using NTIMS, including large in-run fractionation and mass interferences (Aggarwal and Palmer, 1995; Sanyal et al., 1995; Foster et al., 2006). An approach utilizing multi-collector inductively coupled plasma mass spectrometry (MC-ICPMS), which requires a slightly larger sample size compared to some approaches, is the most precise (<1‰) method for analyzing boron isotopes (Foster, 2008). One of the advantages with using the MC-ICPMS approach is that the relative stability of the machine-induced fractionation can easily be corrected (Foster, 2008). The use of MC-ICPMS to analyze boron isotope composition of calcium carbonate samples is less sensitive to the high degrees of fractionation and isobaric interferences compared to NTIMS. The use of MC-ICPMS also allows for a more rapid analysis compared to NTIMS and PTIMS.

Table 1.3: Comparisons of methods for analyzing boron isotope composition

Method	Acronym	Sample Size (ng)	Precision (‰)
Multi-collector inductively-coupled plasma mass spectrometry	MC-ICPMS	250	±0.2
Negative ion thermal mass spectrometry	NTIMS	1	±0.8
Total evaporation negative ion thermal mass spectrometry	TE-NTIMS	< 0.5	±0.7
Positive ion thermal mass spectrometry	PTIMS	1000	±0.4
High resolution inductively coupled plasma mass spectrometry	HR-ICPMS	250	±2
Quadruple inductively coupled plasma mass spectrometry	Q-ICPMS	100	±14
Secondary ion mass spectrometry	SIMS	< 0.1	±4

1.1.6 Applying the boron isotope-pH proxy

Once the proxy has been properly calibrated and the sole incorporation of tetrahedral $B(OH)_4^-$ is verified, calcium carbonate specimens obtained from shallow sediment cores, which minimizes effects of dissolution (Honisch et al., 2007), can be analyzed for boron isotope composition. The optimal carbonates for this application are those with higher concentrations of boron, due to boron isotope analytical limitations, as well as organisms that do not significantly modify seawater during calcium carbonate secretion. Corals composed of aragonite (*i.e. Siderastrea sidereal*) are ideal for applying boron isotope-pH proxy as they contain a high concentration of boron, approximately 60 ppm (Hemming and Hanson, 1992) and growth of corals occurs at the epidermis, in contact with seawater (Hemming and Hanson, 1992) as oppose to internal shell growth associated with internal fluids at a lower pH as observed in molluscs.

By analyzing calcium carbonate for boron isotope compositions and calculating the pH of the seawater at the time of formation, it is used in conjunction with alkalinity or total inorganic carbon concentration to reconstruct dissolved PCO_2. This can then be used to infer atmospheric carbon dioxide concentrations at the time. There is no reliable record of the variations of alkalinity nor total inorganic carbon concentrations over long time scales, however these parameters can be constrained by understanding variations in carbonate compensation depth (CCD) of the ocean using historical patterns of carbonate sedimentation (Pearson and Palmer, 2000). This thesis focuses on validating the reconstructions of seawater pH and estimations of alkalinity and total inorganic carbon concentrations over Earth's history will not be further discussed.

1.1 Carbon Isotope Composition of Marine Carbonates and DIC

Utilizing calcium carbonate to evaluate boron isotope compositions also allows the possibility to understand the carbon isotope systematics in the marine carbonate system, which is critical to reviewing biogeochemical cycling of carbon and fluctuations in atmospheric carbon dioxide (pCO_2) levels. A sound understanding of isotope fractionation factors is a prerequisite for interpreting stable isotope abundance patterns in nature. In isotope studies of carbon in the environment, quantification of isotope fractionation between the dissolved inorganic species and both atmospheric and dissolved CO_2 is of critical importance. Exchange of CO_2 between the atmosphere and ocean affects the carbon isotope composition of surface waters (Lynch-Stieglitz et al., 1995) and as anthropogenic CO_2 emissions increase resulting in a greater uptake of CO_2 by the oceans, a shift may be seen in the carbon isotope compositions of dissolved inorganic carbon (DIC). The carbon isotopic signature of carbon dioxide dissolved in the ocean cannot be measured directly; however, it is in equilibrium with the DIC species and can be further extrapolated with the use of fractionation factors between the different species. The carbon isotope compositions of DIC in the ocean are also significant in understanding paleoproductivity (Zachos et al., 1989) and tracing sources and sinks of marine carbon (Buhl et al., 1991; Blair et al., 1994; Quay et al., 1992).

Reconstructing the carbon isotope compositions of planktonic and benthic foraminifera in the ocean also has many applications, including monitoring variations in atmospheric CO_2 by outlining organic carbon burial (e.g. Vincent and Berger, 1985), deep water circulation patterns (e.g. Duplessy et al., 1984; Mix and Fairbanks, 1985; Oppo and Fairbanks, 1987; Raymo et al., 1990; Billups, 2002; Venz and Hodell, 2002),

paleoclimate and paleoenvironmental studies (e.g. Yan et al., 2009) as well as being used in conjunction with oxygen isotope records to reconstruct climate aberrations (e.g. Zachos et al., 2001). Taking into account importance of applications of carbon isotope compositions of calcium carbonate and DIC, as well as the observation that many take place in an oceanic environment, it is of considerable importance to evaluate the effect seawater may have on carbon isotope fractionation.

Dissolved inorganic carbon (DIC) consists of $CO_{2\,(aq)}$, H_2CO_3, HCO_3^-, and CO_3^{2-}. The concentration of H_2CO_3 at 25 °C is slightly less than 0.3%, and therefore it is convention to infer that all $CO_{2\,(aq)}$ exists as H_2CO_3 (Eby, 2004). The speciation depends on the pH of the system, with H_2CO_3 dominating below pH 6.4, HCO_3^- between 6.4 and 10.3, and CO_3^{2-} being the dominant species in systems with a pH greater than 10.3 (Clark and Fritz, 1997). It is important to understand the dominant species of DIC in the solution because each individual DIC species has slightly different isotope compositions with respect to $CO_{2\,(g)}$ (Table 1.4).

Table 1.4: Fractionation factors for carbonic acid species relative to $CO_{2\,(g)}$[a]

Species	Equation[a]
H_2CO_3	$1000\ln\alpha = -0.91 + 0.0063 \times 10^6/T^2$
HCO_3^-	$1000\ln\alpha = -4.54 + 1.099 \times 10^6/T^2$
CO_3^{2-}	$1000\ln\alpha = -3.4 + 0.87 \times 10^6/T^2$
$CaCO_3$ (s)	$1000\ln\alpha = -3.63 + 1.194 \times 10^6/T^2$

[a]From Deines et al. (1974)

Isotope equilibrium values between calcium carbonate and dissolved inorganic carbon are generally derived from inorganic precipitate data (Hoefs, 2009). An issue

associated with conducting experiments to determine carbon isotope fractionation among species is the separation of the dissolved carbon phases (H_2CO_3, HCO_3^-, CO_3^{2-}) because equilibrium between the phases is reached within seconds (Hoefs, 2009). However, a complicated factor associated with using natural samples to establish carbon isotope fractionation factors is that shell carbonate is sensitive to vital effects, which generates uncertainty in quantifying the fractionation between the shell and carbon solution. Previous studies have used laboratory experiments to analyze parameters (i.e. mineralogy, precipitation rate, and temperature) that may influence the fractionation of carbon between dissolved inorganic carbon and calcium carbonate (e.g. Emrich et al., 1970; Turner, 1982; Grossman and Ku, 1986; Romanek et al., 1992).

1.1.1 Controls on carbon isotope fractionation

Studies have been conducted in efforts to evaluate carbon isotope fractionation between calcium carbonate, or CO_2, and DIC (e.g. Emrich et al., 1970; Mook et al., 1974; Romanek et al., 1992). This can be complicated because in order to estimate these relationships, the dominant DIC species must be known because equilibrium fractionation ($\alpha_{a\text{-}b}$) depends on the carbon speciation i.e. the proportion of H_2CO_3, HCO_3^-, and CO_3^{2-}, as well as the individual fractionation factor of each species with respect to $CO_{2\,(g)}$ or calcium carbonate. This study uses $1000\ln\alpha_{a\text{-}b}$ notation, where $\alpha_{a\text{-}b}$ is defined as

$$\alpha_{A-B} = \frac{R_A}{R_B} = \frac{1000 + \delta_A}{1000 + \delta_B} \tag{1.10}$$

Where 'A' and 'B' denote the chemical compounds. In the notation used throughout this thesis, a comparison of the published fractionation factors can be seen in Table 1.3.

Table 1.5: Previously published aragonite-DIC fractionation factors

Author(s)	Temp. Range (°C)	Ionic Strength (mol kg^{-1})	$1000ln\alpha_{CaCO3\text{-}DIC(aq)}$	$1000ln\alpha_{CaCO3\text{-}HCO3^-}$
This study	25°C	~0.7	3.26 ±0.18	–
Mook and Vogel, (1968)	25°C	n/a	–	1.499
Rubinson and Clayton, (1969)	25°C	≤ 0.5	–	2.79 ±0.2
Emrich et al., (1970)[a]	20°C	n/a	–	1.85 ±0.23
Romanek et al., (1992)	25°C	≤ 0.065	–	2.9 ±0.6
Owen et al., (2008)	9.2-15.6°C	(~30)[b]	1.31 ±0.03	–

[a]Mineralogy not specific
[b]In salinity (psu)

There are conflicting reviews regarding temperature dependence of the carbon isotope equilibrium fractionation between calcium carbonate and dissolved inorganic carbon (Emrich et al., 1970; Grossman and Ku, 1986; Romanek et al., 1992). Emrich et al. (1970) identified carbon isotope fractionation between $CO_{2\,(g)}$, HCO_3^-, and calcium carbonate between 20 °C and 60 °C utilizing inorganic precipitation experiments, while Grossman and Ku (1986) studied live modern aragonitic foraminifera, gastropods and scaphopods, including *Hoegundina elegans*, from temperatures ranging from 2.6-22.0 °C. Both studies identified a relationship for temperature dependence, however Emrich et al. (1970) noted that an increase in temperature by 1 °C leads to a 0.04‰ increase in $\delta^{13}C$ of calcium carbonate, whereas Grossman and Ku, (1986) reported that a 1 °C rise in temperature results in a decrease of 0.1‰ in shell $\delta^{13}C$, relative to DIC. Romanek et al. (1992) did not find a correlation between carbon isotope fractionation and temperature, however, the methodology consisted of carbonate synthesis experiments which had better control on the temperature, mineralogy, and precipitation rate during calcium carbonate precipitation, which may contributed to the different results.

The importance of mineralogy (aragonite vs. calcite) on carbon isotope fractionation between calcium carbonate and bicarbonate has been established, and it is noted that aragonite is enriched in ^{13}C relative to calcite (Romanek et al., 1992). The influence that ionic strength may have on carbon isotope fractionation between calcium carbonate and DIC has not yet been quantified. Mook and Vogel, (1968) observed a correlation between the fresh:salt water mixing ratio and the carbon isotope composition of carbonate, suggesting that chemical composition of the environment influences $\delta^{13}C_{carb}$. Zhang et al. (1995) suggested that ion complexes would have an effect on the

fractionation of DIC in seawater with respect to gaseous CO_2 after conducting direct measurements in seawater samples and observing that the carbon isotope fractionation between DIC and $CO_{2\,(g)}$ did not agree with values calculated based on C speciation. The presence of ion complexes may have an effect on the carbon isotope fractionation in seawater because there would be a potential increase in various carbonate complexes, e.g. $MgHCO_3$, $MgCO_3$ and $CaCO_3$, which may significantly influence the isotopic fractionation in the system.

It is necessary to evaluate the potential dependence of carbon isotope fractionation on the ionic strength of the precipitating solution because many valuable applications utilizing carbon isotope fractionation factors involve a marine environment, and therefore a high ionic strength. Romanek et al. (1992) determined the carbon isotope fractionation factor between aragonite and bicarbonate as 2.9 ± 0.6 at a constant mineralogy, temperature of 25 °C, and precipitation rate at a low ionic strength (≤0.065 mol kg^{-1}). This is in agreement with the previously published value from a higher ionic strength (≤0.5 mol kg^{-1}) by Rubinson and Clayton (1969), however there is no study equivalent to natural seawater (0.7 mol kg^{-1}).

Owen et al. (2008) cultivated bivalve *Placopecten magellanicus* larval aragonite in high salinity environment and determined that the relationship they calculated between $\delta^{13}C_{aragonite}$ and $\delta^{13}C_{DIC}$ resulted in depleted shell aragonite values compared to the predicted equilibrium relationship presented by Romanek et al., (1992). Within the study by Owen et al. (2008) the dominant DIC species was not identified and utilizing marine bivalves to evaluate this connection introduces the potential for vital effects to contribute to carbon isotopic fractionation. Identifying the biological effects on the carbon isotope

fractionation is necessary prior to applying any proxy utilizing carbon isotope compositions to the carbonate-DIC-CO_2 system, however, the extent to which these vital effects influence is species-specific (McConnaughey et al., 1997). It is necessary to identify a base carbon isotope fractionation factor between carbonate and DIC so that further studies can be conducted to establish the distinct species-related influences. For these reasons, laboratory studies must be conducted where carbonate synthesis conditions can be controlled and the vital and non-equilibrium effects can be eliminated. The results presented within Owen et al. (2008) are of interest because of the significant relationship noted in the carbon isotope fractionation between calcium carbonate and DIC at increased levels of salinity, which does not support comparisons made between Romanek et al. (1992) and Rubinson and Clayton (1969).

1.2 Analytical Techniques for Measurement of $\delta^{18}O_{H2O}$ and $\delta^{13}C_{DIC}$

Within the research presented in this thesis, carbon and oxygen isotope compositions, of dissolved inorganic carbon (DIC) and water respectively, were important parameters to be investigated. The carbon isotope compositions of the DIC in aqueous samples were analyzed in order to evaluate carbon isotope fractionation between aragonite and DIC in high ionic strength environments. From the same solution samples, the oxygen isotope compositions were used to ensure that the system was in isotopic equilibrium throughout aragonite synthesis. The oxygen isotope composition of water ($\delta^{18}O_{H2O}$) and the dissolved inorganic carbon isotope composition in solution ($\delta^{13}C_{DIC}$) usually require two separate analytical techniques. The $\delta^{18}O_{H2O}$ is typically determined using the modified CO_2-H_2O equilibration technique (Epstein and Mayeda, 1953), where

a small quantity of CO_2 is equilibrated with a surplus of water at a constant temperature. The $\delta^{13}C_{DIC}$ is often obtained via a gas evolution method (Atekwana and Krishnamurthy, 1998), where phosphoric acid (H_3PO_4) reacts with the DIC in a solution sample within a closed system and liberates CO_2 to be collected for $\delta^{13}C_{DIC}$ determination. The development of a technique to simultaneously analyze both of these values from a single sample was of beneficial interest because analyses of $\delta^{18}O_{H2O}$ and $\delta^{13}C_{DIC}$ are also applied to enhance Earth science research within fields including oceanography (i.e. Blair et al., 1994) and hydrology (i.e. Buhl et al., 1991; Gat, 1996). The development of the DIC-CO_2 Gas Equilibration method (DIC-CO_2-GEM) combines the principles of two conventional methods into one simple process using continuous flow isotope ratio mass spectrometry (CF-IRMS).

1.3 Thesis Structure

Chapter 1 provided an overview of the boron isotope-pH proxy, the associated hypotheses and previous research completed on the topic. It also provided a background to the carbon isotope fractionation between calcium carbonate and dissolved inorganic carbon (DIC) and the relevance to this research. There was also an introduction to a new method for the analysis of the oxygen isotope composition of water and carbon isotope composition of DIC of an aqueous sample simultaneously.

Chapter 2 and 3 are written in paper format. Chapter 2 will focus on refining the boron isotope-pH proxy. One hypothesis associated with the proxy suggests that only tetrahedral borate is incorporated into the carbonate crystal lattice. Since borate is isotopically different from boric acid, the boron isotope composition of calcium

carbonate should be the same of that for borate. In this research, calcium carbonate is synthesized from three different pH values and the boron isotope composition is compared to the calculated boron isotope composition of borate at the given pH value. This comparison will address the hypothesis stating only the tetrahedral borate ion is incorporated into the carbonate lattice, which is critical to the application of the boron isotope-pH proxy. The carbon isotope fractionation between aragonite and DIC in high ionic strength solutions will also be explored.

Chapter 3 will focus on developing new methodology for measuring the oxygen isotope composition of water and carbon isotope composition of DIC simultaneously from a single solution sample. This method requires small sample sizes on a Finnigan GasBench II headspace autosampler with a Thermo Finnigan Delta plus XP isotope ratio mass spectrometer and is termed the DIC-CO_2 Gas Equilibration method (DIC-CO_2-GEM).

Chapter 4 contains the conclusions of this thesis. This chapter will provide an overview of the research that has been completed within this thesis, including the candidate's contributions to the research where multiple authors were involved, and identify the applications associated with the findings. It will also outline future avenues for this research that will contribute to the applications of the boron isotope-pH proxy.

References

Aggarwal J. K. and Palmer M. R. (1995) Boron Isotope Analysis: A Review. **120,** 1301-1307.

Aggarwal J., Böhm F., Foster G., Halas S., Hönisch B., Jiang S., Kosler J., Liba A., Rodushkin I. and Sheehan T. (2009) How well do non-traditional stable isotope results compare between different laboratories: results from the interlaboratory comparison of boron isotope measurements. *J. Anal. At. Spectrom.* **24,** 825-831.

Arrhenius S. (1896) XXXI. On the influence of carbonic acid in the air upon the temperature of the ground. *The London, Edinburgh, and Dublin Philosophical Magazine and Journal of Science* **41,** 237-276.

Billups K. (2002) Late Miocene through early Pliocene deep water circulation and climate change viewed from the sub-Antarctic South Atlantic. *Palaeogeogr. , Palaeoclimatol. , Palaeoecol.* **185,** 287-307.

Blair N. E., Plaia G. R., Boehme S. E., DeMaster D. J. and Levin L. A. (1994) The remineralization of organic carbon on the North Carolina continental slope. *Deep Sea Research Part II: Topical Studies in Oceanography* **41,** 755-766.

Bryne R. H., Yao W., Klochko K., Tossell J. A. and Kaufman A. J. (2006) Experimental evaluation of the isotopic exchange equilibrium $^{10}B(OH)_3 + {}^{11}B(OH)_4^- = {}^{11}B(OH)_3 + {}^{10}B(OH)_4^-$ in aqueous solution. **53,** 684-688.

Bryne R. and Kester D. (1974) Inorganic speciation of boron in seawater. *J. Mar. Res.* **32,** 119-127.

Buch K. (1933) On boric acid in the sea and its influence on the carbonic acid equilibrium. *Journal du Conseil* **8,** 309-325.

Buhl D., Neuser R., Richter D., Riedel D., Roberts B., Strauss H. and Veizer J. (1991) Nature and nurture: environmental isotope story of the river Rhine. *Naturwissenschaften* **78,** 337-346.

Chamberlin T. C. (1899) An attempt to frame a working hypothesis of the cause of glacial periods on an atmospheric basis. *J. Geol.* **7,** 545-584.

Clark I. D. and Fritz P. (1997) *Environmental isotopes in hydrogeology.* CRC press,

Deines P., Langmuir D. and Harmon R. S. (1974) Stable carbon isotope ratios and the existence of a gas phase in the evolution of carbonate ground waters. *Geochim. Cosmochim. Acta* **38,** 1147-1164.

DelValls T. and Dickson A. (1998) The pH of buffers based on 2-amino-2-hydroxymethyl-1, 3-propanediol ('tris') in synthetic sea water. *Deep-Sea Research Part I* **45,** 1541-1554.

Dickson A. G. (1993) The measurement of seawater pH. *Mar. Chem.* **44,** 131-142.

Dickson A. G. (1993) pH buffers for sea water media based on the total hydrogen ion concentration scale. *Deep Sea Research Part I: Oceanographic Research Papers* **40,** 107-118.

Dickson A. G. (1990) Thermodynamics of the dissociation of boric acid in synthetic seawater from 273.15 to 318.15 K. *Deep Sea Research Part A.Oceanographic Research Papers* **37,** 755-766.

Duplessy J. C., Shackleton N. J., Matthews R. K., Prell W., Ruddiman W. F., Caralp M. and Hendy C. H. (1984) ^{13}C Record of benthic foraminifera in the last interglacial

ocean: Implications for the carbon cycle and the global deep water circulation. *Quatern. Res.* **21,** 225-243.
Dyrssen D. and Hansson I. (1973) Ionic medium effects in seawater — a comparison of acidity constants of carbonic acid and boric acid in sodium chloride and synthetic seawater. *Mar. Chem.* **1,** 137-149.
Eby G. N. (2004) *Principles of environmental geochemistry.* Brooks/Cole Pub Co,
Emrich K., Ehhalt D. and Vogel J. (1970) Carbon isotope fractionation during the precipitation of calcium carbonate. *Earth Planet. Sci. Lett.* **8,** 363-371.
Foster G. L. (2008) Seawater pH, pCO_2 and $[CO_3^{2-}]$ variations in the Carribean Sea over the last 130 kyr: A boron isotope and B/Ca study of foraminifera. **271,** 254-266.
Foster G. L., Ni Y., Haley B. and Elliott T. (2006) Accurate and precise isotopic measurement of sub-nanogram sized samples of foraminiferal hosted boron by total evaporation NTIMS. *Chem. Geol.* **230,** 161-174.
Furst M., Lowenstam H. and Burnett D. (1976) Radiographic study of the distribution of boron in recent mollusc shells. *Geochim. Cosmochim. Acta* **40,** 1381-1386.
Gat J. R. (1996) Oxygen and hydrogen isotopes in the hydrologic cycle. *Annu. Rev. Earth Planet. Sci.* **24,** 225-262.
Gonfiantini R., Tonarini S., Gröning M., Adorni-Braccesi A., Al-Ammar A. S., Astner M., Bächler S., Barnes R. M., Bassett R. L. and Cocherie A. (2003) Intercomparison of boron isotope and concentration measurements. Part II: evaluation of results. *Geostandards Newsletter* **27,** 41-57.
Grossman E. L. and Ku T. (1986) Oxygen and carbon isotope fractionation in biogenic aragonite: temperature effects. *Chemical Geology: Isotope Geoscience section* **59,** 59-74.
Hansson I. (1973) A new set of acidity constants for carbonic acid and boric acid in sea water. **20,** 461-478.
Hansson I. (1973) A new set of pH-scales and standard buffers for sea water. **20,** 479-491.
Hemming N. G. and Hönisch B. (2007) Chapter Seventeen Boron Isotopes in Marine Carbonate Sediments and the pH of the Ocean. *Developments in Marine Geology* **1,** 717-734.
Hemming N. G. and Hanson G. N. (1992) Boron isotopic composition and concentration in modern marine carbonates. **56,** 371-379.
Hemming N. G., Reeder R. J. and Hanson G. N. (1995) Mineral-fluid partitioning and isotopic fractionation of boron in synthetic calcium carbonate. **59,** 371-379.
Hemming N. and Hanson G. (1994) A procedure for the isotopic analysis of boron by negative thermal ionization mass spectrometry. *Chem. Geol.* **114,** 147-156.
Hershey J. P., Fernandez M., Milne P. J. and Millero F. J. (1986) The ionization of boric acid in NaCl, Na-Ca-Cl and Na-Mg-Cl solutions at 25° C. *Geochim. Cosmochim. Acta* **50,** 143-148.
Hickman H. J. (1970) The liquid junction potential—the free diffusion junction. *Chemical Engineering Science* **25,** 381-398.
Hobbs M. Y. and Reardon E. J. (1999) Effect of pH on boron coprecipitation by calcite: Further evidence for nonequilibrium partitioning of trace elements. **63,** 1013-1021.
Hoefs J. (2009) *Stable isotope geochemistry.* Springer,

Honisch B., Hemming N. G. and Loose B. (2007) Comment on "A critical evaluation of the boron isotope-pH proxy: The accuracy of ancient ocean pH estimates" by M. Pagani, D. Lemarchand, A. Spivack and J. Gaillardet. **71,** 1636-1641.

Kakihana H., Kotaka M., Satoh S., Nomura M. and Okamoto M. (1977) Fundamental studies on the ion-exchange separation of boron isotopes. **50,** 158-163.

Kerrick D. M. and Caldeira K. (1998) Metamorphic CO_2 degassing from orogenic belts. *Chem. Geol.* **145,** 213-232.

Kitano Y., Okumura M. and Idogaki M. (1978) Coprecipitation of borate-boron with calcium carbonate. **12,** 183-189.

Klochko K., Cody G. D., Tossell J. A., Dera P. and Kaufman A. J. (2009) Re-evaluating boron speciation in biogenic calcite and aragonite using ^{11}B MAS NMR. **73,** 1890-1900.

Klochko K., Kaufman A. J., Yao W., Bryne R. H. and Tossell J. A. (2006) Experimental measurement of boron isotope fractionation in seawater. **248,** 276-285.

Lemarchand D., Gaillardet J., Lewin E. and Allegre C. (2002) Boron isotope systematics in large rivers: implications for the marine boron budget and paleo-pH reconstruction over the Cenozoic. *Chem. Geol.* **190,** 123-140.

Lemarchand D., Gaillardet J., Lewin E. and Allègre C. (2000) The influence of rivers on marine boron isotopes and implications for reconstructing past ocean pH. *Nature* **408,** 951-954.

Liu Y. and Tossell J. A. (2005) Ab initio molecular orbital calculations for boron isotope fractionations on boric acids and borates. *Geochim. Cosmochim. Acta* **69,** 3995-4006.

Lyman J. (1958) Buffer mechanism of seawater.

Lynch-Stieglitz J., Stocker T. F., Broecker W. S. and Fairbanks R. G. (1995) The influence of air-sea exchange on the isotopic composition of oceanic carbon: Observations and modeling. *Global Biogeochem. Cycles* **9,** 653-665.

McConnaughey T. A., Burdett J., Whelan J. F. and Paull C. K. (1997) Carbon isotopes in biological carbonates: respiration and photosynthesis. *Geochim. Cosmochim. Acta* **61,** 611-622.

McCrea J. M. (1950) On the isotopic chemistry of carbonates and a paleotemperature scale. *J. Chem. Phys.* **18,** 849.

Meyer K., Yu M., Jost A., Kelley B. and Payne J. (2011) $\delta^{13}C$ evidence that high primary productivity delayed recovery from end-Permian mass extinction. *Earth Planet. Sci. Lett.* **302,** 378-384.

Millero F. (1982) Use of models to determine ionic interactions in natural waters. *Thalassia Jugosl.* **18,** 253-291.

Milliman J. D. (1974) *Recent sedimentary carbonates, part 1. Marine carbonates.*

Mix A. C. and Fairbanks R. G. (1985) North Atlantic surface-ocean control of Pleistocene deep-ocean circulation. *Earth Planet. Sci. Lett.* **73,** 231-243.

Mook W., Bommerson J. and Staverman W. (1974) Carbon isotope fractionation between dissolved bicarbonate and gaseous carbon dioxide. *Earth Planet. Sci. Lett.* **22,** 169-176.

Mook W. and Vogel J. (1968) Isotopic equilibrium between shells and their environment. *Science* **159,** 874-875.

Nomura M., Kanzaki T., Ozawa T., Okamoto M. and Kakihana H. (1982) Boron isotopic composition of fumarolic condensates from some volcanoes in Japanese island arcs. *Geochim. Cosmochim. Acta* **46,** 2403-2406.

Oi T. (2000) Ab initio molecular orbital calculations of reduced partition function ratios of polyboric acids and polyborate anions. *ZEITSCHRIFT FUR NATURFORSCHUNG A* **55,** 623-628.

Oi T., Nomura M., Musashi M., Ossaka T., Okamoto M. and Kakihana H. (1989) Boron isotopic compositions of some boron minerals. *Geochim. Cosmochim. Acta* **53,** 3189-3195.

Oppo D. W. and Fairbanks R. G. (1987) Variability in the deep and intermediate water circulation of the Atlantic Ocean during the past 25,000 years: Northern Hemisphere modulation of the Southern Ocean. *Earth Planet. Sci. Lett.* **86,** 1-15.

Owen B. B. and King E. J. (1943) The effect of sodium chloride upon the ionization of boric acid at various temperatures. *Journal of the American Chemical Society* **65,**

Owen E. F., Wanamaker A. D., Feindel S. C., Schöne B. R. and Rawson P. D. (2008) Stable carbon and oxygen isotope fractionation in bivalve (*Placopecten magellanicus)* larval aragonite. *Geochim. Cosmochim. Acta* **72,** 4687-4698.

Owen R. M. and Rea D. K. (1985) Sea-floor hydrothermal activity links climate to tectonics: The Eocene carbon dioxide greenhouse. *Science* **227,** 166-169.

Pagani M., Lemarchand D., Spivack A. and Gaillardet J. (2005) A critical evaluation of the boron isotope-pH proxy: The accuracy of ancient ocean pH estimates. **69,** 953-961.

Palmer M., Spivack A. and Edmond J. (1987) Temperature and pH controls over isotopic fractionation during adsorption of boron on marine clay. *Geochim. Cosmochim. Acta* **51,** 2319-2323.

Paquette J. and Reeder R. J. (1995) Relationship between surface structure, growth mechanism, and trace element incorporation in calcite. *Geochim. Cosmochim. Acta* **59,** 735-749.

Pearson P. N. and Palmer M. R. (2000) Atmospheric carbon dioxide concentrations over the past 60 million years. **406**, 695-699.

Quay P. D., Wilbur D. O., Richey J. E., Hedges J. I. and Devol A. H. (1992) Carbon Cycling in the Amazon River: Implications from the $\delta^{13}C$ Compositions of Particles and Solutes. *Limnol. Oceanogr.* **37,** 857-871.

Rae J. W. B., Foster G. L., Schmidt D. N. and Elliott T. (2011) Boron isotopes and B/Ca in benthic foraminifera: Proxies for the deep ocean carbonate system. **302,** 403-413.

Ramette R. W., Culberson C. H. and Bates R. G. (1977) Acid-base properties of tris (hydroxymethyl) aminomethane (Tris) buffers in sea water from 5 to 40^{o}C. *Anal. Chem.* **49,** 867-870.

Raymo M., Ruddiman W., Shackleton N. and Oppo D. (1990) Evolution of Atlantic-Pacific $\delta^{13}C$ gradients over the last 2.5 my. *Earth Planet. Sci. Lett.* **97,** 353-368.

Raymo M. and Ruddiman W. F. (1992) Tectonic forcing of late Cenozoic climate. *Nature* **359,** 117-122.

Rollion-Bard C., Blamart D., Trebosc J., Tricot G., Mussi A. and Cuif J. -. (2011) Boron isotopes as pH proxy: A new look at boron speciation in deep-sea corals using ^{11}B MAS NMR and EELS. **75,** 1003-1012.

Romanek C. S., Grossman E. L. and Morse J. W. (1992) Carbon isotopic fractionation in synthetic aragonite and calcite: Effects of temperature and precipitation rate. *Geochim. Cosmochim. Acta* **56,** 419-430.

Roy R. N., Roy L. N., Vogel K. M., Porter-Moore C., Pearson T., Good C. E., Millero F. J. and Campbell D. M. (1993) The dissociation constants of carbonic acid in seawater at salinities 5 to 45 and temperatures 0 to 45 C. *Mar. Chem.* **44,** 249-267.

Rubinson M. and Clayton R. N. (1969) Carbon-13 fractionation between aragonite and calcite. *Geochim. Cosmochim. Acta* **33,** 997-1002.

Rustad J. R. and Bylaska E. J. (2007) Ab initio calculation of isotopic fractionation in $B(OH)_{3(aq)}$ and $BOH_4^-{}_{(aq)}$. *J. Am. Chem. Soc.* **129,** 2222-2223.

Sanyal A., Hemming N. G., Hanson G. N. and Broecker W. S. (1995) Evidence for a higher pH in the glacial ocean from boron isotopes in foraminifera. **373,** 234-236.

Sanyal A., Nugent M., Reeder R. J. and Buma J. (2000) Seawater pH control on the boron isotopic composition of calcite: Evidence from inorganic calcite precipitation experiments. **64,** 1551-1555.

Sanyal A., Hemming N., Broecker W., Lea D. W., Spero H. J. and Hanson G. N. (1996) Oceanic pH control on the boron isotopic composition of foraminifera: evidence from culture experiments. *Paleoceanography* **11,** 513-517.

Schwarcz H., Agyei E. and McMullen C. (1969) Boron isotopic fractionation during clay adsorption from sea-water. *Earth Planet. Sci. Lett.* **6,** 1-5.

Sen S., Stebbins J., Hemming N. and Ghosh B. (1994) Coordination environments of B impurities in calcite and aragonite polymorphs: A ^{11}B MAS NMR study. *Am. Mineral.* **79,** 819-825.

Spivack A., You C. -. and Smith J. (1993) Foraminiferal boron isotope ratios as a proxy for surface ocean pH over the past 21 Myr. **363,** 149-151.

Su C. and Suarez D. L. (1995) Coordination of adsorbed boron: A FTIR spectroscopic study. *Environ. Sci. Technol.* **29,** 302-311.

Taylor S. R. and McLennan S. M. (1985) The continental crust: its composition and evolution.

Tossell J. (2006) Boric acid adsorption on humic acids: ab initio calculation of structures, stabilities, ^{11}B NMR and ^{11}B, ^{10}B isotopic fractionations of surface complexes. *Geochim. Cosmochim. Acta* **70,** 5089-5103.

Tossell J. (2005) Boric acid,"carbonic" acid, and N-containing oxyacids in aqueous solution: Ab initio studies of structure, pK_a, NMR shifts, and isotopic fractionations. *Geochim. Cosmochim. Acta* **69,** 5647-5658.

Turner J. V. (1982) Kinetic fractionation of carbon-13 during calcium carbonate precipitation. *Geochim. Cosmochim. Acta* **46,** 1183-1191.

Vengosh A., Kolodny Y., Starinsky A., Chivas A. R. and McCulloch M. T. (1991) Coprecipitation and isotopic fractionation of boron in modern biogenic carbonates. *Geochim. Cosmochim. Acta* **55,** 2901-2910.

Venz K. A. and Hodell D. A. (2002) New evidence for changes in Plio–Pleistocene deep water circulation from Southern Ocean ODP Leg 177 Site 1090. *Palaeogeogr. , Palaeoclimatol. , Palaeoecol.* **182,** 197-220.

Vincent E. and Berger W. H. (1985) Carbon dioxide and polar cooling in the Miocene: The Monterey hypothesis. *The carbon cycle and atmospheric CO* **2,** 455-468.

Waskowiak R. (1962) *Geochemische Untersuchungen an rezenten Molluskenschalen mariner Herkunft.* Akademie-Verlag,

Yan H., Lee X., Zhou H., Cheng H., Peng Y. and Zhou Z. (2009) Stable isotope composition of the modern freshwater bivalve Corbicula fluminea. *Geochem. J.* **43,** 379.

Zachos J., Pagani M., Sloan L., Thomas E. and Billups K. (2001) Trends, rhythms, and aberrations in global climate 65 Ma to present. *Science* **292,** 686-693.

Zachos J. C., Arthur M. A. and Dean W. E. (1989) Geochemical evidence for suppression of pelagic marine productivity at the Cretaceous/Tertiary boundary.

Zeebe R. E. (2005) Stable boron isotope fractionation between dissolved $B(OH)_3$ and $B(OH)_4^-$. **69,** 2753-2766.

Zeebe R. E., Sanyal A., Ortiz J. D. and Wolf-Gladrow D. A. (2001) A theoretical study of the kinetics of the boric acid-borate equilibrium in seawater. **73,** 113-124.

Zhang J., Quay P. and Wilbur D. (1995) Carbon isotope fractionation during gas-water exchange and dissolution of CO_2. *Geochim. Cosmochim. Acta* **59,** 107-114.

Chapter 2: Investigation of stable isotope systematics in the aragonite-CO_2-H_2O system: Multi-element approach

Christa D. Klein Gebbinck,[a], Sang-Tae Kim[a], Michael Henehan[b], and Gavin L. Foster [b]

[a]School of Geography and Earth Sciences, McMaster University, 1280 Main Street West, Hamilton, ON, L8S 4K1, Canada
[b]Ocean and Earth Sciences, University of Southampton Waterfront Campus, National Oceanography Centre, Southampton, European Way, Southampton SO14 3ZH, UK

Status: Intent to submit to Geochimica et Cosmochimica Acta

Abstract

The application of boron isotope compositions in marine carbonates to reconstruct ancient seawater pH has wide appeal in identifying fluctuations in atmospheric pCO_2 concentrations, if proved to be reliable. Inorganic experiments to spontaneously nucleate the calcium carbonate polymorph aragonite at stable pH values (~7.15, ~8.50, ~9.15) in high ionic strength solutions (0.7 mol kg^{-1}) were conducted to identify the dependence of carbonate boron isotope composition ($\delta^{11}B_{carb}$) on the pH of the precipitating solution. The results show a distinct correlation between boron isotope composition and solution pH and support the hypothesis that $B(OH)_4^-$ is the dominant species incorporated into the crystal lattice, however, without an appropriate boric acid dissociation constant and isotope equilibrium constant to apply, the sole incorporation of $B(OH)_4^-$ cannot be confirmed. The results of this study suggest that boron isotope compositions of marine carbonate require further quantification from artificial seawater solutions where appropriate constants can be used and more clearly verify the proxy.

In addition, the carbon isotope fractionation between aragonite and dissolved inorganic carbon (DIC) was quantified in high ionic strength (0.7 mol kg^{-1}) at 25 °C

$$1000 \ln \alpha_{aragonite-DIC} = 3.26 \pm 0.18$$

Which is in agreement to previous studies conducted in low ionic strength solutions, suggesting that the carbon isotope fractionation between aragonite and DIC is independent of ionic strength up to 0.7 mol kg^{-1}.

2.1 Introduction

A reconstruction of atmospheric carbon dioxide concentrations (expressed as partial pressure: pCO2) over the course of Earth's history is important for evaluating concurrent fluctuations. In 1880, pCO_2 increased from 280 to 300 parts per million (ppm) and from 335 to 340 ppm in 1980 (Siegenthaler and Oeschger, 1978; Hansen et al., 1981). A connection made between CO_2 concentrations in the atmosphere and climate change first initiated experimentally by Tyndall (1861) lead to further propositions by Arrhenius (1896) suggesting that high levels of CO_2 in the atmosphere caused warming during the Cenozoic. In order to quantify the impact of climate change as a response to increases in pCO_2, it is important to understand these relationships throughout Earth's history and potential causal effects. Previous studies have attempted to accurately reconstruct pCO_2, using approaches including ice core analysis (e.g. Barnola, 1999), stomatal indices (e.g. Retallack, 2001), and paleovegetation (e.g. Cerling et al., 1993).

Calcium carbonate is ubiquitous in the oceanic system and is a useful tool for many paleoclimate studies because many calcium carbonate organisms are precipitated in equilibrium with seawater, such as aragonitic specimens, *Hoeglundina elegans,* and calcitic specimens, *Uvigerina curticosta* (e.g. Grossman and Ku, 1986), and therefore have the ability to relay chemical information of the environment during the time of formation. The controls on stable isotope fractionation in the carbonate-CO_2-water system can lead to a greater understanding of Earth's history by providing information (e.g. temperature) of past environments.

The correlation between the boron isotope composition of marine carbonates and seawater pH has the potential to reconstruct ancient pCO_2 concentrations (Spivack et al.,

1993; Pearson and Palmer, 2000; Palmer and Pearson, 2003; Henehan et al., 2013). The connection relies on the understanding that as pCO_2 concentrations fluctuate the concentration of dissolved CO_2 in seawater changes to maintain equilibrium and subsequently causes a shift in pH. Applications of the boron isotope-pH proxy have wide appeal in addressing the carbonate-CO_2-water system if they are properly calibrated.

2.2.1 The boron-isotope pH proxy

Boron has two stable isotopes, ^{11}B and ^{10}B, comprising 80.2% and 19.8% of total boron respectively (Kakihana et al., 1977). The two dominant aqueous boron species in seawater are trigonal boric acid, $B(OH)_3$, and tetrahedral borate, $B(OH)_4^-$ (Hershey et al., 1986). The concentrations of these species are a function of pH and can be described by the dissociation of boric acid in seawater:

$$B(OH)_3 + H_2O \leftrightarrow B(OH)_4^- + H^+ \tag{2.1}$$

The dissociation constant of boric acid can be defined by:

$$K_B^* = \frac{[H^+]\cdot[B(OH)_4^-]}{[B(OH)_3]} \tag{2.2}$$

By determining pK_B^* of $B(OH)_3$, the concentration of each species can be calculated as a function of pH (Dickson, 1990; Pagani et al., 2005). The pK_B^* constant of boric acid has been experimentally tested under various conditions, including a range of temperatures, chemical compositions, and ionic strengths (Table 2.1). Using a pK_B^* of 8.597, the value quantified in synthetic seawater with an ionic strength of 0.7 mol kg^{-1} at 25 °C (Dickson, 1990), at pH < 8.6, virtually all boron species exists as $B(OH)_3$, whereas $B(OH)_4^-$ is

dominant when pH > 8.6 (Figure 2.1) (Hershey et al., 1986; Hemming and Hanson, 1992; Klochko et al., 2006).

The boron isotope equilibrium reaction between the two aqueous species is described as,

$$^{10}B(OH)_3 + ^{11}B(OH)_4^- \leftrightarrow ^{11}B(OH)_3 + ^{10}B(OH)_4^- \quad (2.3)$$

Where the boron isotope equilibrium constant is defined as:

$$^{11\text{–}10}K_B = \frac{[^{11}B(OH)_3]\cdot[^{10}B(OH)_4^-]}{[^{10}B(OH)_3]\cdot[^{11}B(OH)_4^-]} \quad (2.4)$$

The $^{11\text{-}10}K_B$ constant has been quantified theoretically and experimentally (Table 2.2), and the accepted value that was experimentally determined in synthetic seawater with an ionic strength of 0.7 mol kg^{-1} at 25 °C is 1.0272 (Klochko et al., 2006). The boron isotope-pH proxy relies on the boron isotope fractionation between $B(OH)_3$ and $B(OH)_4^-$. Due to variations in coordination and in the vibrational frequencies of the aqueous species of boron, the heavier isotope ^{11}B is preferentially incorporated into $B(OH)_3$ and, as a result, $B(OH)_3$ is enriched in ^{11}B relative to $B(OH)_4^-$ (Kakihana et al., 1977; Nomura et al., 1982; Oi et al., 1989; Vengosh et al., 1991) by a constant factor of ~27‰ (Klochko et al., 2006). As the relative concentrations of the aqueous boron species change as a function of pH, so does their respective boron isotope composition (Figure 2.2). Boron isotope composition is presented using delta notation as $\delta^{11}B$:

$$\delta^{11}B = \left(\frac{R_{sample}}{R_{std}} - 1\right)\cdot 1000 \quad (2.5)$$

where $\delta^{11}B$ is expressed in permil (‰), R_{sample} is the $^{11}B/^{10}B$ of sample and R_{std} is the $^{11}B/^{10}B$ of NIST-SRM 951 boric acid standard.

The boron isotope-pH proxy is based on the hypothesis that only tetrahedral $B(OH)_4^-$ is incorporated into the aragonite crystal structure (Vengosh et al., 1991; Hemming and Hanson, 1992). The pH is related to the boron isotope composition of calcium carbonate, $\delta^{11}B_{carb}$, by the following equation:

$$pH = pK_B^* - \log\left(\frac{\delta^{11}B_{SW} - \delta^{11}B_{carb}}{\delta^{11}B_{SW} - {}^{11-10}K_B\delta^{11}B_{carb} - 1000 \cdot ({}^{11-10}K_B - 1)}\right) \quad (2.6)$$

The concentration and boron isotope composition of $B(OH)_4^-$ is a function of pH and as a result, it is expected for the boron isotope composition of carbonates precipitated at a given pH value to be equal to that for borate at the same pH if only $B(OH)_4^-$ is being incorporated into aragonite.

The development of a geochemical proxy based on natural samples is challenging due to ambiguity in tracing environments from which the samples were formed (e.g., pH, temperature, salinity). Therefore, laboratory studies, which allow control over all parameters, are essential to better understand the boron isotope systematics of marine carbonates. Previous studies have used boron isotope compositions and total boron concentrations in synthetic minerals to evaluate the mechanisms of boron incorporation into calcium carbonate. Hemming et al. (1995) found the boron isotope composition of carbonate, $\delta^{11}B_{carb}$, to be equal to $\delta^{11}B_{B(OH)4-}$, while Sanyal et al. (2000) found $\delta^{11}B_{carb}$ to be isotopically lighter than $\delta^{11}B_{B(OH)4-}$ for a given pH value. Aside from the disagreements between Hemming et al. (1995) and Sanyal et al. (2000), neither study synthesized calcium carbonate samples from a wide enough pH range to reliably outline the dependence of carbonate boron isotope compositions on pH.

In this study, aragonite was synthesized at a range of stable pH values from pH 7.10 to 9.18 using total scale, with a thermostated modified constant addition technique,

to investigate the boron, carbon, and oxygen isotope systematics in the aragonite-CO_2-H_2O system. More specifically, the boron isotope composition of aragonite at given a pH value was determined and compared to the boron isotope composition calculated for $B(OH)_4^-$ in seawater at the same pH value.

In addition, carbon isotope fractionation between aragonite and dissolved inorganic carbon (DIC) was examined. Previous investigations have identified the effects of temperature, mineralogy, and precipitation rates (e.g. Romanek et al., 1992), however, this study determined fractionation of carbon isotopes within solutions of high ionic strength (0.7 mol kg^{-1}). A sound understanding of carbon isotope fractionations is essential due to the useful applications of carbon isotope compositions in paleoenvironmental studies, such as reconstructing Earth's temporal changes and productivity (e.g. Holser et al., 1989; Zachos et al., 1989; Meyer et al., 2011). Taking into account that the samples utilized for many paleo proxies are likely of marine origin, it is of considerable importance to specifically evaluate the effect seawater may have on carbon isotope fractionation between aragonite and DIC.

2.2 Experimental Methods

2.2.1 Solution preparation and synthesis of aragonite

Starting solutions were gravimetrically prepared using deionized water (~18 MΩ cm) and ACS grade $NaHCO_3$ and/or Na_2CO_3, depending on the intended starting pH of the experimental solution, $B(OH)_3$ and NaCl,. A minimum of 7 days in a temperature monitored water bath at 25 ± 0.01°C was allotted to ensure that oxygen isotope

equilibrium between the DIC species and water was established. Immediately prior to beginning each synthesis experiment, ACS grade $MgCl_2 \cdot 6H_2O$ and $CaCl_2 \cdot 2H_2O$ were added to the isotopically equilibrated starting solutions. The ratio of $MgCl_2 \cdot 6H_2O$ to $CaCl_2 \cdot 2H_2O$ was 4:1 in order to precipitate aragonite rather than calcite (Morse et al., 2007). The starting solution was then held in a closed reaction chamber at 25.04 ±0.03 °C with two titrants being injected at a continuous rate of 0.5 mL hr^{-1}. In order to have a consistent initial $\delta^{18}O_{H2O}$, the two titrants were prepared with deionized water collected at the same time as the water for the starting solution that they accompanied. One of the titrant solutions was composed of ACS grade $NaHCO_3$ and/or Na_2CO_3, depending on the intended pH of the system and NaCl with the second titrant solution consisting of ACS grade $CaCl_2 \cdot 2H_2O$, $B(OH)_3$, and NaCl. Table 2.3 outlines the solution chemistries and experimental conditions.

The addition of the titrant solutions supersaturated the starting solution with respect to calcium carbonate and provoked spontaneous nucleation, a phase change from the dissolved inorganic carbon species to the precipitation of aragonite, without requiring seed material. A stable pH was maintained throughout aragonite precipitation by adjusting the chemical compositions of the starting and titrant solutions accordingly. The temperature of the experimental solution in the closed reaction chamber was monitored daily using a Thermo Scientific Traceable® digital thermometer. For further description of the experimental set-up used in this study see Appendix A.

For boron isotope analysis, the experimental solution was sampled before and after the synthesis experiment with a 60-mL plastic syringe, filtered through a 0.45 μm Millipore Durapore® syringe filter, and stored in two 1.5 mL vials. The 1.5 mL vials used

to collect solution for boron isotope analysis were cleaned in 3M HCl at 80 °C overnight, rinsed thoroughly with deionized water and stored in a closed high-density polyethylene bottle. The vials were rinsed a minimum of 3 times with deionized water and given a final rinse with the experimental solution immediately prior to injection of the sample. It was ensured that the acid solution used to clean the vials did not come into contact with borosilicate glass to avoid risking isotopic exchange with boron in the experimental solution. The experimental solution was also sampled before and after the synthesis experiment with a 60 mL plastic syringe and stored in a 50 mL vial for oxygen and carbon isotope analysis.

2.2.2 Seawater pH buffer

The experimental solution has an ionic strength of ~0.7 mol kg^{-1}, similar to the ionic strength of natural seawater. Determining the pH of seawater can be complicated because in a high ionic strength solution, the methods employed to measure the pH are not compatible with those that define pH from a low ionic strength media (Dickson, 1993) due to the difference in the liquid junction potential between the solution and electrode (Hickman, 1970). For this reason, it is inaccurate to assume that pH measurements taken directly from an electrode that is inserted into the experimental solution are appropriate.

The pH of the solution was measured daily with a ROSS® Sure-Flow combination pH electrode. The electrode was calibrated against three NIST buffers (pH = 4.00, 7.00, and 10.00) and one Tris buffer (pH = 8.1). All pH buffers were kept in a temperature controlled water bath at 25 ±0.01 °C in order to maintain consistent temperature between

all solutions involved in the experimental procedure. The Tris buffer contained an ionic concentration similar to that of the experimental solution and was used to convert the pH values obtained using the NIST buffers (pH_{NBS} scale) to total scale.

The Tris buffer was prepared following the protocol outlined in Millero et al. (1993). ACS grade KCl, Na_2SO_4, and NaCl salts were dried at 90°C over a 24 hour period. The buffer was then prepared gravimetrically using deionized water, the dried salts, as well as Tris and Tris-HCl. In order to determine all values according to the total scale, the difference between the RmV measured with the pH electrode for the Tris buffer solution (pH = 8.1) and the calculated RmV for a pH of 8.1 using the calibration with NIST buffer solutions (pH = 4.00, 7.00, and 10.00) quantifies the correction factor (~0.28 pH units). This value is then applied to the pH values of the experimental solutions obtained by the ROSS® pH electrode, calibrated by the NIST buffers. All pH measurements are reported using the total scale, which allows the results to be consistent with recent measurements for the dissociation of boric acid in seawater.

2.2.3 Isotopic analysis of aragonite

The mineralogy of all synthesized calcium carbonate samples was quantified through x-ray diffraction (XRD) analysis. The carbon and oxygen isotope compositions of the calcium carbonate samples were determined on a VG OPTIMA isotope ratio mass spectrometer at McMaster University, equipped with an ISOCARB automated common acid bath at 90 °C. The oxygen isotope compositions were normalized to the recommended values for standards NBS 18 and NBS 19 of 7.16‰ and 28.65‰ relative to SMOW, respectively. The acid fractionation factor applied to calculate $\delta^{18}O$ of

aragonite is 1.01063 (Kim et al., 2007). The carbon isotope compositions were normalized to the recommended values for standards NBS 18 and NBS 19 of −5.01‰ and 1.95‰ relative to PDB, respectively.

2.2.4 Isotopic analysis of solutions

For oxygen isotope analysis of aqueous samples, a modified CO_2-H_2O equilibration technique (Epstein and Mayeda, 1953) was employed using a Gas Bench II headspace autosampler with a Thermo Finnigan Delta plus XP isotope ratio mass spectrometer at McMaster University, in Hamilton, Ontario. Exetainer® vials were flushed and filled with a 0.2% CO_2 and 99.8% He mixture with a double needle (Figure 2.3) and a flow of 100 mL min^{-1}. Using a 1 mL syringe, 0.2 mL of water sample was injected into the vial, allowed at least 27 hours to equilibrate at 25 ±0.1 °C and finally, the CO_2 in the headspace was analyzed (Figure 2.4). For full details, refer to Section 3.2.1. Samples were analyzed in duplicates with standards, USGS RSIL W-67400 and USGS RSIL W-64444, with oxygen isotope compositions of -1.97‰ and 51.14‰, respectively, as well as laboratory water standards, MRSI-STD-W1 and MRSI-STD-W2, previously calibrated against both SMOW and SLAP, as 0.58‰ and 28.08‰, respectively, before and after all samples.

The carbon isotope composition of DIC was determined using a gas evolution method (Atekwana and Krishnamurthy, 1998) on the Gas Bench II using CF-IRMS at McMaster University. For this method, Exetainer® vials were preloaded with 0.2 mL 103% H_3PO_4, capped using a new septa and then flushed and filled with 99.999% He. The He filled tubes were then injected with 0.2 mL of water sample using 1 mL syringes

and equilibrated overnight at 25 ±0.1 °C. Laboratory standards containing DIC, as well as international standards NBS 18 and NBS 19 carbonates, were analyzed at the beginning and end of each session. To review details and procedures on the preparation of laboratory standards for DIC analysis see Section 3.1.

2.2.5 Analysis of $\delta^{11}B$

The boron isotope composition of aragonite samples was analyzed at the National Oceanography Centre, Southampton (NOCS), using multicollector inductively coupled plasma mass spectrometry (MC-ICPMS) (Foster, 2008). Samples of 1-3 mg of synthetic aragonite were cleaned to remove any boron that may have adhered to the carbonates from the experimental solution. Carbonate samples were rinsed with ~500 µL of boron-free MilliQ (18.2 MΩ cm) water, ultrasonicated for 30 seconds and then centrifuged for 4 minutes. This step was repeated five times, and each time the supernatant extracted was kept for B/Ca analysis on the Thermo XSeries II Quadropole ICPMS to check for the efficiency of rinsing. After transfer to Teflon centrifuge tubes, samples were subject to a weak acid leach (in 0.0005M HNO_3) to remove any remaining adsorbed boron and three further rinses of MilliQ water to remove the weak acid. Samples were then dissolved via addition of 0.5M HNO_3.

For the accurate analysis of boron isotope composition, boron must be separated from calcium carbonate matrix (Foster et al., in review). To this end, samples were buffered with boron-free 2M sodium acetate-0.5M acetic acid buffer and passed through 20 µL columns of boron-specific anion exchange resin, Amberlite IRA 743 (Kiss, 1988; Lemarchand et al., 2002). Matrix and buffer were removed with ten 160 µl rinses of

boron-free MilliQ water before sample boron was eluted in five 106 µl rinses of 0.5M HNO_3. A further 106 µl of 0.5M HNO_3 was then passed through columns, and boron concentrations in this elution tail checked to ensure >99.9% elution efficiency.

A Thermo Neptune MC-ICPMS is utilized for boron isotope analysis. The instrument is ideal due to the high sensitivities for boron that can be attained (600-800 mV for a 50 ppb boron solution), as well as the adaptable and customizable introduction system. For the generation of boron isotope measurements, it is of critical importance to implement adequate tuning of the MC-ICPMS. At NOCS, the instrument is allotted 1-2 hours to 'warm up' at approximate tuning conditions prior to tuning (using a 50 ppb solution of NIST SRM 951). First, the inlet system and source lenses are tuned for maximum sensitivity and peak shape may then be optimized for maximum $^{11}B/^{10}B$ stability prior to boron isotope analyses (Foster, 2008). Besides peak shape and intensity, it is critical to stabilize machine-induced fractionation as much as possible. The instrument is tuned for stability by analyzing the isotopic ratio of NIST SRM 951 across a range of sample gas input levels.

If tuning and stability is satisfactory, any in-run drift in instrumental mass fractionation is gradual and measurements of 50 ppb solutions of NIST SRM 951 boric acid standard before and after sample analysis will be within uncertainty of each other. In contrast, inadequate tuning and sub-optimal machine performance is outlined by large jumps between measured boron isotope compositions between bracketing standards. The NIST SRM 951 can be used to correct for machine-induced isotopic fractionation and is also used to normalize the $^{11}B/^{10}B$ ratios of samples to delta notation.

Boron is a contaminant and prior to measurements, efforts to reduce analytical blank are critical to the production of accurate $\delta^{11}B$ data. These measures include (1) a reduction in airborne particulate boron, (2) purification of all reagents involved in sample preparation, (3) effective cleaning protocols for sample vessels, and (4) correct analyst practices. To permit accurate characterization of fall-in blank, reagent-borne blank, and any possible contamination from the autosampler vials, measurements of 'blank pots' surrounds every three samples. These 'blank pots' consist of 1.5 mL autosampler vials filled with HNO_3 equal to sample volumes.

Samples are measured in duplicates and the mean $\delta^{11}B$ is calculated. Note that replicate measurements are independent, and do not share bracketing standards or blanks. In-house precision was assessed using standards and corals containing a range of boron concentrations and give a $\delta^{11}B$ an external reproducibility at 2σ of 0.23‰ at 50 ppb and 0.33‰ at 10 ppb.

2.3 Results and Discussion

2.3.1 Confirmation of mineralogy and isotopically equilibrated conditions

The modified constant addition method effectively precipitated sample sizes ranging from 58.8 mg to 389.1 mg depending on the chemical composition of the experiment (refer to Table 2.3). Mineralogy of all samples was confirmed to be 100% aragonite with XRD analysis (Figure 2.5, see Appendix A for results of all samples).

In order to confirm that the experimental system was in isotopic equilibrium during the precipitation of aragonite, the relationship between the oxygen isotope compositions

of the precipitating solution and synthesized aragonite were compared to the published equilibrium aragonite-water oxygen isotope fractionation equation

$$1000 \ln \alpha_{aragonite-water} = 17.88 \pm 0.13(10^3 / T) - 31.14 \pm 0.46 \quad (2.7)$$

(Kim et al., 2007). The oxygen isotope fractionation ($1000\ln\alpha_{aragonite\text{-}water}$) for the experiments conducted in this study at 25 °C ranged from 28.80 to 29.15 and averaged 28.97 ±0.11 (Table 2.4). The calculated $1000\ln\alpha_{aragonite\text{-}water}$ 25 °C from the published relationship is 28.83 ±0.59 and therefore, the experimental system in this study was in isotopic equilibrium throughout aragonite synthesis (Figure 2.6). This investigation is critical when looking at isotope fractionation relationships involved within the system (i.e., boron) that are not as well established.

2.3.2 Boron isotope compositions in synthetic aragonite

The boron isotope compositions of inorganic aragonite ($\delta^{11}B_{carb}$) precipitated from pH values from 7.10 to 9.18 are reported in Table 2.5. The stability of pH throughout aragonite synthesis experiments is included in Appendix A. The $\delta^{11}B_{carb}$ increases from 14.54‰ at pH 7.10 to 34.96‰ at pH 9.15. The $\delta^{11}B$ of the experimental solution was constant for all experiments at approximately 39.85‰. The results of increasing $\delta^{11}B_{carb}$ with increasing pH, and decreasing boron isotope fractionation between solution and carbonate with increasing pH, strongly supports the hypothesis that only $B(OH)_4^-$ is incorporated into the crystal lattice and current applications of the boron isotope-pH proxy (e.g. Spivack et al., 1993; Sanyal et al., 1995).

A comparison of the trend in $\delta^{11}B_{carb}$ with pH to the calculated $\delta^{11}B_{B(OH)4-}$ with pH is not straightforward. The pK_B^* and $^{11\text{-}10}K_B$ constants have not been determined in experimental conditions similar to those utilized in this study (for details see Tables 2.1 and 2.2). Based on similarities in experimental solution compositions, the most applicable pK_B^* values of 8.597 (Dickson, 1990) and 8.830 (Hershey et al., 1986), as well as $^{11\text{-}10}K_B$ values 1.0250 and 1.0272 (Klochko et al., 2006), are considered in order to further interpret the boron isotope compositions of synthesized aragonite (Figure 2.7). If only borate is being incorporated into the aragonite crystal lattice, it is likely that the pK_B^* value is closer to 8.597 and the $^{11\text{-}10}K_B$ value is closer to 1.0250. Applying arbitrary values to form a line of 'best fit' for our data would actually have a pK_B^* value of 8.64 and the $^{11\text{-}10}K_B$ value approximately 1.0254, however it is uncertain as to whether or not only the $B(OH)_4^-$ ion was incorporated into the carbonate lattice, and if $B(OH)_3$ was also taken up, these constants would not be valid in calculating $\delta^{11}B_{B(OH)4-}$ with pH. As a result, previously established values for pK_B^* and $^{11\text{-}10}K_B$ were applied to compare $\delta^{11}B_{carb}$ to $\delta^{11}B_{B(OH)4-}$.

The chemical compositions outlined in this study are preliminary steps to examining the boron isotope proxy and further experimental studies incorporating more seawater constituents are necessary to clearly outline the systematic processes. The inorganic aragonite samples from this study are intended to undergo ^{11}B magic angle spinning nuclear magnetic resonance (MAS NMR) spectroscopy analysis to further classify boron coordination within the crystal lattice. The application of MAS NMR analysis will be beneficial in terms of identifying whether trigonal or tetrahedral boron is

present, however, will not provide an indication of whether or not coordination transformations may have occurred.

2.3.3 Carbon isotope fractionation between aragonite and DIC

In the experiments where starting solution and titrants were prepared using only one carbon source (i.e., Na_2CO_3) and the isotopic composition of DIC in the solution did not significantly change over the duration of the experiment, the carbon isotope fractionation between precipitated aragonite and DIC was examined (Table 2.6). The $\delta^{13}C$ values of the slowly precipitated aragonite and DIC, from solutions with an ionic strength of 0.7 mol kg^{-1} at 25 °C (n =10), yielded the following carbon isotope fractionation factor

$$1000 \ln \alpha_{aragonite-DIC} = 3.26 \pm 0.18 \quad (2.8)$$

Where $\alpha_{aragonite\text{-}DIC}$ is defined as

$$\alpha_{aragonite-DIC} = \frac{1000 + \delta^{13}C_{aragonite}}{1000 + \delta^{13}C_{DIC}} \quad (2.9)$$

The previously published value from Romanek et al. (1992) using an ionic strength of ≤0.065 mol kg^{-1}, at 25 °C is

$$1000 \ln \alpha_{aragonite-HCO_3^-} = 2.9 \pm 0.6 \quad (2.10)$$

In order to compare the results presented here and previously published by Romanek et al. (1992), where the fractionation of carbon between aragonite and HCO_3^- was quantified, the dominant DIC species present for this study was identified by the pH of the solution. The pH of the experiments for this investigation ranged from 9.14 to 9.18

and by applying the equilibrium constants for the carbonate system (i.e. K_1 and K_2, See Appendix), an estimate for the concentrations of the DIC species can be calculated. To determine the exact concentrations of the individual DIC species in high ionic strength solutions, consideration must be taken to account for the formation of ion pairs (i.e., $MgHCO_3$, etc.), however, a direct application of the equilibrium constants is sufficient to confirm the primary species. The dominant DIC species by a factor of 10 is HCO_3^-, and therefore, the results of this study are comparable and can infer that an ionic strength up to 0.7 mol kg^{-1} does not significantly influence the fractionation of carbon between aragonite and dissolved inorganic carbon (Figure 2.8).

2.4 Conclusion

Calcium carbonate in the form of aragonite was synthesized from high ionic strength solutions at 25 °C with stable pH values ranging from 7.10 to 9.18 using a modified constant addition method. The boron isotope composition of aragonite was compared to the predicted equilibrium boron isotope composition of $B(OH)_4^-$ in seawater at the same pH value. Boron isotope compositions analyzed by MC-ICPMS were interpreted by considering pK_B^* constants 8.597 and 8.830, as well as $^{11\text{-}10}K_B$ of 1.250 and 1.272, as the chemical compositions of the experimental solutions in this study were not as simple or complex as the experimental solutions where the constants were quantified. The trend observed in $\delta^{11}B_{carb}$ with increasing pH is suggestive of only having $B(OH)_4^-$ incorporated into the crystal lattice.

The carbon isotope fractionation in high ionic strength solutions at 25 °C was quantified between aragonite and dissolved inorganic carbon (DIC), which yielded the relationship

$$1000 \ln \alpha_{aragonite-DIC} = 3.26 \pm 0.18$$

The calculated fractionation factor of carbon between aragonite and DIC is comparable to previously published values for aragonite and HCO_3^- fractionation factors obtained in low ionic strength solutions because in the solutions from this study HCO_3^- is the dominant species present. An understanding of parameters that can influence carbon isotope fractionation in the natural environment is key to identify so that further investigation of additional relationships, such as metabolic and kinetic effects, can be accurately quantified.

Further research on the dependence of boron isotope compositions of marine carbonates on pH is required, however, it is likely that the boron isotope-pH proxy is a feasible tool in reconstructing seawater pH and can be used in conjunction with seawater alkalinity or the dissolved inorganic carbon concentrations to outline pCO_2 concentrations in Earth's history (Zeebe and Wolf-Gladrow, 2001). The generation of models for historical pCO_2 trends using ancient seawater pH will give a more elaborate understanding of cause and effect relationships between climate and CO_2 concentrations in the past.

References

Arrhenius S. (1896) XXXI. On the influence of carbonic acid in the air upon the temperature of the ground. *The London, Edinburgh, and Dublin Philosophical Magazine and Journal of Science* **41,** 237-276.

Atekwana E. and Krishnamurthy R. (1998) Seasonal variations of dissolved inorganic carbon and $\delta^{13}C$ of surface waters: application of a modified gas evolution technique. *Journal of Hydrology* **205,** 265-278.

Barnola J. M. (1999) Status of the atmospheric CO2 reconstruction from ice cores analyses. *Tellus B* **51,** 151-155.

Cerling T. E., Wang Y. and Quade J. (1993) Expansion of C4 ecosystems as an indicator of global ecological change in the late Miocene. *Nature* **361,** 344-345.

Dickson A. G. (1993) The measurement of seawater pH. *Mar. Chem.* **44,** 131-142.

Dickson A. G. (1990) Thermodynamics of the dissociation of boric acid in synthetic seawater from 273.15 to 318.15 K. *Deep Sea Research Part A.Oceanographic Research Papers* **37,** 755-766.

Foster G. L. (2008) Seawater pH, pCO_2 and $[CO_3^{2-}]$ variations in the Caribbean Sea over the last 130 kyr: A boron isotope and B/Ca study of foraminifera. **271,** 254-266.

Grossman E. L. and Ku T. (1986) Oxygen and carbon isotope fractionation in biogenic aragonite: temperature effects. *Chemical Geology: Isotope Geoscience section* **59,** 59-74.

Hansen J., Johnson D., Lacis A., Lebedeff S., Lee P., Rind D. and Russell G. (1981) Climate impact of increasing atmospheric carbon dioxide. *Science* **213,** 28.

Hemming N. G. and Hanson G. N. (1992) Boron isotopic composition and concentration in modern marine carbonates. **56,** 371-379.

Henehan M. J., Rae J. W. B., Foster G. L., Erez J., Prentice K. C., Kucera M., Bostock H. C., Martinez-Boti M. A., Milton J. A., Wilson P. A., Marshall B. J. and Elliott T. (2013) Calibration of the boron isotope proxy in the planktonic foraminifera *Globigerinoides ruber* for use in palaeo-CO_2 reconstruction. *Earth and Planetary Science Letters* **364,** 111-122.

Hershey J. P., Fernandez M., Milne P. J. and Millero F. J. (1986) The ionization of boric acid in NaCl, Na-Ca-Cl and Na-Mg-Cl solutions at 25° C. *Geochim. Cosmochim. Acta* **50,** 143-148.

Hickman H. J. (1970) The liquid junction potential—the free diffusion junction. *Chemical Engineering Science* **25,** 381-398.

Kakihana H., Kotaka M., Satoh S., Nomura M. and Okamoto M. (1977) Fundamental studies on the ion-exchange separation of boron isotopes. **50,** 158-163.

Kim S. T., O'Neil J. R., Hillaire-Marcel C. and Mucci A. (2007) Oxygen isotope fractionation between synthetic aragonite and water: Influence of temperature and Mg^{2+} concentration. *Geochim. Cosmochim. Acta* **71,** 4704-4715.

Kim S., Mucci A. and Taylor B. E. (2007) Phosphoric acid fractionation factors for calcite and aragonite between 25 and 75 C: revisited. *Chem. Geol.* **246,** 135-146.

Kiss E. (1988) Ion-exchange separation and spectrophotometric determination of boron in geological materials. *Anal. Chim. Acta* **211,** 243-256.

Klochko K., Kaufman A. J., Yao W., Bryne R. H. and Tossell J. A. (2006) Experimental measurement of boron isotope fractionation in seawater. **248,** 276-285.

Lemarchand D., Gaillardet J., Lewin E. and Allegre C. (2002) Boron isotope systematics in large rivers: implications for the marine boron budget and paleo-pH reconstruction over the Cenozoic. *Chem. Geol.* **190,** 123-140.

Liu Y. and Tossell J. A. (2005) Ab initio molecular orbital calculations for boron isotope fractionations on boric acids and borates. *Geochim. Cosmochim. Acta* **69,** 3995-4006.

Meyer K., Yu M., Jost A., Kelley B. and Payne J. (2011) $\delta^{13}C$ evidence that high primary productivity delayed recovery from end-Permian mass extinction. *Earth Planet. Sci. Lett.* **302,** 378-384.

Millero F. J., Zhang J. Z., Fiol S., Sotolongo S., Roy R. N., Lee K. and Mane S. (1993) The use of buffers to measure the pH of seawater. *Mar. Chem.* **44,** 143-152.

Morse J. W., Arvidson R. S. and Luttge A. (2007) Calcium carbonate formation and dissolution. *Chemical Reviews-Columbus* **107,** 342-381.

Oi T. (2000) Ab initio molecular orbital calculations of reduced partition function ratios of polyboric acids and polyborate anions. *ZEITSCHRIFT FUR NATURFORSCHUNG A* **55,** 623-628.

Palmer M. and Pearson P. N. (2003) A 23,000-year record of surface water pH and PCO_2 in the Western Equatorial Pacific Ocean. *Science* **300,** 480-482.

Pearson P. N. and Palmer M. R. (2000) Atmospheric carbon dioxide concentrations over the past 60 million years. **406,** 695-699.

Retallack G. J. (2002) Carbon dioxide and climate over the past 300 Myr. *Philosophical Transactions of the Royal Society of London.Series A: Mathematical, Physical and Engineering Sciences* **360,** 659-673.

Romanek C. S., Grossman E. L. and Morse J. W. (1992) Carbon isotopic fractionation in synthetic aragonite and calcite: Effects of temperature and precipitation rate. *Geochim. Cosmochim. Acta* **56,** 419-430.

Rustad J. R. and Bylaska E. J. (2007) Ab initio calculation of isotopic fractionation in $B(OH)_{3(aq)}$ and $BOH_4^-{}_{(aq)}$. *J. Am. Chem. Soc.* **129,** 2222-2223.

Sanyal A., Hemming N. G., Hanson G. N. and Broecker W. S. (1995) Evidence for a higher pH in the glacial ocean from boron isotopes in foraminifera. **373,** 234-236.

Sanyal A., Nugent M., Reeder R. J. and Buma J. (2000) Seawater pH control on the boron isotopic composition of calcite: Evidence from inorganic calcite precipitation experiments. **64,** 1551-1555.

Siegenthaler U. and Oeschger H. (1978) Predicting future atmospheric carbon dioxide levels. *Science* **199,** 388-395.

Spivack A., You C. -. and Smith J. (1993) Foraminiferal boron isotope ratios as a proxy for surface ocean pH over the past 21 Myr. **363,** 149-151.

Tyndall J. (1861) On the Absorption and Radiation of Heat by Gases and Vapours, and on the Physical Connexion of Radiation, Absorption, and Conduction. *The London, Edinburgh and Dublin Philosophical Magazine and Journal of Science* **22,** 169.

Vengosh A., Kolodny Y., Starinsky A., Chivas A. R. and McCulloch M. T. (1991) Coprecipitation and isotopic fractionation of boron in modern biogenic carbonates. *Geochim. Cosmochim. Acta* **55,** 2901-2910.

Vincent E. and Berger W. H. (1985) Carbon dioxide and polar cooling in the Miocene: The Monterey hypothesis. *The carbon cycle and atmospheric CO* **2,** 455-468.

Zachos J., Pagani M., Sloan L., Thomas E. and Billups K. (2001) Trends, rhythms, and aberrations in global climate 65 Ma to present. *Science* **292,** 686-693.

Zachos J. C., Arthur M. A. and Dean W. E. (1989) Geochemical evidence for suppression of pelagic marine productivity at the Cretaceous/Tertiary boundary.

Zeebe R. E. (2005) Stable boron isotope fractionation between dissolved $B(OH)_3$ and $B(OH)_4^-$. **69,** 2753-2766.

Zeebe R. E. and Wolf-Gladrow D. (2001) *CO_2 in Seawater: Equilibrium, Kinetics, Isotopes: Equilibrium, Kinetics, Isotopes.* Elsevier Science.

Table 2.1: Acid dissociation constants (pK_B^*) for $B(OH)_3$ at 25 °C

Author(s)	pH scale	Ionic Strength (mol kg^{-1})	Media	pK_B^*
Buch (1933)	uncertain	(34.4)[a]	Na^+, Ca^{2+}, Cl^-	8.74
Owen and King (1945)	pH_{NBS}	0.725	Na^+, Cl^-	8.831
Lyman (1957)	pH_{NBS}	(33)[a]	Seawater	8.54[b]
Dyrssen and Hansson, (1973)	uncertain	0	pure water	9.237
		0.7	Na^+, Cl^-	8.85
		0.7	synthetic seawater (Na^+, Cl^-, Ca^{2+}, Mg^{2+}, SO_4^{2-})	8.61
Hansson (1973)	pH_T	0.7	Na^+, Mg^{2+}, Ca^{2+}, Cl^-, SO_4^{2-}	8.61
Bryne and Kester (1974)	pH_{NBS}	0.7	Na^+, Ca^{2+}, Cl^-	8.774[c]
			Na^+, Mg^{2+}, Cl^-	8.715[c]
Hershey et al. (1986)	pH_T	0.68	Na^+, Cl^-	8.83
			Na^+, Mg^{2+}, Cl^-	8.725
			Na^+, Ca^{2+}, Cl^-	8.675
Dickson (1990)	pH_T	0.7	Na^+, Mg^{2+}, Ca^{2+}, Cl^-, K^+,SO_4^{2-}	8.597
Tossell (2005)	n/a	n/a	computational	9.2
Bryne et al. (2006)	pH_T	0.6	K^+, Cl^-	8.64

[a]In salinity (psu).
[b]calculated from Pitzer interaction parameters in Hershey et al., (1986).
[c]corrected by Millero (1982).

Table 2.2: Boron isotope fractionation factors cited within the literature

Author(s)	Treatments/Methods	Isotope Equilibrium Constant ($^{11\text{-}10}K_B$)
Kakihana et al., 1977	Ion-exchange separation based on reduced partition function ratios and using spectroscopic data for molecular vibrations	1.0194
Palmer et al., 1987	Adsorption of B from seawater onto marine clay	1.033
Oi, 2000	*Ab initio* molecular orbital theory calculating vibrational frequency at the optimized structure	1.026
Pagani et al., 2005	Best fit with inorganic carbonate precipitation experiments conducted in artificial seawater	1.0267
Zeebe, 2005	*Ab initio* molecular orbital theory and spectroscopic data for molecular vibrations	≥1.030
Liu and Tossell, 2005	*Ab initio* molecular orbital theory using the "water droplet" method	1.027
Tossell (2005)	Quantum mechanical calculations considering vibrational, rotational, and translational contributions to the free energy	1.0322
Bryne et al., 2006	Experimental observations of chemical equilibrium in 0.6 mol kg^{-1} H_2O KCl	1.0285
Klochko et al., 2006	Experimental observations of chemical equilibrium in "pure water", 0.6 mol kg^{-1} H_2O KCl, and 0.7 mol kg^{-1} synthetic seawater, at 25 and 40°C, with 0.01-0.05 mol kg^{-1} total boron concentrations	1.0308, 1.0250, and 1.0272, respectively
Rustad and Bylaska, 2007	*Ab initio* molecular dynamics using Fourier transformation of the velocity autocorrelation function to obtain vibrational densities	1.028

Table 2.3: Experimental conditions and oxygen isotope data for constant addition aragonite precipitation experiments.

Sample Name	Start[a] (mmolal)	Titrant 1[b] (mmolal)	Titrant 2[c] (mmolal)	Duration (hrs)	Sample Size (mg)	Average Temp. (°C)	Average pH (total scale)
CKG-Oct511	5/5/0.5/2/7.9/685	60/20/620	3/20/695	375.23	70.01	25.04	8.52
CKG-Mar2112-C	5/5/0.5/2/7.9/685	60/20/620	3/20/695	411.05	45.33	25.01	8.51
CKG-Apr2712-D	5/5/0.5/2/7.9/685	60/20/620	3/20/695	405.87	42.67	24.99	8.56
CKG-Aug312-D2	0/10/0.25/1/7.9/685	0/80/510	5/20/695	406.88	263.51	25.05	8.99
CKG-Aug3012-E	5/5/0.5/2/7.9/685	60/20/620	3/20/695	626.88	79.34	24.94	8.49
CKG-Sept2512-D2	0/10/0.25/1/7.9/685	0/80/510	5/20/695	595.17	92.44	25.06	9.18
CKG-Oct2912-E	5/5/0.5/2/7.9/685	60/20/620	3/20/695	595.17	71.39	25.03	8.52
CKG-Oct2912-E2	5/5/0.5/2/7.9/685	60/20/620	3/20/695	599.73	88.08	25.06	8.49
CKG-Dec512-D	0/10/0.25/1/7.9/685	0/80/510	5/20/695	599.73	79.85	25.08	9.14
CKG-Dec512-D2	0/10/0.25/1/7.9/685	0/80/510	5/20/695	479.40	67.07	25.05	9.14
CKG-Dec1412-C	7.5/2.5/10/40/7.9/592	16/4/685	5/20/695	599.73	270.13	25.03	7.27
CKG-Feb2513-C	0/10/0.25/1/7.9/685	0/80/510	5/20/695	450.82	75.21	25.05	9.15
CKG-Feb2513-D	0/10/0.25/1/7.9/685	0/80/510	5/20/695	450.82	58.76	25.07	9.15
CKG-Feb2513-E	10/0/10/40/7.9/570	60/20/620	10/20/695	283.03	389.06	25.08	7.10
CKG-Apr313-C	10/0/10/40/7.9/570	60/20/620	10/20/695	307.25	339.86	25.03	7.31
CKG-Apr313-D	10/0/10/40/7.9/570	60/20/620	10/20/695	211.58	334.98	25.06	7.28
CKG-Apr313-E	10/0/10/40/7.9/570	60/20/620	10/20/695	67.22	67.00	25.06	7.32

[a] $NaHCO_3/Na_2CO_3/Ca/Mg/B/NaCl$
[b] $NaHCO_3/Na_2CO_3/NaCl$
[c] $B/Ca/NaCl$

Table 2.4: Oxygen isotope compositions of aragonite and water confirming equilibrium conditions for synthesis experiments

Sample Name	$\delta^{18}O_{aragonite}$ (‰)	$\delta^{18}O_{water}$ (‰)	$\alpha_{(aragonite\text{-}H2O)}$	$1000ln\alpha_{(aragonite\text{-}H2O)}$
CKG-Oct511	22.45	-6.76	1.0294	28.99
CKG-Mar2112-C	22.52	-6.63	1.0293	28.92
CKG-Apr2712-D	22.45	-6.70	1.0293	28.92
CKG-Aug312-D2	22.59	-6.73	1.0295	29.09
CKG-Aug3012-E	22.51	-6.62	1.0293	28.90
CKG-Sept2512-D2	22.59	-6.52	1.0293	28.88
CKG-Oct2912-E	22.56	-6.51	1.0293	28.84
CKG-Oct2912-E2	22.53	-6.49	1.0292	28.80
CKG-Dec512-D	22.67	-6.41	1.0293	28.84
CKG-Dec512-D2	22.69	-6.43	1.0293	28.89
CKG-Dec1412-C	22.96	-6.43	1.0296	29.15
CKG-Feb2513-C	22.65	-6.60	1.0294	29.02
CKG-Feb2513-D	22.63	-6.57	1.0294	28.97
CKG-Feb2513-E	22.67	-6.64	1.0295	29.08
CKG-Apr313-C	22.64	-6.69	1.0295	29.10
CKG-Apr313-D	22.60	-6.68	1.0295	29.05
CKG-Apr313-E	22.49	-6.74	1.0294	29.01
		Average:	1.0294	28.97
		StDevp:	0.00	0.10

Table 2.5: Boron isotope compositions of aragonite synthesized from 0.7 mol kg^{-1} solution at 25 °C

Sample	Average pH	σ	$\delta^{11}B_{carb}$ (‰)
CKG-Oct511	8.52	0.03	24.81
CKG-Mar2112-C	8.51	0.02	24.62
CKG-Apr2712-D	8.56	0.04	24.50
CKG-Aug312-D2	8.99	0.05	31.26
CKG-Aug3012-E	8.49	0.03	24.45
CKG-Sept2512-D2	9.18	0.03	34.19
CKG-Oct2912-E	8.52	0.02	24.65
CKG-Oct2912-E2	8.49	0.03	24.65
CKG-Dec512-D	9.14	0.06	34.81
CKG-Dec512-D2	9.14	0.05	34.85
CKG-Dec1412-C	7.27	0.08	15.62
CKG-Feb2513-C	9.15	0.05	34.96
CKG-Feb2513-D	9.15	0.05	24.85
CKG-Feb2513-E	7.10	0.03	14.54
CKG-Apr313-C	7.31	0.13	14.94
CKG-Apr313-D	7.28	0.11	14.84
CKG-Apr313-E	7.32	0.12	14.86

σ = Standard deviation based on population (stdevp).

Table 2.6: Determining carbon isotope fractionation between dissolved inorganic carbon and aragonite in high ionic strength (0.7 mol kg^{-1}) conditions

Sample[a]	$\delta^{13}C_{aragonite}$ (‰)	$\delta^{13}C_{DIC}$ (‰)	$\alpha_{(aragonite\text{-}DIC)}$	$1000ln\alpha_{(aragonite\text{-}DIC)}$
CKG-Sept2512-D2-S	1.06	-2.06	1.0031	3.12
CKG-Sept2512-D2-E		-2.23	1.0031	3.12
CKG-Dec512-D-S	1.05	-2.01	1.0031	3.07
CKG-Dec512-D-E		-2.13	1.0032	3.19
CKG-Dec512-D2-S	1.17	-2.11	1.0033	3.28
CKG-Dec512-D2-E		-2.37	1.0035	3.54
CKG-Feb2513-C-S	1.20	-2.05	1.0033	3.26
CKG-Feb2513-C-S-E		-2.41	1.0036	3.62
CKG-Feb2513-D-S	1.08	-2.04	1.0031	3.12
CKG-Feb2513-D-E		-2.29	1.0034	3.37
		Average:	1.0033	3.26
		StDevp:	0.00	0.18

[a]At end of sample name, 'S' refers to values at start of experiment, and 'E' values at end of experiment.

Figures

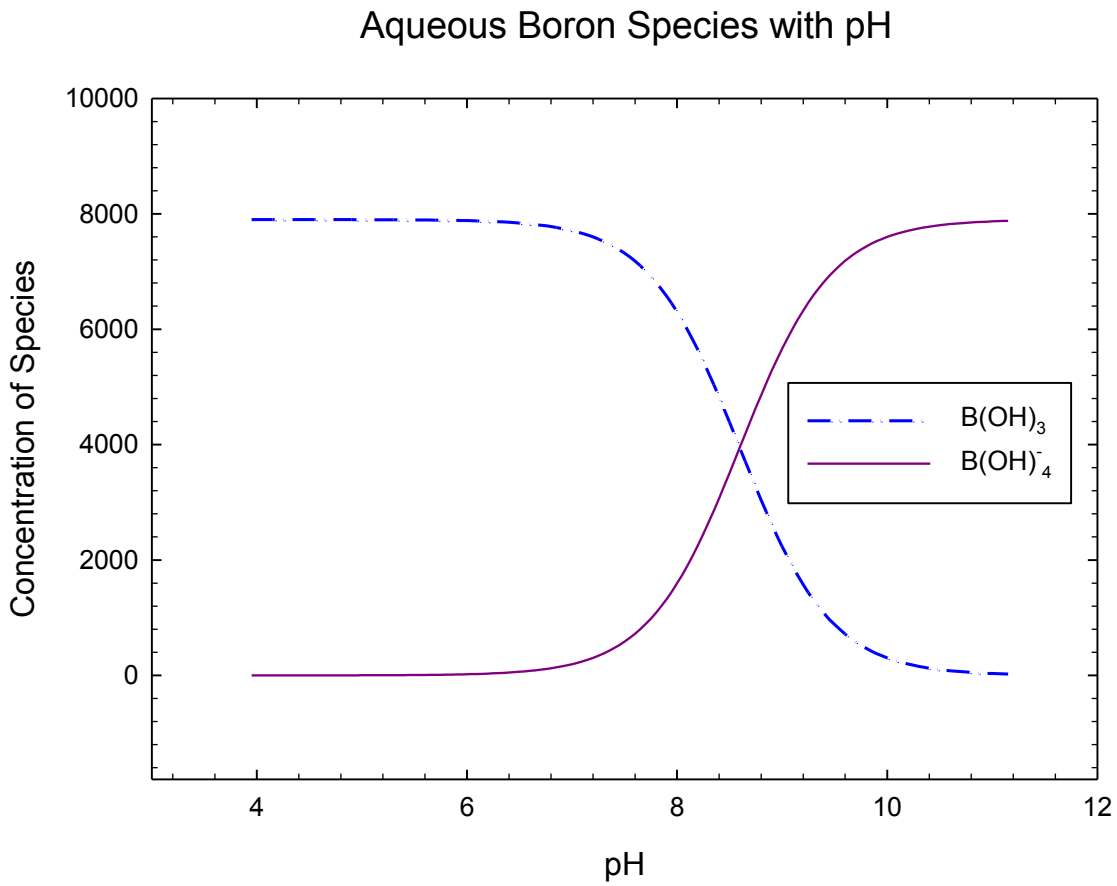

Figure 2.1: Distribution of aqueous boron species in seawater as a function of pH, $pK_B = 8.597$ at 25°C (Dickson, 1990).

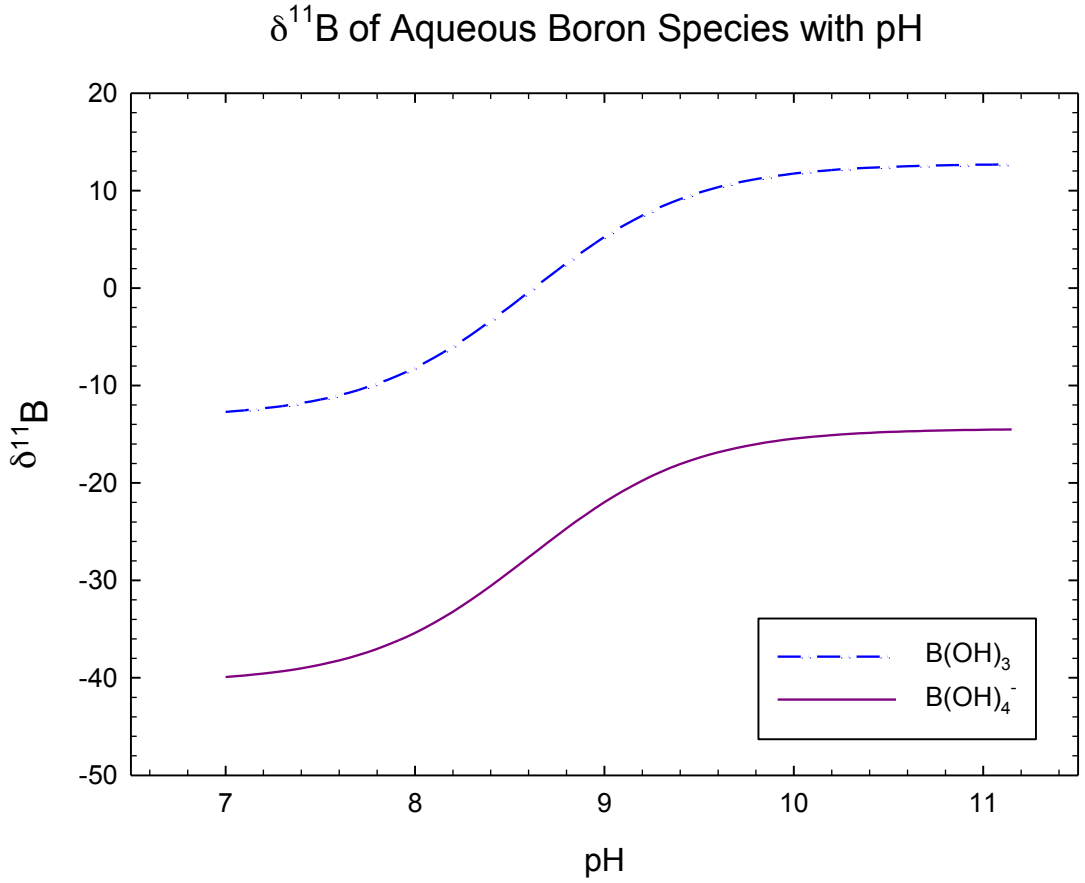

Figure 2.2: $\delta^{11}B$ of $B(OH)_3$ and $B(OH)_4^-$ in seawater as a function of pH ($^{11\text{-}10}K_B$ = 1.0272 (Klochko et al., 2006).

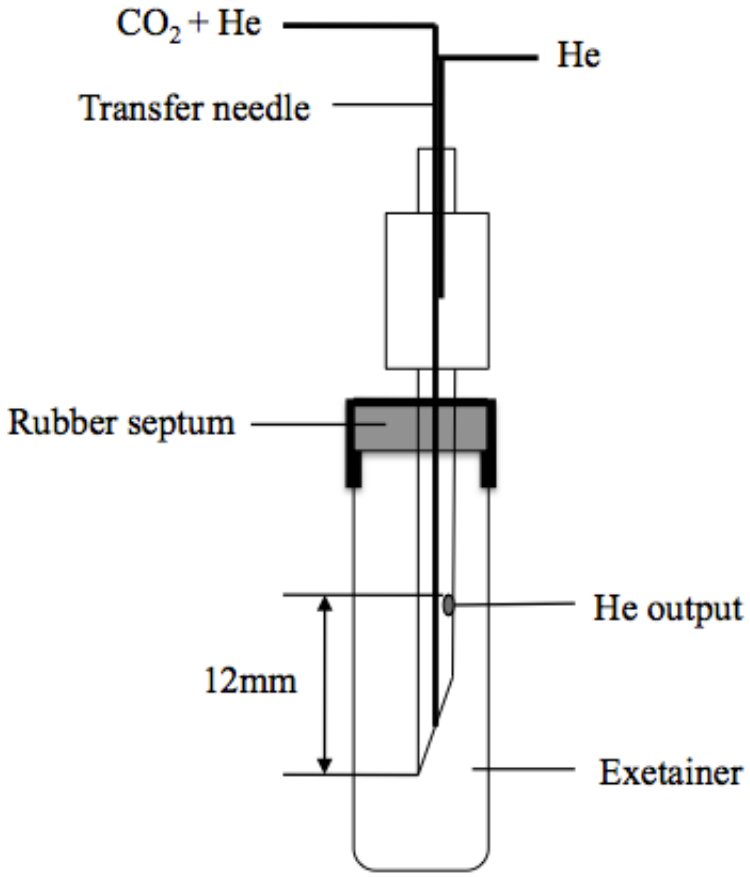

Figure 2.3: Diagram outlining the needle used to flush and fill the Exetainer® vials on the ThermoFinnigan Gas Bench II

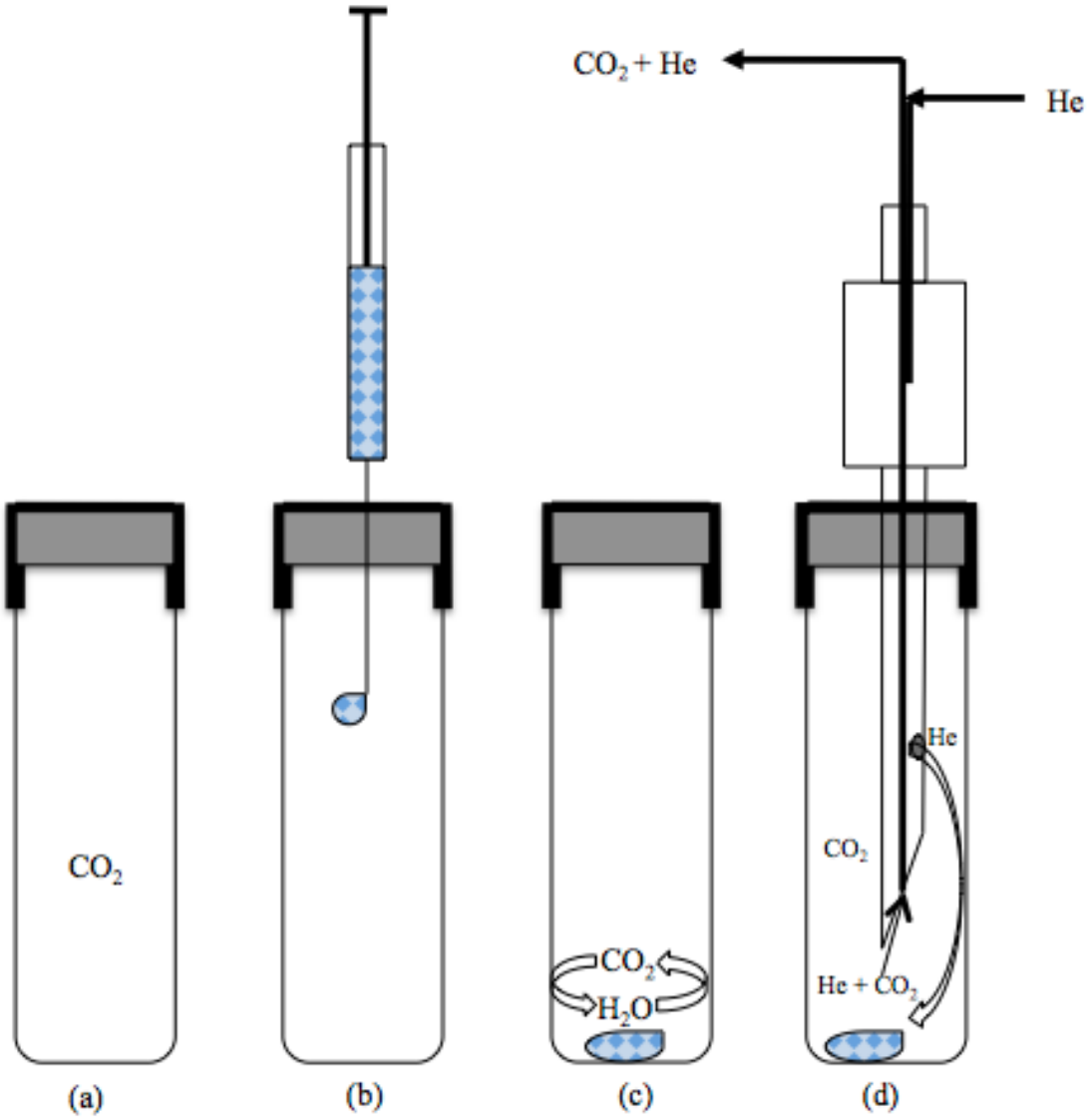

Figure 2.4: (a) After the Exetainer® has been flushed and filled with 0.2% CO_2 and 99.8% He, (b) water samples are added and (c) allotted a minimum of 27 hours to exchange and reach isotopic equilibrium at 25 ±0.1°C. After equilibration, (d) CO_2 in the headspace is sampled and the isotopic ratio is determined.

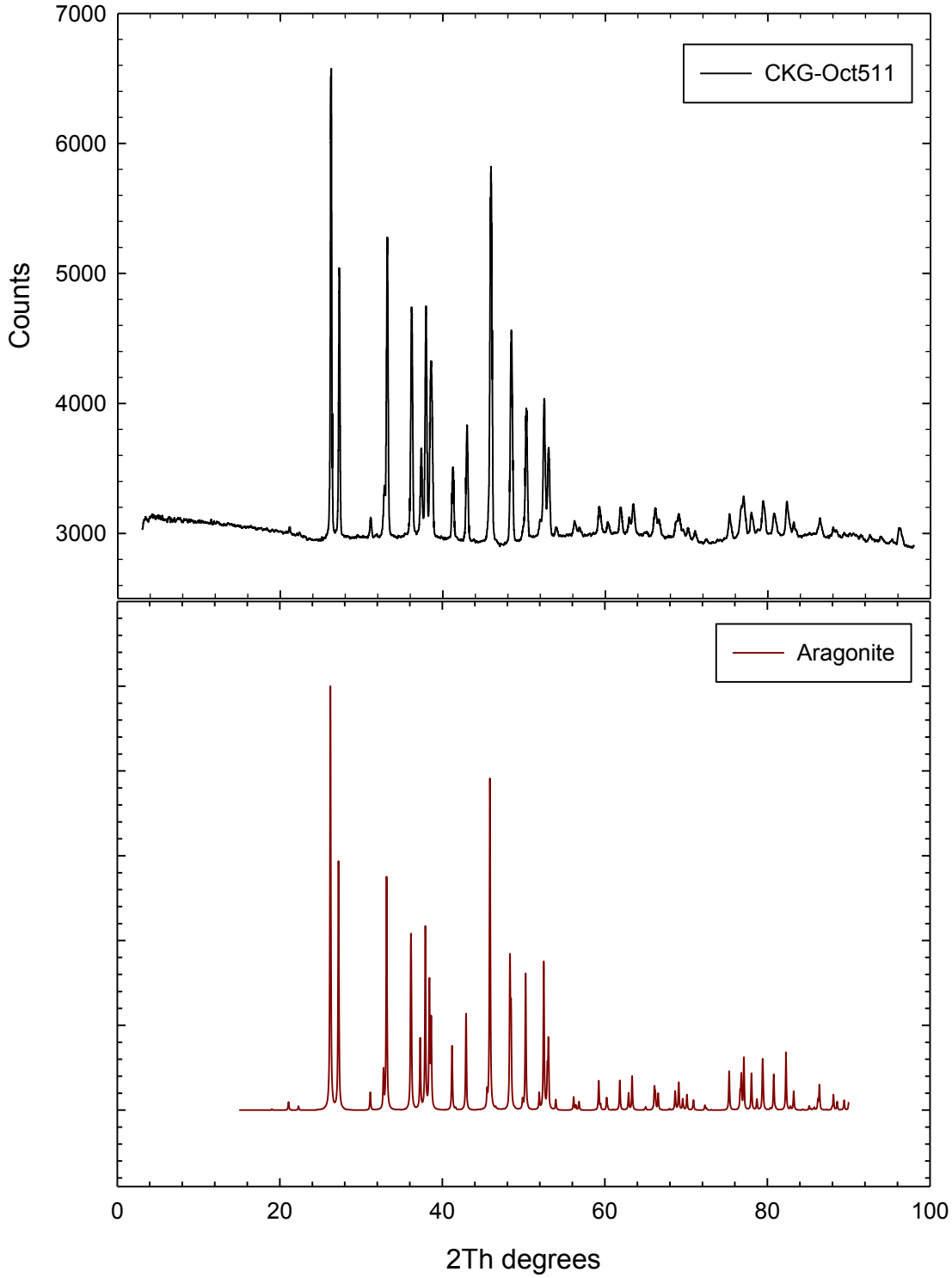

Figure 2.5: X-ray diffraction analysis confirming that calcium carbonate sample is 100% aragonite.

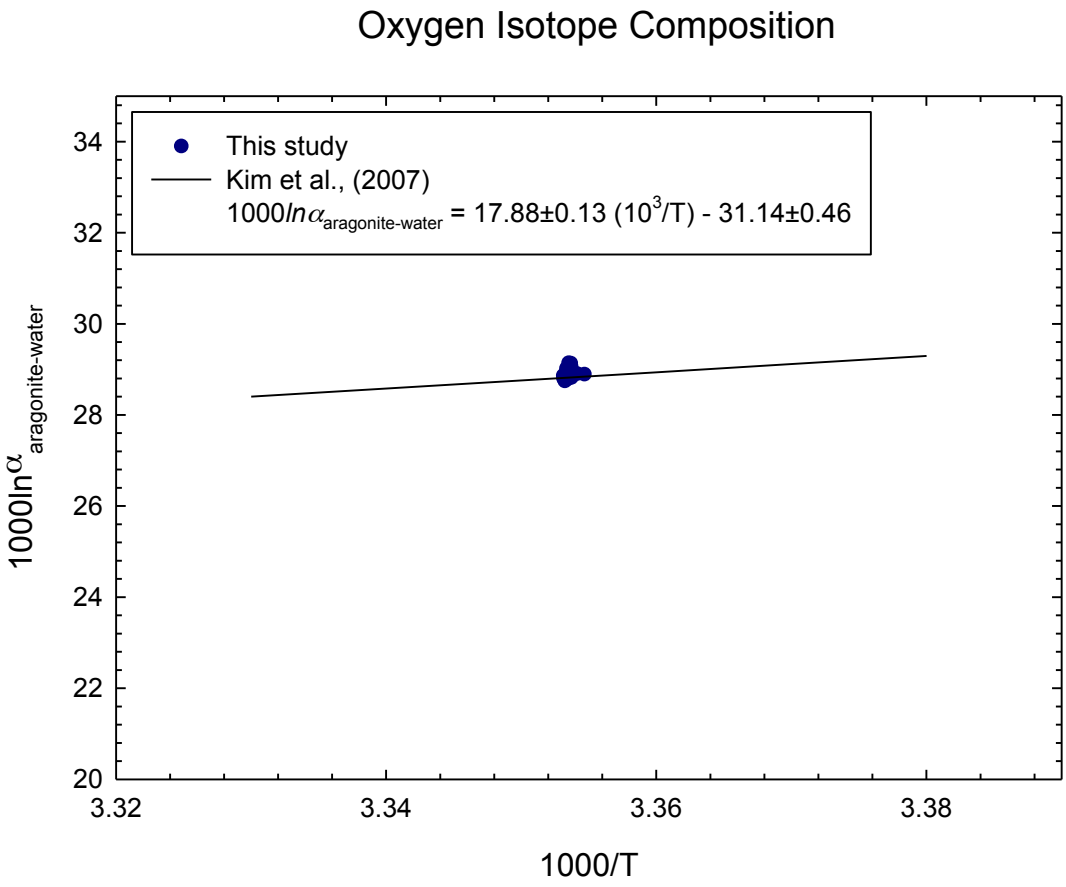

Figure 2.6: Oxygen isotope compositions of parent solution and precipitated aragonite confirm that experimental system was in isotopic equilibrium during synthesis.

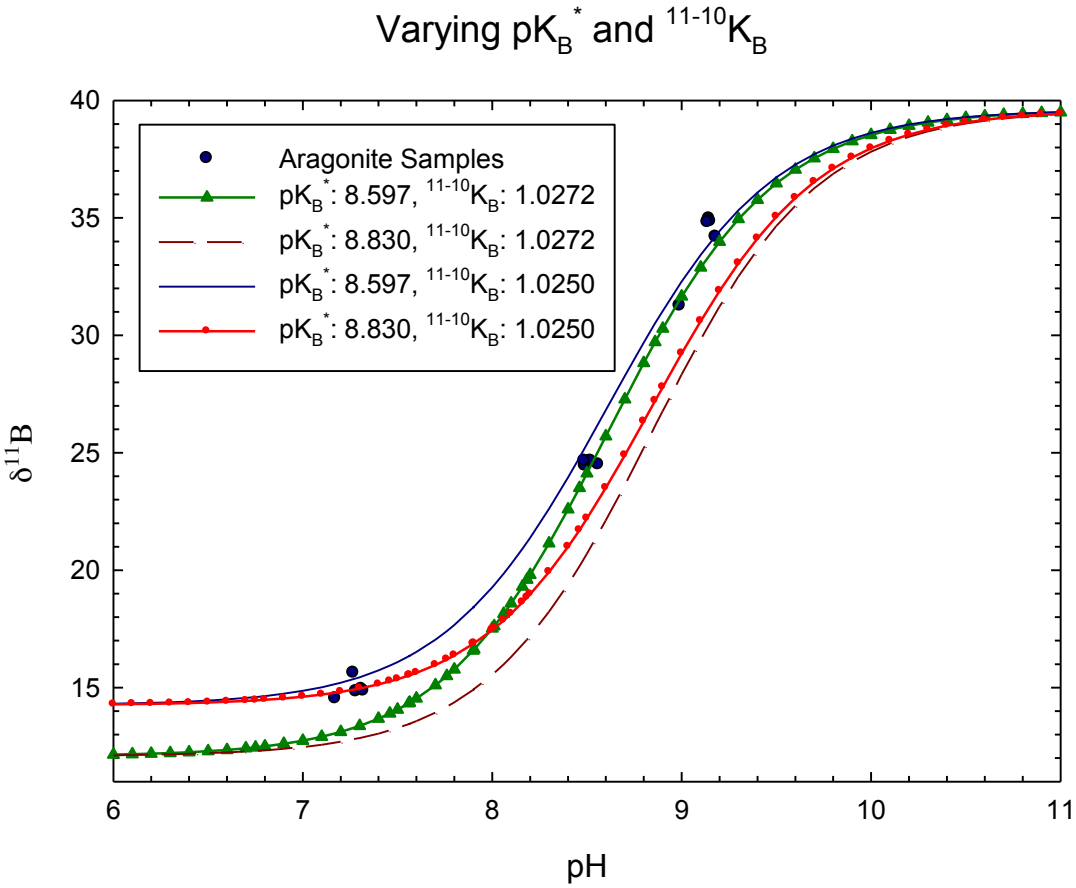

Figure 2.7: The boron isotope composition of synthetic aragonite against the boron isotope composition of seawater $B(OH)_4^-$ using the most correct values for $^{11\text{-}10}K_B$ including 1.0250 from 0.6 mol kg^{-1} H_2O KCl at 25 °C and 1.0272 from 0.7 mol kg^{-1} synthetic seawater (Klochko et al., 2006), as well as the most correct published pK_B^* values of 8.597 from 0.7 mol kg^{-1} synthetic seawater at 25 °C (Dickson, 1990) and 8.830 from 0.68 mol kg^{-1} pure NaCl solution (Hershey et al., 1986).

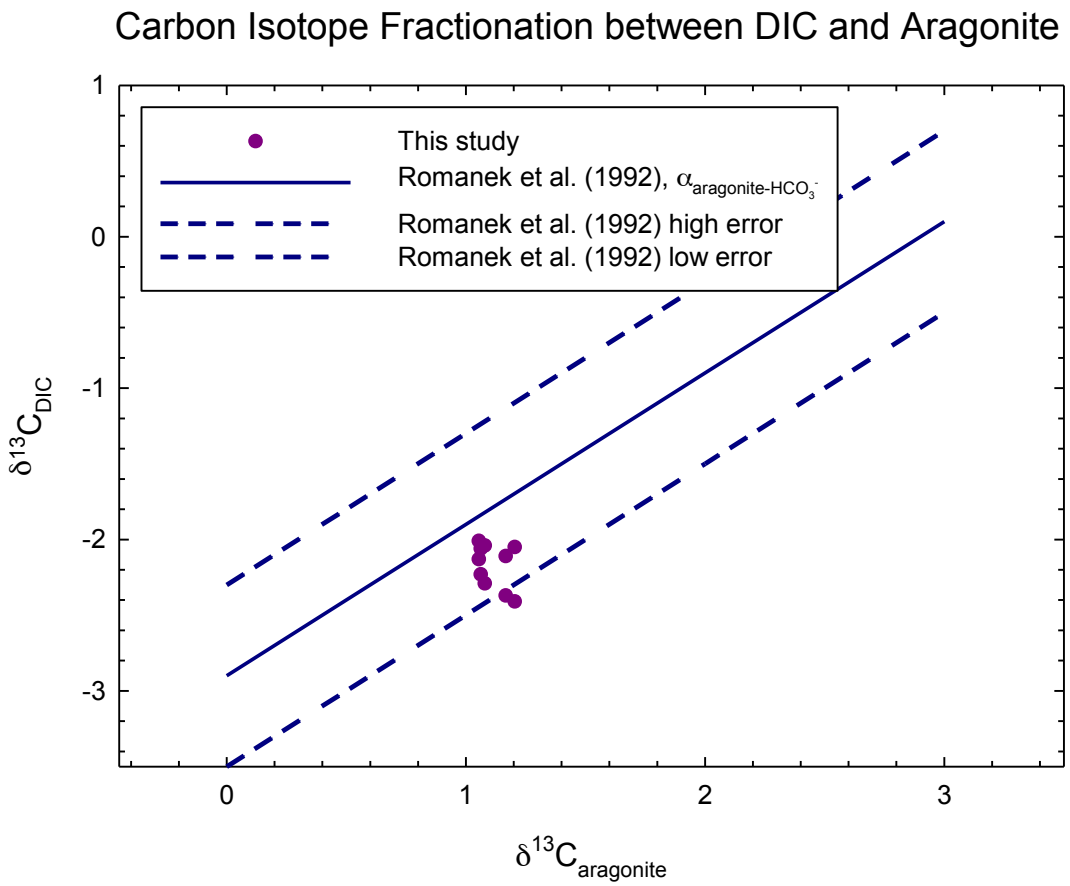

Figure 2.8: Comparing fractionation factors for carbon isotopes between aragonite and dissolved inorganic carbon at 25 °C using arbitrary values calculated with Romanek et al. (1992)'s fractionation factor of 2.9 ±0.6‰ for low ionic strength systems to the high ionic strength (0.7 mol kg^{-1}) systems utilized in this study.

Chapter 3: A new online technique for the simultaneous analysis of $\delta^{13}C$ of dissolved inorganic carbon (DIC) and $\delta^{18}O$ of water from a single solution sample using continuous flow isotope ratio mass spectrometry (CF-IRMS)

Christa D. Klein Gebbinck[a], Sang-Tae Kim[a], Martin Knyf[a], and Jillian Wyman[a]

[a]School of Geography and Earth Sciences, McMaster University, 1280 Main Street West, Hamilton, ON, L8S 4K1, Canada

Status: To be submitted to Rapid Communications in Mass Spectrometry

Abstract

RATIONAL: Accurate measurements of the oxygen isotope composition of water and carbon isotope composition of dissolved inorganic carbon are essential to understanding systematic processes occurring on Earth. In the past, these isotope compositions have been obtained through two separate analytical techniques that require a larger amount of sample and increased analysis time. In addition, developments to combine the measurements into one convenient technique utilize either elaborate offline hardware or complex calculations involving pH measurements.

METHODS: In this study, a new DIC-CO_2 Gas Equilibration Method, DIC-CO_2-GEM, was developed for simultaneous analysis of $\delta^{18}O_{H2O}$ and $\delta^{13}C_{DIC}$. The instrument employed was a Gas Bench II autosampler coupled with a Delta Plus XP isotope ratio mass spectrometer. In this method, 0.01 mL of 103% H_3PO_4 acid liberates CO_2 from 0.2 mL of a DIC-containing water sample and the mixture is equilibrated at a constant temperature for a minimum of 27 hours. The CO_2 is then sampled and both $\delta^{18}O_{H2O}$ and $\delta^{13}C_{DIC}$ are obtained.

RESULTS: The $\delta^{18}O_{H2O}$ values from this new method are precise and differ only slightly (<0.15‰) from previously obtained values using conventional methods. The $\delta^{13}C_{DIC}$ values obtained using the new method are also reproducible between replicates and comparable (<0.22 ‰) to those from traditional techniques. Using this new method, unknown DIC concentrations from samples can also be calculated within an acceptable error (~0.3 mmolal).

CONCLUSIONS: This new method is suitable for the direct measurement of both $\delta^{18}O_{H2O}$ and $\delta^{13}C_{DIC}$ simultaneously from small solution samples using CF-IRMS. In addition, the method is effective in determining the unknown DIC concentrations in sample solutions.

3.1 Introduction

The fundamental application of stable isotope analyses has greatly enhanced research outlining the mechanisms of Earth's processes both past and present. The oxygen isotope study of water reservoirs in the hydrosphere is important for understanding physiochemical processes in the water cycle, such as precipitation, evaporation, and condensation (Gat, 1996; Kendall and Coplen, 2001; Craig, 1961). The carbon isotope study of dissolved inorganic carbon (DIC) is essential to investigate biogeochemical cycling of carbon because it has been shown to effectively trace carbon sources and sinks, such as carbon from the ocean or that originated from the microbial respiration of organic matter (Kroopnick, 1985; e.g. Buhl et al., 1991; Blair et al., 1994; Quay et al., 1992). As a result, significant efforts have been made by numerous scientists to improve the analytical techniques for the oxygen isotope composition of water and the carbon isotope composition of DIC by reducing sample sizes and/or increasing analytical precisions (Tables 3.1 and 3.2).

For example, the oxygen isotope composition of water ($\delta^{18}O_{H2O}$) is typically measured using the CO_2-H_2O equilibration technique, which was developed by Cohn and Urey (1938) in the late nineteen thirties. This approach determines the oxygen isotope composition of CO_2 via isotope ratio mass spectrometry (IRMS) after CO_2 and H_2O are isotopically equilibrated at a constant temperature. Epstein and Mayeda (1953) modified Cohn and Urey's CO_2- H_2O equilibration technique and successfully studied the oxygen isotope ratio of natural waters.

Several improvements were made to the classic CO_2-H_2O equilibration technique over the past sixty years, the most significant of which are (1) the use of pre-evacuated glass vials (Socki et al., 1992) that could be disposed of after use and (2) equilibrating a small quantity of

CO_2 with a surplus of water such that the oxygen isotope composition of CO_2 is dictated by the oxygen isotope composition of water analyzed. Other approaches for the measurement of $\delta^{18}O_{H2O}$ include (1) conversion techniques, where water is converted to CO_2 by BrF_5, ClF_3, or guanidine hydrochloride, (2) pyrolysis, where water is converted to CO and H_2 at a high temperature, and (3) electrolysis, where water is transformed into oxygen gas using an electrolyte (i.e. $CuSO_4$) (see Table 3.1 for details).

The carbon isotope composition of DIC ($\delta^{13}C_{DIC}$) in aqueous solutions is often determined by either a direct precipitation method (e.g. Gleason et al., 1969) or a gas evolution method (e.g. Mook, 1968). The direct precipitation method involves the addition of a $SrCl_2$-NH_4OH or $BaCl_2$-NH_4OH solution directly to an aqueous sample, with subsequent instantaneous precipitation of $SrCO_3$ or $BaCO_3$. The carbonate is then filtered and dried in preparation for measuring its carbon isotope composition, which reflects the $\delta^{13}C_{DIC}$ of the aqueous sample. The direct precipitation method requires large sample sizes (Capasso et al., 2005), is tedious and time consuming, involving the preparation of $SrCl_2$-NH_4OH or $BaCl_2$-NH_4OH solution, filtering, and drying the precipitated carbonates prior to the isotopic analysis. In contrast, for the gas evolution method, the DIC in a water sample is converted to gaseous CO_2 by acidification (Atekwana and Krishnamurthy, 1998). The extracted CO_2 is then introduced to a mass spectrometer for isotopic analysis.

Most of the conventional off-line extraction methods described above have been adapted to comply with a new generation of isotope ratio mass spectrometry (IRMS). For instance, the introduction of gas-chromatography coupled with continuous-flow mass spectrometry (CF-IRMS) eliminates the cryogenic purification of CO_2 from water on a glass vacuum line in the classic CO_2-H_2O equilibration technique. In addition, a much smaller sample size is generally

required for the analysis of $\delta^{18}O_{H2O}$ as well as $\delta^{13}C_{DIC}$ in the on-line CF-IRMS compared to the conventional off-line and dual-inlet IRMS methods.

It should be noted that the oxygen isotope composition of water and the carbon isotope composition of DIC were analyzed separately in the methods discussed above. There have also been a few attempts to develop a single method to obtain both isotopic compositions. Graber and Aharon (1991) implemented an off-line extraction technique that required a custom vacuum line and used 0.3 mL of 100% phosphoric acid to extract CO_2 from a ~2 mL DIC-containing water sample. They isolated the liberated CO_2 immediately, without equilibration with water, for its carbon isotope composition via IRMS to determine $\delta^{13}C_{DIC}$. In addition, they applied a correction factor of -1.10‰ to the measured oxygen isotope composition of CO_2 to calculate $\delta^{18}O_{H2O}$. Yang and Jiang (2012) utilized an online version of the classic CO_2-H_2O equilibration method that also determined $\delta^{13}C_{DIC}$ by measuring the pH and temperature of the sample, and applying the carbon isotope fractionation factor between gaseous CO_2 and DIC.

This study aims to establish an analytical method in which $\delta^{18}O_{H2O}$ and $\delta^{13}C_{DIC}$ can be simultaneously determined from a single solution sample. In our DIC-CO_2 Gas Equilibration Method (DIC-CO_2-GEM), phosphoric acid (H_3PO_4) is added to a DIC-containing aqueous sample to liberate CO_2, which then equilibrates with the sample solution at a constant temperature of 25 °C. Upon completion, the isotopic compositions of the CO_2 gas are measured using CF-IRMS. The DIC-CO_2-GEM requires ~0.2 mL of sample solution for DIC concentrations tested in this study, ranging from 2 to 15 mmolal.

3.2 Experimental Methods

3.2.1 Preparation of DIC-CO_2-GEM standard solutions

Standard solutions containing DIC are required to determine both $\delta^{18}O_{H2O}$ and $\delta^{13}C_{DIC}$ of sample solutions. Six DIC-CO_2-GEM standard solutions were gravimetrically prepared with ACS grade sodium bicarbonate or sodium carbonate to concentrations from 5 to 10 mmolal. Of the six DIC-CO_2-GEM standard solutions, four were prepared with DIC-free deionized water (~18 MΩ cm), while isotopically light DIC-free iceberg water from Newfoundland, Canada was used for the other two standard solutions (Table 3.3). The deionized water and iceberg water were confirmed to be DIC-free, yielding no trace of CO_2, on the basis of the gas evolution method (Atekwana and Krishnamurthy, 1998).

In addition, two sets of secondary standard solutions of varying DIC concentrations (2, 5, 8, 10 and 15 mmolal) were prepared, one set with sodium bicarbonate ($NaHCO_3$: pH = ~8.28) and the other set with sodium carbonate (Na_2CO_3: pH = ~10.87). These secondary standard solutions were used not only to estimate the DIC concentration of sample solutions, but also to identify potential limitations of the DIC-CO_2-GEM in measuring $\delta^{18}O_{H2O}$ and $\delta^{13}C_{DIC}$ precisely.

3.2.2 Stable isotope compositions of DIC-CO_2-GEM standard solutions

3.2.2.1 Oxygen isotope composition: modified CO_2-H_2O equilibration technique

A modified version of the classic CO_2-H_2O equilibration technique was employed to determine the oxygen isotope compositions of the DIC-CO_2-GEM standard solutions using a Gas Bench II headspace autosampler (Thermo Finnigan, Bremen, Germany) with a Thermo Finnigan Delta plus XP isotope ratio mass spectrometer at McMaster University, Canada. Non-evacuated

Labco RK borosilicate Exetainer® round bottom vials (Labco Limited, Lampeter, United Kingdom), with dimensions of 104 mm by 15.5 mm and 12 mL and a screw cap, were used for CO_2 equilibration with the standard solutions. The Exetainer® vials were cleaned by soaking in 5% H_3PO_4 solution for 1-2 hours after each use, and then rinsed twice with hot tap water, four times with distilled water, twice with deionized water, and finally dried at 70 °C overnight. The caps were cleaned using neutral pH soap, then also rinsed multiple times with deionized water, and dried at room temperature. The screw cap was fitted with a new septa before each use.

In our modified CO_2-H_2O equilibration technique at McMaster University, Exetainer® vials were flushed and filled with a 0.2 % CO_2 and 99.8 % He mixture. A 0.2 mL aliquot of the standard solution was subsequently injected using a 1 mL syringe, equilibrated with CO_2 for a minimum of 27 hours at 25 ±0.1 °C, and finally the isotopic composition of CO_2 is analyzed using CF-IRMS.

3.2.2.2 Carbon isotope composition: gas evolution technique

The gas evolution method(Atekwana and Krishnamurthy, 1998) was used to obtain the carbon isotope compositions for all the DIC-CO_2-GEM standard solutions, as well as sample solutions, used in this study. Exetainer® vials were preloaded with 0.2 mL 103% H_3PO_4, capped with a new septa and then flushed with 99.999% He. The flushed vial is then injected with 0.2 mL of the standard solution using a 1 mL syringe. The H_3PO_4 reacted with DIC in the standard solution to quasi-instantaneously produce CO_2 that is equilibrated with the standard solution for a minimum of 27 hours at 25 ±0.1 °C, followed by the isotopic analysis using CF-IRMS.

3.2.3 Simultaneous measurement of $\delta^{18}O_{H2O}$ and $\delta^{13}C_{DIC}$ from the same aqueous solution: DIC evolved CO_2 gas equilibration method (DIC-CO_2-GEM)

3.2.3.1 Overall description

This study combines the modified CO_2-H_2O equilibration technique and gas evolution method to engineer the DIC-CO_2 Gas Equilibration Method (DIC-CO_2-GEM), employing CF-IRMS to analyze both $\delta^{18}O_{H2O}$ and $\delta^{13}C_{DIC}$ from a single solution sample. Using a 1 mL syringe, ~0.01 mL (1 drop = ~0.01 mL) of 103% H_3PO_4 is loaded into Exetainer® vials which are then capped and flushed with 99.999% He. After flushing with pure He gas, Exetainer® vials are injected with 0.2 mL DIC-containing solution sample using 1 mL syringes. The DIC in the solution reacts with the H_3PO_4 and is subsequently converted to CO_2. The DIC is composed of three carbonic acid species: H_2CO_3, HCO_3^-, and CO_3^{2-}, with the dominant species being dictated by the pH of the solution. By lowering the pH of the sample solution below 1, the equilibrium will shift towards gaseous CO_2 (Graber and Aharon, 1991). The evolved CO_2 gas in the headspace is equilibrated with the solution sample for a minimum of 27 hours at 25 ±0.1 °C before isotopic analysis (Figure 3.1).

3.2.3.2 Normalization of raw data: $\delta^{18}O_{H2O}$

To normalize the oxygen isotope composition of the sample solution from raw isotope data, six DIC-CO_2-GEM standard solutions (see section 3.2.1. for details) were analyzed with the sample solutions. At the beginning and end of each run, duplicates of Exetainer® vials containing only 0.2 % CO_2 and 99.8 % He were analyzed to compare the start and end isotopic composition of the reference gas and no shift in carbon or oxygen isotope compositions was observed. The oxygen isotope compositions of the standard solutions were pre-determined with the modified

CO_2-H_2O equilibration technique described in Section 3.2.2.1. For DIC-CO_2-GEM, it is essential that the standard solutions be treated the same way as the sample solutions as described in Section 3.2.3.1.

3.2.3.3 Normalization of raw data: $\delta^{13}C_{DIC}$

The carbon isotope compositions of the sample solutions were normalized to the $\delta^{13}C$ values of the DIC-CO_2-GEM standard solutions in combination with NBS 18 (-5.01 ‰) and NBS 19 (+1.95 ‰). The carbon isotope compositions of the DIC-CO_2-GEM standard solutions were determined through isotopic analysis of $NaHCO_3$ or Na_2CO_3 salts used for the preparation of the standard solutions via VG OPTIMA isotope ratio mass spectrometer (VG Analytical, Manchester, England) equipped with an ISOCARB common acid bath system at 90 °C. For each DIC-CO_2-GEM sequence, ~150 µg of NBS 18 and NBS 19 were pre-loaded into Exetainer® vials, capped and flushed with 99.999 % He. Upon completion, ~0.1 mL (10 drops = ~0.1 mL) 103 % H_3PO_4 was injected to the side of the vial using a 1 mL syringe. The acid retreated down the side of the vial and reacted with carbonate standards to produce CO_2 for isotopic analysis (Figure 3.2). The duplicates of NBS 18 and NBS 19 analyzed at the beginning of each run were in agreement with those at the end. Reports of shifts in $\delta^{18}O$ of carbonate as a function of reaction time with the phosphoric acid in a previous study (Révész and Landwehr, 2002) were not observed at the reaction temperature of 25 °C used in this study.

3.3 Results and Discussion

3.3.1 Initial development of DIC-CO_2-GEM

3.3.1.1 Influence of acid on oxygen isotope exchange kinetics between CO_2 and H_2O

The oxygen isotope compositions of MRSI-DIC-STD-1, MRSI-DIC-STD-2, and MRSI-DIC-STD-3 are -6.75‰, -6.74‰, and -6.56‰, respectively (Table 3.4). However, they were determined to be -6.05‰, -5.98‰, and -8.23‰ when 0.2 mL H_3PO_4 was used in an early stage of DIC-CO_2-GEM development. The deviation in the oxygen isotope compositions from the actual isotopic composition of the DIC-CO_2-GEM standard solutions was investigated by testing the effect of acid on oxygen isotope exchange between CO_2 and DIC-free water. The DIC-CO_2-GEM, outlined in Section 3.2.3.1, was used for this examination except that Exetainer® vials were flushed with the CO_2-He gas mixture, instead of pure He gas. Two types of DIC-free water, deionized water at McMaster University and iceberg water from Newfoundland, Canada, were utilized. Figure 3.3 and Table 3.5 show that as the amount of the acid increases, the oxygen isotope composition of CO_2 that was equilibrated with either the deionized water or the iceberg water, becomes closer to the initial oxygen isotope composition of CO_2 (-4.70‰) used for the equilibration. This suggests that the rate of oxygen isotope exchange between CO_2 and water significantly decreases as the amount of acid pre-loaded into the vial increases. This trend is not obvious for iceberg water because the oxygen isotope composition of the initial CO_2 is very close to the oxygen isotope composition of CO_2 that was equilibrated with the iceberg water without the addition of acid.

The isotopic exchange reaction between aqueous and gaseous CO_2 constitutes the rate-determining step in the hydration of CO_2, with the rate being influenced by a variety of factors including the chemical composition of samples and solution pH. Mills and Urey (1940) alluded

to the relationship between pH and oxygen isotope exchange, however to the best of knowledge, no prior study has acknowledged that there may be implications if pH is significantly decreased. It has become apparent from Figure 3 that a high amount of H_3PO_4 may shift all carbonic acid species to gaseous CO_2, and as a result, there is no aqueous CO_2 available for oxygen isotope exchange with the gaseous CO_2.

3.3.1.2 Optimization of acid volume for DIC-CO_2-GEM

The amount of H_3PO_4 utilized proved to be an important parameter to ensure the precision and accuracy of $\delta^{18}O_{H2O}$ measurement. Table 3.4 shows that a decrease in the amount of H_3PO_4 pre-loaded into the Exetainer® vial displayed a better agreement between the two techniques (described in Sections 3.2.2.1. and 3.2.3.1.). For example, in the early test using 0.2 mL acid, the oxygen isotope composition of MRSI-DIC-STD-3 was -8.23‰ and with a decrease in the amount of H_3PO_4 to 0.05 mL and 0.01 mL of H_3PO_4 the oxygen isotope composition was -6.84‰ and -6.64‰, respectively (see Table 3.4). It was noted that using 0.01 mL of H_3PO_4 acid to liberate CO_2 from the standard and sample solutions achieved better reproducibility for $\delta^{18}O_{H2O}$ between replicates, less than 0.1‰, than trials using 0.05 mL of H_3PO_4 acid, where standard deviations averaged 0.18‰ (Table 3.4). As a result, the optimal amount of H_3PO_4 for DIC-CO_2-GEM is 0.01 mL.

3.3.1.3 Effect of acid amount on $\delta^{13}C_{DIC}$

The amount of H_3PO_4 pre-loaded into the Exetainer® vials tested throughout DIC-CO_2-GEM development did not significantly affect $\delta^{13}C_{DIC}$ (Table 3.4) because as the pH is reduced below 1, the chemical equilibrium among dissolved carbon species in solution shifts so that

gaseous CO_2 becomes the dominant species and its carbon isotope composition reflects $\delta^{13}C_{DIC}$. The reduction of pH below 1 was verified with litmus paper after all amounts of acid tested during method development, from 0.01 to 0.6 mL, on various samples after DIC-CO_2-GEM analysis.

The slight shift in carbon isotope compositions of standard solutions that can be seen in Table 3.4, for example from -26.33‰ with 0.2 mL H_3PO_4 to -25.91‰ with 0.01 mL in MRSI-DIC-STD-1, is likely due to degassing of CO_2 from the solution over time. The analysis of $\delta^{13}C_{DIC}$ with 0.2 mL of H_3PO_4 was completed shortly after solution preparation, whereas tests with 0.01 mL of acid were conducted approximately five months afterwards. It should be noted that standard solutions should be prepared regularly in large volumes and the exposure to atmospheric CO_2 minimized to reduce CO_2 degassing.

3.3.2 DIC-CO_2-GEM compared to conventional methods

3.3.2.1 DIC-CO_2-GEM vs. the classical CO_2-H_2O equilibration technique: Oxygen isotopes

The reliability of DIC-CO_2-GEM was determined by comparing $\delta^{18}O_{H2O}$ of sample solutions obtained using DIC-CO_2-GEM to those previously determined using the modified CO_2-H_2O equilibration technique. The results obtained by DIC-CO_2-GEM are consistent with those from the conventional technique with closest results being ±0.00‰ and the largest difference being ±0.15‰ (Table 3.7). Therefore, DIC-CO_2-GEM is a viable alternative to the classical CO_2-H_2O equilibration technique.

3.3.2.2 DIC-CO_2-GEM vs. the Gas evolution method: Carbon isotopes

The effectiveness of DIC-CO_2-GEM for carbon isotope analysis was quantified by comparing obtained $\delta^{13}C_{DIC}$ values to those determined using the gas evolution method. Taking into consideration the shift in $\delta^{13}C_{DIC}$ over time in standard solutions (described in Section 3.3.1.3.), the gas evolution method was completed a second time, within a week of DIC-CO_2-GEM analysis, for sample solutions that had been stored, in order to eliminate discrepancies due to potential shifts in carbon isotope compositions of DIC over time. The results between the two methods are consistent, with $\delta^{13}C_{DIC}$ from DIC-CO_2-GEM differing from the gas evolution method by ±0.00‰ to ±0.22‰ and with a precision for DIC-CO_2-GEM of ±0.17‰ (Table 3.8). The DIC-CO_2-GEM is a practical substitute to the gas evolution method.

3.3.3 Determination of DIC concentrations in samples

The DIC concentrations of samples can be estimated using the secondary standard solutions containing 2 to 15 mmolal of DIC. The known concentrations of DIC are used to calibrate an equation that relates the amount of CO_2 liberated from the water sample by H_3PO_4 to mmolal of DIC in the aqueous solution (Figure 3.4). While this approach may not be as precise compared to methods curbed for this analysis (e.g. coulometry, Johnson et al., 1985), it is capable of determining concentrations within a maximum error of ±0.7 mmolal, with the average error within ±0.3 mmolal, which is acceptable for many applications.

3.4 Conclusions

The oxygen isotope composition of water and carbon isotope composition of dissolved inorganic carbon are traditionally determined through two separate methods, requiring greater

analysis time and sample sizes. In many instances, specifically where sample size is limited, it is desirable to maximize the yield of information while minimizing resources. By combining fundamental principles associated with the modified CO_2-H_2O equilibration technique and the gas evolution method, often used to obtain $\delta^{18}O_{H2O}$ and $\delta^{13}C_{DIC}$ values respectively, the DIC-CO_2-GEM accurately obtains both parameters in a single analysis.

This novel approach uses a small amount of 103% phosphoric acid to liberate CO_2 from a DIC-containing solution sample. In this study, 0.01mL of H_3PO_4 was sufficient for analysis of solutions containing 2 to 15 mmolal of DIC. The $\delta^{18}O_{H2O}$ reproducibility is acceptable at less than 0.1‰, as well as for $\delta^{13}C_{DIC}$, 0.17‰, and both are consistent to the conventional approaches, ±0.00‰ to ±0.15‰ for $\delta^{18}O_{H2O}$ compared to our modified CO_2-H_2O equilibration technique and ±0.00‰ to ±0.22‰ for $\delta^{13}C_{DIC}$ versus the gas evolution method.

The method developed in this study, termed the DIC-CO_2-GEM, utilizes CF-IRMS to directly measure the $\delta^{18}O_{H2O}$ and $\delta^{13}C_{DIC}$ from solution samples simultaneously. Determination of these values in a single analysis is an advantage in terms of revealing more information while reducing sample sizes, instrumental use, and time. The generation of more data from one small sample will benefit many practical applications.

References

Atekwana E. and Krishnamurthy R. (1998) Seasonal variations of dissolved inorganic carbon and $\delta^{13}C$ of surface waters: application of a modified gas evolution technique. *Journal of Hydrology* **205,** 265-278.

Blair N. E., Plaia G. R., Boehme S. E., DeMaster D. J. and Levin L. A. (1994) The remineralization of organic carbon on the North Carolina continental slope. *Deep Sea Research Part II: Topical Studies in Oceanography* **41,** 755-766.

Brand W., Tegtmeyer A. and Hilkert A. (1994) Compound-specific isotope analysis: Extending toward $^{15}N/^{14}N$ and $^{18}O/^{16}O$. *Org. Geochem.* **21,** 585-594.

Buhl D., Neuser R., Richter D., Riedel D., Roberts B., Strauss H. and Veizer J. (1991) Nature and nurture: environmental isotope story of the river Rhine. *Naturwissenschaften* **78,** 337-346.

Burns S. J. (1998) Carbon isotopic evidence for coupled sulfate reduction-methane oxidation in Amazon Fan sediments. *Geochim. Cosmochim. Acta* **62,** 797-804.

Capasso G., Favara R., Grassa F., Inguaggiato S. and Longo M. (2005) On-line technique for preparation and measuring stable carbon isotope of total dissolved inorganic carbon in water samples ($\delta^{13}C_{TDIC}$). *Annals Geophysics* **48,** 159-166.

Cohn M. and Urey H. C. (1938) Oxygen exchange reactions of organic compounds and water. *J. Am. Chem. Soc.* **60,** 679-687.

Craig H. (1961) Isotopic variations in meteoric waters. *Science* **133,** 1702-1703.

Dugan Jr J. P., Borthwick J., Harmon R. S., Gagnier M. A., Glahn J. E., Kinsel E. P., MacLeod S., Viglino J. A. and Hess J. W. (1985) Guanidine hydrochloride method for determination of water oxygen isotope ratios and the oxygen-18 fractionation between carbon dioxide and water at 25 C. *Anal. Chem.* **57,** 1734-1736.

Epstein S. and Mayeda T. (1953) Variation of $^{18}O/^{16}O$ content of waters from natural sources. *Geochim. Cosmochim. Acta* **4,** 213-224.

Fessenden J. E., Cook C. S., Lott M. J. and Ehleringer J. R. (2002) Rapid ^{18}O analysis of small water and CO_2 samples using a continuous-flow isotope ratio mass spectrometer. *Rapid Communications in Mass Spectrometry* **16,** 1257-1260.

Gat J. R. (1996) Oxygen and hydrogen isotopes in the hydrologic cycle. *Annu. Rev. Earth Planet. Sci.* **24,** 225-262.

Gleason J. I. M. D., Friedman I. and HANSHAW B. B. (1969) Extraction of dissolved carbonate species from natural water for carbon-isotope analysis.

Graber E. and Aharon P. (1991) An improved microextraction technique for measuring dissolved inorganic carbon (DIC), $\delta^{13}C_{DIC}$ and $\delta^{18}O_{H2O}$ from milliliter-size water samples. *Chemical geology.Isotope geoscience section* **94,** 137-144.

Johnson K. M., King A. E. and Sieburth J. M. (1985) Coulometric TCO_2 analyses for marine studies; an introduction. *Mar. Chem.* **16,** 61-82.

Kendall C. and Coplen T. B. (2001) Distribution of oxygen-18 and deuterium in river waters across the United States. *Hydrol. Process.* **15,** 1363-1393.

Kroopnick P. (1974) The dissolved O_2-CO_2-^{13}C system in the eastern equatorial Pacific. **21,** 211-227.

Kroopnick P. (1985) The distribution of ^{13}C of ΣCO_2 in the world oceans. *Deep Sea Research Part A. Oceanographic Research Papers* **32,** 57-84.

Meijer H. and Li W. (1998) The use of electrolysis for accurate $\delta^{17}O$ and $\delta^{18}O$ isotope measurements in water. *Isotopes Environ. Health Stud.* **34,** 349-369.

Mills G. A. and Urey H. C. (1940) The Kinetics of Isotopic Exchange between Carbon Dioxide, Bicarbonate Ion, Carbonate Ion and Water. *J. Am. Chem. Soc.* **62,** 1019-1026.

Miyajima T., Yamada Y., Hanba Y. T., Yoshii K., KOITABASHI K. and Wada E. (1995) Determining the stable isotope ratio of total dissolved inorganic carbon in lake water by GC/C/IRMS. *Limnol. Oceanogr.* **40,** 994-1000.

Mook W. G. (1968) *Geochemistry of the stable carbon and oxygen isotopes of natural waters in the Netherlands.*

O'Neil J. R. and Epstein S. (1966) A method for oxygen isotope analysis of milligram quantities of water and some of its applications. *Journal of Geophysical Research* **71,** 4955-4961.

Quay P. D., Wilbur D. O., Richey J. E., Hedges J. I. and Devol A. H. (1992) Carbon Cycling in the Amazon River: Implications from the $\delta^{13}C$ Compositions of Particles and Solutes. *Limnol. Oceanogr.* **37,** 857-871.

Révész K. M. and Landwehr J. M. (2002) $\delta^{13}C$ and $\delta^{18}O$ isotopic composition of $CaCO_3$ measured by continuous flow isotope ratio mass spectrometry: statistical evaluation and verification by application to Devils Hole core DH-11 calcite. *Rapid Communications in Mass Spectrometry* **16,** 2102-2114.

Socki R. A., Karlsson H. R. and Gibson Jr E. K. (1992) Extraction technique for the determination of oxygen-18 in water using preevacuated glass vials. *Anal. Chem.* **64,** 829-831.

Taylor C. and Fox V. (1996) An isotopic study of dissolved inorganic carbon in the catchment of the Waimakariri River and deep ground water of the North Canterbury Plains, New Zealand. *Journal of Hydrology* **186,** 161-190.

Torres M. E., Mix A. C. and Rugh W. D. (2005) Precise $\delta^{13}C$ analysis of dissolved inorganic carbon in natural waters using automated headspace sampling and continuous-flow mass spectrometry. *Limnol.Oceanogr.: Methods* **3,** 349-360.

Yang T. and Jiang S. (2012) A new method to determine carbon isotopic composition of dissolved inorganic carbon in seawater and pore waters by CO_2-water equilibrium. *Rapid Communications in Mass Spectrometry* **26,** 805-810.

Tables

Table 3.1: Variations in methods of measuring $\delta^{18}O$ of water samples

References	Method	Principle of Method	Sample Size (µL)	Precision (‰, 1σ)
Epstein and Mayeda, 1953	Equilibration	CO_2-H_2O equilibration on custom glass extraction line	2500	0.1
O'Neil and Epstein, 1966	Conversion	Using BrF_5 or ClF_3 to convert H_2O directly to CO_2	5-10	0.1-0.2
Dugan et al., 1985	Conversion	React H_2O with guanidine hydrochloride to convert directly to CO_2	10	0.078
Brand et al., 1994	Conversion	Pyrolysis of H_2O to CO using CF-MS	2-10	0.2-0.3
Meijer and Li, 1998	Electrolysis	$CuSO_4$ used as electrolyte to convert H_2O to O_2	1000	0.1
Fessenden et al., 2002	Equilibration	CO_2-H_2O equilibration using CF-IRMS	>100	0.12
This study	Equilibration	Acidification and CO_2-H_2O equilibration using CF-IRMS	200	0.15

Table 3.2: Variations in methods of measuring $\delta^{13}C$ of dissolved inorganic carbon (DIC)

References	Method	Principle of Method	Sample Size (mL)	Precision (‰, 1σ)
Mook, 1968	Gas Evolution	Convert DIC to CO_2 by acidification with H_3PO_4 acid on vacuum line and analyze with dual inlet mass spectrometry	5-10	0.1
Gleason et al., 1969	Precipitation	Precipitate DIC as carbonate by adding $SrCl_2$-NH_4OH, $BaCl_2$-NaOH or $Ba(OH)_2$	20-1000	0.1
Kroopnick, 1974	Gas Evolution	Convert DIC to CO_2 by acidification with H_3PO_4 acid offline and strip with nitrogen, analyze with dual inlet mass spectrometry	250	0.04
Taylor and Fox, 1996	Precipitation and Gas Evolution	Precipitate DIC, collect, dry, and react with H_3PO_4 to simultaneously determine DIC concentration and $\delta^{13}C_{DIC}$	300-1000	0.1
Miyajima et al., 1995	Vapour Phase Equilibrium	Acidify sample with HCl to liberate $CO_{2(g)}$ for analysis on gas chromatograph and use mass balance to calculate $\delta^{13}C$ of sample	68	0.1
Burns, 1998	Gas Evolution	Convert DIC to CO_2 by acidification with H_3PO_4 acid on vacuum line and analyze with dual inlet mass spectrometry	~2	0.04
Torres et al., 2005	Gas Evolution	Convert DIC to CO_2 by acidification with H_3PO_4 acid online and analyze using CF-IRMS	0.3-0.5	0.04
This study	Gas Evolution	Convert DIC to CO_2 by acidification with H_3PO_4 acid online, equilibrate, and analyze using CF-IRMS	0.2	0.22

Table 3.3: Details of laboratory standards used in this study

Standard Name	Water used	$\delta^{18}O_{H2O}$ (‰)	σ	Carbonate Used[c]	$\delta^{13}C_{salt}$ (‰)	σ	DIC conc. (mmolal)
MRSI-DIC-STD-1	Deionized water	-6.75	0.00	$NaHCO_3$-A	-25.81	0.18[d]	5
MRSI-DIC-STD-2	Deionized water	-6.74	0.01	$NaHCO_3$-C	-2.56	0.07	5
MRSI-DIC-STD-3	Deionized water	-6.56	0.06	Na_2CO_3-A	-1.99	0.13[d]	10
MRSI-DIC-STD-4	Deionized water	-6.76	0.01	Na_2CO_3-A	-1.99	0.13[d]	6
MRSI-ICEBERG-1	Iceberg water[b]	-30.38	0.03	$NaHCO_3$-A	-25.81	0.18[d]	5
MRSI-ICEBERG-2	Iceberg water[b]	-30.38	0.03	Na_2CO_3-A	-1.99	0.13[d]	5
MRSI-STD-W1[a]	Deep Sea water	-0.58	0.02	n/a	n/a	n/a	n/a

σ = Standard deviation of population.

conc. = Concentration.

[a]McMaster Research Group for Stable Isotopologues (MRSI) laboratory standard.

[b]Iceberg located off coast of Newfoundland, Canada.

[c]A and C indicate the specific salt added.

[d]Excludes 1σ outliers.

Table 3.4: Testing the potential effects of various amounts of acid on measured oxygen and carbon isotope compositions

Name	DIC-CO_2-GEM																Previous Methods	
	$\delta^{18}O_{H2O}$ (‰)									$\delta^{13}C_{DIC}$ (‰)									$\delta^{18}O_{H2O}$ (‰)[b]	$\delta^{13}C$ (‰)[c]
	Amount of H_3PO_4 added (mL)									Amount of H_3PO_4 added (mL)										
	0.2	σ	*n*	0.05	σ	*n*	0.01	σ	*n*	0.2	σ	*n*	0.05	σ	*n*	0.01	σ	*n*		
Standards																				
MRSI-DIC-STD-1	-6.05	0.38	7	-6.59	0.17	8	-6.74	0.12	17	-25.91	0.07	7	-26.14	0.07	8	-26.33	0.08	17	-6.75	-25.81
MRSI-DIC-STD-2	-5.98	0.30	7	-6.81	0.08	2	-6.78	0.18	14	-2.64	0.08	7	-2.57	0.06	2	-2.43	0.06	14	-6.74	-2.56
MRSI-DIC-STD-3	-8.23	0.09	7	-6.84	0.35	4	-6.64	0.05	10	-2.05	0.06	7	-2.04	0.05	4	-1.98	0.13	10	-6.56	-1.99
MRSI-DIC-STD-4	–	–	–	-6.75	0.05	4	-6.76	0.07	17	–	–	–	-2.46	0.03	4	-2.48	0.19	17	-6.76	-1.99
MRSI-ICEBERG-1	-29.57	0.06	4	-30.26	0.22	8	-30.37	0.06	17	-25.78	0.02	4	-25.34	0.12	8	-25.11	0.28	17	-30.38	-25.81
MRSI-ICEBERG-2	-31.24	0.04	2	-30.53	0.26	6	-30.39	0.09	17	-2.23	0.06	2	-2.37	0.13	6	-2.55	0.31	17	-30.38	-1.99
MRSI-STD-W1[a]	-0.59	0.87	7	-0.60	0.07	6	-0.58	0.09	9	n/a	–	–	n/a	–	–	n/a	–	–	-0.58	n/a
Samples																				
#CKG-Sept2512-D2-S	–	–	–	-6.53	0.26	8	-6.51	0.04	8	–	–	–	-2.43	0.07	8	-2.41	0.17	8	-6.59	-2.37
#CKG-Oct2912-E-E	–	–	–	-6.44	0.22	8	-6.52	0.04	8	–	–	–	-18.23	0.06	8	-17.80	0.09	8	-6.49	-17.80
#CKG-Apr313-D-E	–	–	–	-6.53	0.18	8	-6.71	0.05	8	–	–	–	-20.48	0.06	8	-20.13	0.09	8	-6.73	-19.95

σ = Standard deviation based on population (stdevp).

n = number of samples.

[a]McMaster Research Group for Stable Isotopologues (MRSI) laboratory standard.

[b]Determined using CO_2-H_2O equilibration technique (Section 2.2.1.).

[c]For standard solutions determined via IRMS of salt used (Section 2.3.3.), for sample solutions determined via gas evolution (Section 2.2.2.).

Table 3.5: Effect of acid on exchange of oxygen isotopes between CO_2 and H_2O

Sample Name	$\delta^{18}O_{CO2}$ (‰)														
	Amount of H_3PO_4 added (mL)														
	0.0	σ	*n*	0.1	σ	*n*	0.2	σ	*n*	0.4	σ	*n*	0.6	σ	*n*
0.2% CO_2 + 99.8% He	-4.70	0.13	2	–	–	–	-4.70	0.04	2	–	–	–	–	–	–
Deionized water	20.86	0.00	2	9.20	0.31	2	0.95	0.33	2	-2.31	0.02	2	-2.51	0.10	2
Iceberg water	-3.43	0.03	2	–	–	–	–	–	–	–	–	–	-4.59	0.04	2

σ = Standard deviation based on population (stdevp).

n = number of samples.

Table 3.6: Comparing the oxygen isotope coompositions between the different methods

	DIC-CO_2-GEM			CO_2-H_2O Equilibration			Difference[a]
Sample Name	$\delta^{18}O_{H2O}$ (‰)	σ	*n*	$\delta^{18}O_{H2O}$ (‰)	σ	*n*	(‰)
#CKG-Aug312-D2-S	-6.75	0.03	3	-6.70	0.01	2	-0.05
#CKG-Aug312-D2-E	-6.64	0.04	3	-6.79	0.05	2	0.15
#CKG-Aug3012-E-S	-6.68	0.03	2	-6.68	0.02	2	0.00
#CKG-Aug3012-E-E	-6.56	0.03	3	-6.59	0.02	2	0.03
#CKG-Sept2512-D2-S	-6.51	0.04	8	-6.59	0.03	2	0.08
#CKG-Sept2512-D2-E	-6.51	0.05	3	-6.48	0.01	2	-0.03
#CKG-Oct2912-E-S	-6.67	0.03	3	-6.56	0.01	2	-0.11
#CKG-Oct2912-E-E	-6.52	0.04	8	-6.49	0.00	2	-0.03
#CKG-Apr313-D-S	-6.81	0.04	3	-6.71	0.00	2	-0.10
#CKG-Apr313-D-E	-6.71	0.05	8	-6.73	0.02	2	0.02
#CKG-Apr313-E-S	-6.91	0.15	3	-6.76	0.00	2	-0.15
#CKG-Apr313-E-E	-6.80	0.05	3	-6.70	0.07	2	-0.10

σ = Standard deviation based on population (stdevp).

n = number of samples.

[a]Difference between DIC-CO_2-GEM and classical CO_2-H_2O equilibration technique.

Table 3.7: Comparing the carbon isotope compositions between different methods

	DIC-CO_2-GEM			Gas Evolution			Difference[a]
Sample Name	$\delta^{13}C_{DIC}$ (‰)	σ	*n*	$\delta^{13}C_{DIC}$ (‰)	σ	*n*	(‰)
#CKG-Aug312-D2-S	-3.61	0.03	3	-3.56	0.02	2	-0.05
#CKG-Aug312-D2-E	-2.78	0.17	3	-2.62	0.00	2	-0.16
#CKG-Aug3012-E-S	-13.87	0.04	2	-13.87	0.01	2	0.00
#CKG-Aug3012-E-E	-17.98	0.06	3	-17.97	0.00	2	-0.01
#CKG-Sept2512-D2-S	-2.41	0.17	8	-2.37	0.01	2	-0.04
#CKG-Sept2512-D2-E	-2.39	0.16	3	-2.27	0.01	2	-0.12
#CKG-Oct2912-E-S	-14.04	0.13	3	-13.96	0.03	2	-0.08
#CKG-Oct2912-E-E	-17.80	0.09	8	-17.80	0.00	2	0.00
#CKG-Apr313-D-S	-24.65	0.05	3	-24.48	0.02	2	-0.17
#CKG-Apr313-D-E	-20.13	0.09	8	-19.95	0.00	2	-0.18
#CKG-Apr313-E-S	-24.80	0.15	3	-24.58	0.02	2	-0.22
#CKG-Apr313-E-E	-22.79	0.04	3	-22.62	0.00	2	-0.17

σ = Standard deviation based on population (stdevp).

n = number of samples.

[a]Difference between DIC-CO_2-GEM and gas evolution method.

Figures

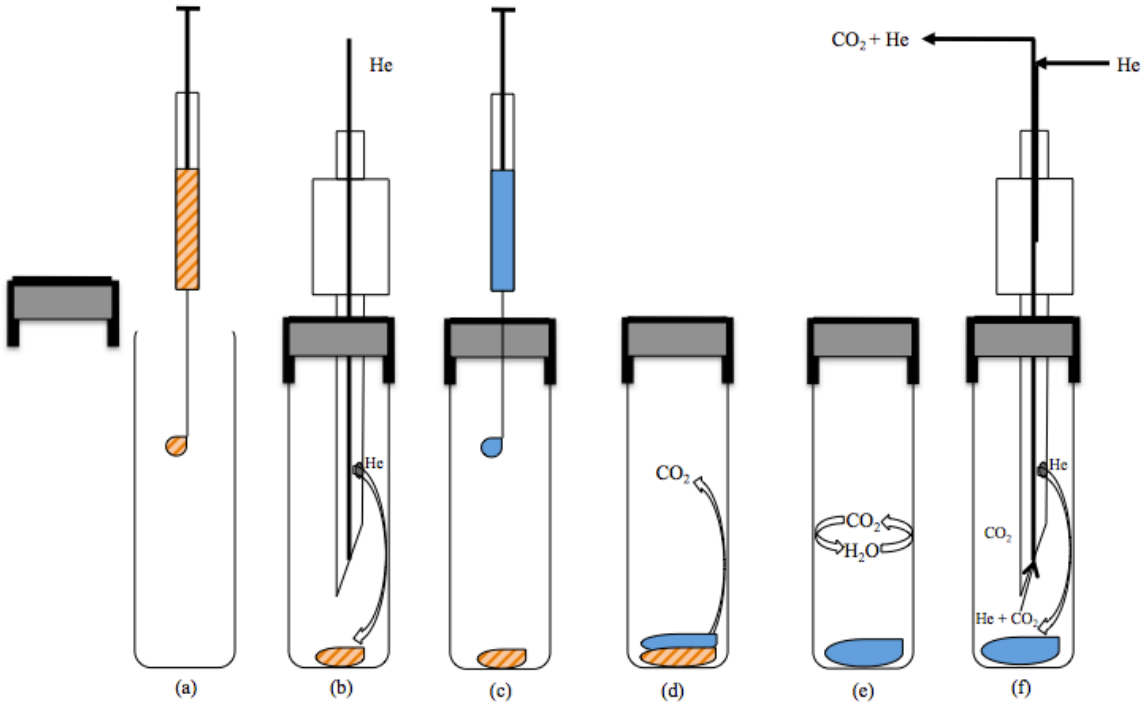

Figure 3.1: For the combined DIC-CO_2-GEM, to prepare the vial for Gas Bench II analysis, (a) 12mm Exetainer® vials are preloaded with an aliquot of H_3PO_4, capped and then (b) flushed and filled with helium using the double needle on the Gas Bench II. Once filled with helium, (c) water sample is added to the vial and (d) the H_3PO_4 will react with the DIC in the sample and produce CO_2 in the headspace. (d) A minimum of 27 hours at 25 ±0.1°C is allotted for equilibration between CO_2 and H_2O, and then (e) headspace CO_2 is sampled on the Gas Bench II.

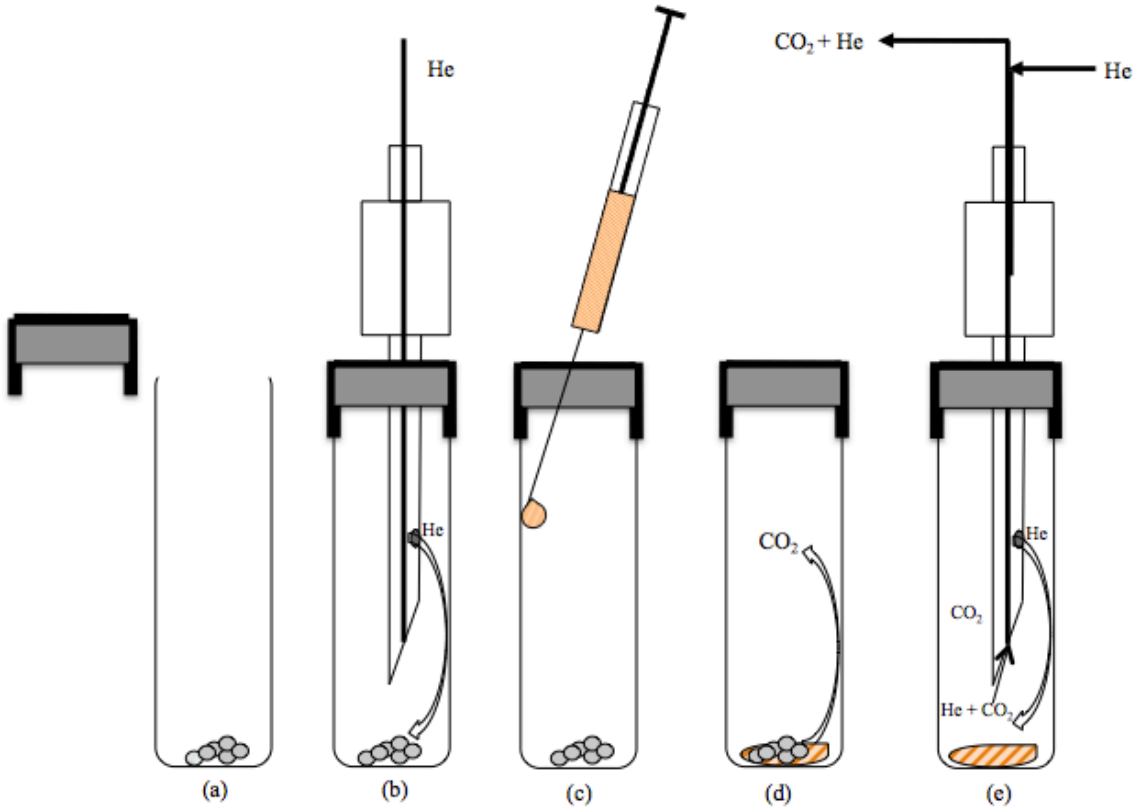

Figure 3.2: To run standards NBS 18 and NBS 19 on Gas Bench II, (a) 12mm Exetainer® vials are preloaded with at least 150 µg of carbonate, and (b) flushed and filled with He. (c) Using a 1-mL syringe, 20 drops of 100% H_3PO_4 is then added to the glass side of the vial and it will slide down the side and (d) have time to reach a temperature of 25°C by the time it reacts with the carbonate to produce CO_2 gas. The CO_2 in the headspace is then (e) analyzed following the Gas Bench II sampling procedure.

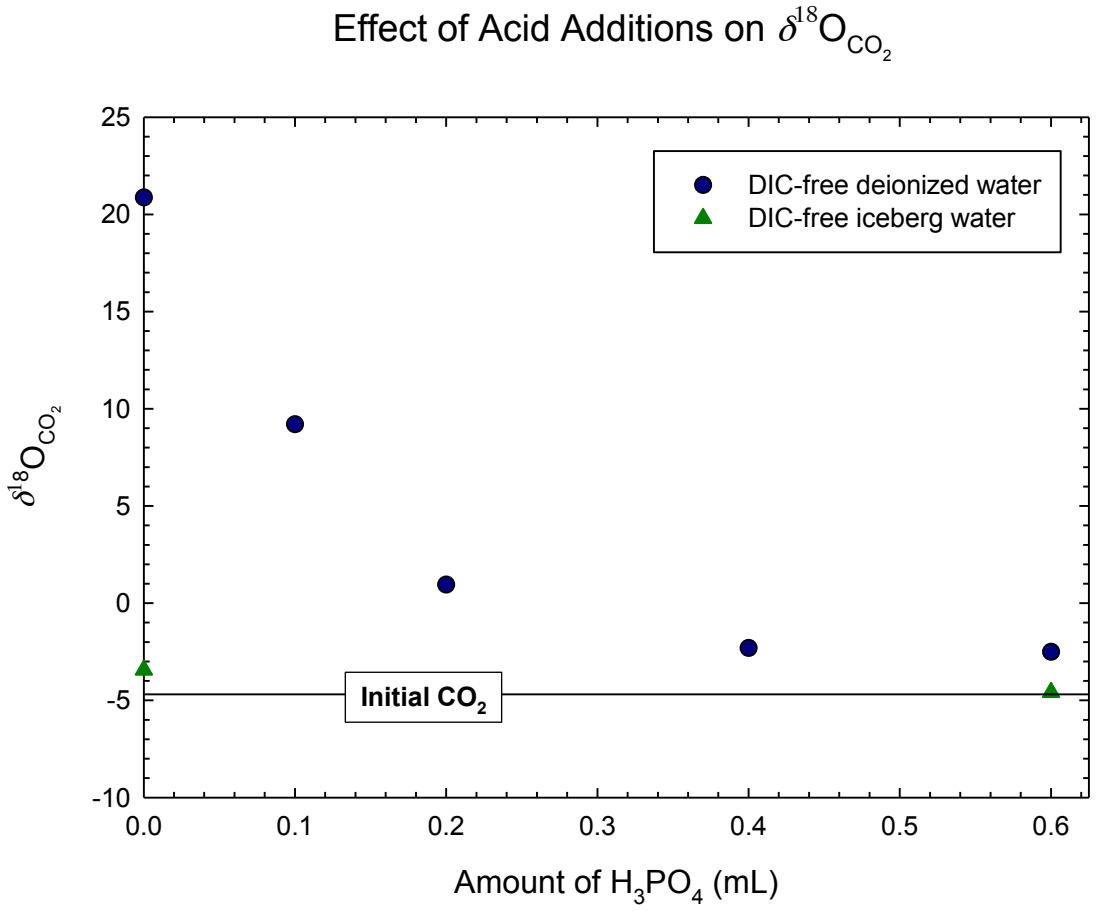

Figure 3.3: Effect of varying amounts of 103% H_3PO_4 acid on the oxygen isotope composition of DIC-free water. With increasing amount of acid, the oxygen isotope composition of headspace CO_2 becomes closer to the initial CO_2 values, showing a decrease in the kinetics of oxygen isotope exchange between CO_2 and H_2O due to smaller amounts of dissolved CO_2 remaining in solution.

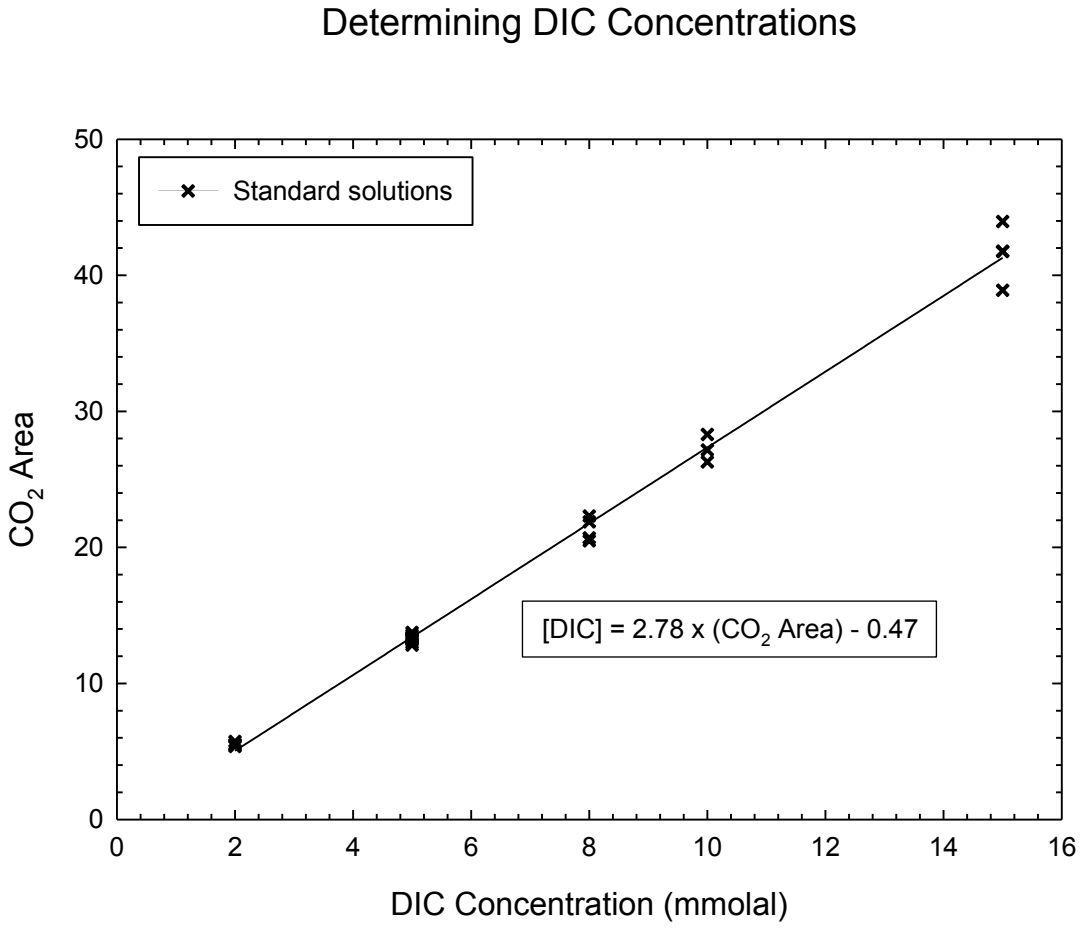

Figure 3.4: Calibration between the known DIC concentrations (mmolal) of standard solutions and the area for the amount of CO_2 evolved from the water sample.

Chapter 4: Conclusions: Thesis Summary and Areas for Future Research

The potential contribution of the boron isotope-pH proxy to understanding the history of atmospheric CO_2 is invaluable if properly calibrated. The changes in seawater pH reflect fluctuations in atmospheric CO_2 concentrations (i.e. anthropogenic contributions) because atmospheric CO_2 is in equilibrium with CO_2 dissolved in the ocean. Potential increases in atmospheric CO_2 will cause a reduction in seawater pH. The research conducted consisted of synthesizing aragonite through spontaneous nucleation at stable pH values and analyzing the boron, oxygen, and carbon isotope compositions of both aragonite and the precipitating solution. This thesis focused on studying the dependence of the boron isotope composition ($\delta^{11}B$) of synthetic calcium carbonate on the pH of the precipitating solution. The $\delta^{11}B$ of aragonite systematically increased, and boron isotope fractionation between aragonite and solution decreased, with increasing pH, supporting the hypothesis that only $B(OH)_4^-$ is incorporated into the crystal lattice. The carbon isotope fractionation between the synthetic aragonite and dissolved inorganic carbon, in the high ionic strength solutions utilized in this study, is consistent with previously published carbon isotope fractionation factors quantified using low ionic strength environments.

Within the boron isotope-pH study, the oxygen isotope composition of water ($\delta^{18}O_{H2O}$) and the carbon isotope composition of dissolved inorganic carbon ($\delta^{13}C_{DIC}$) were of significance to confirming equilibrium conditions within the experimental system. The measurements of $\delta^{18}O_{H2O}$ and $\delta^{13}C_{DIC}$ are typically accomplished through two separate methods, and it was of benefit for this research, as well as applicable to paleoenvironmental studies, to establish a method to analyze both parameters

simultaneously. This thesis introduced the DIC-CO_2 Gas Equilibration Method (DIC-CO_2-GEM) that utilized continuous-flow isotope ratio mass spectrometry (CF-IRMS) to accurately analyze small aliquots DIC-containing water samples for $\delta^{18}O_{H2O}$ and $\delta^{13}C_{DIC}$.

Chapter 1 provided an introduction to the fundamentals of the boron isotope-pH proxy, the mechanisms of carbon isotope fractionation between calcium carbonate and DIC, and an overview of methodology with regards to the oxygen isotope composition of water and carbon isotope composition of DIC measurements. Chapter 2 aimed to investigate the boron isotope compositions of synthetic aragonite from a range of stable pH values as well as examine carbon fractionation between aragonite and DIC. Chapter 3 involved the development of a new analytical technique to analyze $\delta^{18}O_{H2O}$ and $\delta^{13}C_{DIC}$ simultaneously from a DIC-containing water sample using CF-IRMS. Chapter 4 briefly summarized the results of the research conducted, and will outline the candidate's contributions for Chapters 2 and 3, the application to this work in paleoenvironmental studies, as well as identify future avenues of research for the boron isotope-pH proxy.

4.1. Candidate's Contributions to Collaborative Research

4.1.1. Investigation of stable isotope systematics in the aragonite-CO_2-H_2O system: Multi-element approach

In this collaborative work, my contributions consisted of most of the experimental work including conducting modified constant addition experiments, using PHREEQC-I software to calculate chemical compositions for experimental solutions to test various parameters in attempt to maintain a stable pH throughout aragonite synthesis, analysis of

the carbonate samples via IRMS and solution samples for oxygen and carbon via CF-IRMS, as well as interpreting the data. The candidate completed the write up with suggested editorial changes being made by the collaborating authors.

4.1.2. A new online technique for the simultaneous analysis of $\delta^{13}C$ of dissolved inorganic carbon (DIC) and $\delta^{18}O$ of water from a single solution sample using continuous flow isotope ratio mass spectrometry (CF-IRMS)

In this collaborative work, my contributions included assisting in the development of the initial idea, the preparation of standard solutions, all standard and sample analyses, testing of various parameters, as well as data interpretation. The candidate completed the write up with suggested editorial changes being made by the collaborating authors.

4.2. Applications to Paleoenvironmental Studies

The reconstruction of atmospheric CO_2 is of interest due to present day atmospheric carbon dioxide concentrations and the implications that it may have on global climate. To understand how increasing CO_2 may influence radiative forcings it is essential to review aberrations that may have occurred in the past because current climate models are not always effective. The boron isotope-pH proxy has been developed to estimate the pH of ancient seawater, which is affected by equilibrium changes between atmospheric and dissolved CO_2, and can be used in conjunction with either alkalinity or total inorganic carbon concentration to reconstruct atmospheric pCO_2.

This thesis contributes to the evaluation of the robustness of the pH proxy by experimentally observing whether it is only the aqueous species borate ($B(OH)_4^-$) that contributes to the boron isotope composition of carbonates. By assessing boron incorporation into aragonite through inorganic synthesis experiments the environmental components can be controlled to eliminate unknown influences. This is a preliminary step in understanding boron isotope systematics and the validity of current applications of the boron isotope-pH proxy. Isotopic characterization of calcium carbonate (i.e. oxygen and carbon) already reveals a wide range of information with regards to Earth's history including temperature, ocean circulation patterns, productivity, and temporal changes. Including material regarding paleo-pH, which is governed by carbonate equilibra, makes it possible to make quantitative estimates of atmospheric pCO_2.

By addressing the fundamental mechanisms associated with boron incorporation and potential influences of boric acid on the boron isotope compositions in aragonite, further culture and natural sample studies can be conducted to evaluate the existence of species-specific vital effects. Therefore, the foraminiferal species that qualify as suitable candidates can be used for pH reconstructions and the accuracy of historical models of past pCO_2 models can be confirmed.

The isotope compositions of many elements are determined for application in various paleo proxies. By combining the measurement of $\delta^{18}O_{H2O}$ and $\delta^{13}C_{DIC}$ into one simultaneous approach, the required sample size and analytical time is reduced. The simplicity of the DIC-CO_2-GEM experimental procedure to obtain two variables is appealing because little added effort is required compared to conventional approaches.

Conveniently, information revealed for both $\delta^{18}O_{H2O}$ and $\delta^{13}C_{DIC}$ can delve a vast amount of knowledge, for instance tracing water masses and carbon fluxes simultaneously.

4.3. Future Research Areas for CO_2-H_2O Isotope Systematics in Calcium Carbonate

A future avenue to consider includes the determination of boron isotope incorporation into the other dominant polymorph of calcium carbonate, calcite. Previous indications of coordination changes occurring during $B(OH)_4^-$ uptake into calcite suggest that it must be considered independently and that systematic processes occurring at the carbonate surface are likely specific to crystal habit. It is also of interest to conduct nuclear magnetic resonance (NMR) on the synthetic aragonite samples to determine if trigonal and/or tetrahedral forms of borate are present in the crystal lattice. Even though NMR studies do not indicate whether or not boric acid may have contributed to the boron isotope composition of aragonite, it will generate information regarding boron coordination and probable changes during uptake, which will give a better understanding of the mechanisms of boron incorporation into aragonite.

As previously mentioned, the chemical composition of the experiments used in this study was a preliminary step to mimicking artificial seawater. The complexity of the system must be increased step-wise so that important parameters, i.e. pH and ionic strength, can still be controlled. The addition of the major constituents in seawater into the solutions including K^+ and SO_4^{2-}, during aragonite synthesis will allow for more appropriate applications of pK_B^* and $^{11\text{-}10}K_B$, as well as a more direct comparison to the processes occurring in the natural environment. The evaluation of boron incorporation into aragonite or calcite over a range of ionic strengths and temperatures would be

essential to outlining potential controls on the system. Eventually, it is also important to conduct inorganic carbonate experiments with boron concentrations that are more similar to the natural environment, however, this is challenging due to the limits of detection for boron isotope analysis.

The boron isotope-pH proxy is limited by the residence time of boron in seawater, approximately 20 Myr. This still gives a wide range for interpretation into changes in seawater pH, however it is of interest to review how $\delta^{11}B_{seawater}$ may have fluctuated over the course of Earth's history and identify causes of these changes. Investigations into potential deviations in the $\delta^{11}B_{seawater}$ has significant implications to the prediction of $\delta^{11}B_{B(OH)4-}$ which is essential to reconstruct pH from foraminifera.

The solutions prepared for some experiments gave insight to carbon isotope fractionation between calcium carbonate and DIC at a high ionic strength (0.7 mol kg^{-1}). It is of interest to curb solutions to be more ideal for understanding carbon isotope systematics and assess the fractionation over a range of ionic strengths and temperatures. A more detailed interpretation of fractionation factors would benefit studies looking to determine if natural calcium carbonate specimens precipitated in carbon isotope equilibrium with ambient water.

The influences of species-specific biogenic effects on boron and carbon isotope fractionation must be identified in order to properly apply the boron isotope-pH proxy and carbon isotope fractionation factors. Processes including photosynthesis and respiration, with some species being more or less influenced than other species, can affect carbon isotope compositions of foraminifera. The boron isotope composition of some species can be subject to vital effects by affecting fractionation during the incorporation

of boron into the carbonate lattice or causing a change in pH of the microenvironment. These influences can be identified in controlled environments through the use of culture experiments or specimens from current marine environments. The application of current marine specimens to evaluating vital effects is limiting due to a narrow range in current seawater pH.

A better understanding of the controls of boron incorporation into carbonate will allow for a proper understanding of the boron isotope-pH proxy and in turn, it will be more reliable. The study of isotope systematics in calcium carbonate has already proved to be a useful tool in paleoclimate research, and the ability to generate more information is an asset to reconstructions of Earth's history. Understanding fluctuations in atmospheric CO_2 concentrations over long time scales and correlating these increases or decreases with causal effects will allow for better predictions of future climate projections and complex feedback systems.

Appendix A

Constant Addition Method

The constant addition method consisted of two titrant solutions (one $NaHCO_3$ and/or Na_2CO_3 and NaCl solution and the other a $CaCl_2$-$2H_2O$, $B(OH)_3$, and NaCl solution) simultaneously injected at a constant rate of 0.5 mL/hr into an initial thermally and isotopically equilibrated Na-Ca-Cl-B-CO_3 solution held in an air-tight Teflon® reaction vessel (Figure A.1). The addition of the two titrants supersaturates the initial solution and leads to spontaneous nucleation, the precipitation of calcium carbonate without the use of seed material. A ratio of 4:1 [Mg]:[Ca] allowed the precipitation of aragonite versus other polymorphs. The chemical compositions of the initial solutions as well as the titrant solutions were modified so that the pH would remain stable throughout aragonite precipitation. The solutions were prepared using deionized (18 MΩ cm^{-1}) water and stored in a 25 ±0.03°C water bath for a minimum of 7 days to ensure isotopic equilibrium between water and carbonic acid species. The experimental solution was kept homogeneous throughout aragonite precipitation by being constantly stirred by a magnetic floating stirrer. An aliquot of experimental solution was sampled for boron, oxygen and carbon isotope analysis prior to beginning the experiment, as well as before termination. A Millipore 0.45 μm Durapore® syringe filter was used to collect solution samples for boron analysis.

The pH of the system was monitored daily using a ThermoScientific pH electrode and calibrated with NIST-traceable pH buffers (4.00, 7.00, and 10.00) and a TRIS buffer (8.10) at 25 °C. The temperature of the system was examined using a ThermoScientific Traceable thermometer. For experiments where pH was slightly increasing (higher range

pH experiments), 1% HCl was added in small amounts (1-3 mL) and pH recordings were retaken. At the end of the experiment, the solution was filtered through a Millipore 0.45 μm Durapore® filter, dried in an oven at 70 °C overnight and collected for isotopic analysis.

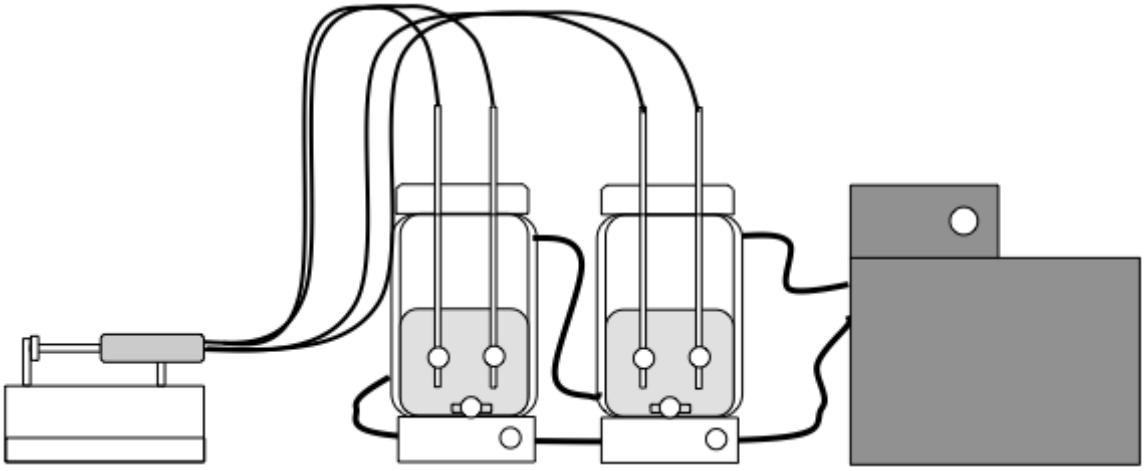

Figure A.1: The constant addition method consisting of a syringe pump fitted with four syringes, one consisting of a $NaHCO_3$ and/or Na_2CO_3 solution and one of a $CaCl_2$ and $B(OH)_3$ solution for each experiment. The temperature of the system is held at 25.04 ±0.03°C with a water bath constantly flowing water through the double walled experimental chambers. The titrants are injected at a constant rate of 0.5 mL/hr into an initial solution that is constantly being stirred.

The concentration of carbonate species in the experimental solution were roughly calculated using pH data, as well as total DIC concentrations for each experiment. The following equations were used to determine the concentration of each carbonate species in solution:

Total carbonate concentration in solution:

$$C_T = H_2CO_{3(aq)} + HCO_3^- + CO_3^{2-}$$

$$C_T = [H_2CO_{3(aq)}]\left(1 + \frac{K_{a1}}{[H^+]}\right) + \left(1 + \frac{K_{a1}K_{a2}}{[H^+]^2}\right)$$

$$C_T = [H_2CO_{3(aq)}](\alpha_H)$$

Subsequent equations:

$$[H_2CO_{3(aq)}] = \frac{C_T}{\alpha_H}$$

$$[HCO_3^-] = \frac{C_T K_{a1}}{[H^+]\alpha_H}$$

$$[CO_3^{2-}] = \frac{C_T K_{a1} K_{a2}}{[H^+]^2 \alpha_H}$$

Where:

C_T = Total concentration of carbonate species in solution (mmolal)

$[H_2CO_3]$ = Concentration of H_2CO_3 in solution (mmolal)

$[HCO_3^-]$ = Concentration of HCO_3^- in solution (mmolal)

$[CO_3^{2-}]$ = Concentration of CO_3^{2-} in solution (mmolal)

$[H^+]$ = Concentration of hydrogen ions in solution

K_{a1} = First dissociation constant for the carbonate system

K_{a2} = Second dissociation constant for the carbonate system

$$\alpha_H = \left(1 + \frac{K_{a1}}{[H^+]} + \frac{K_{a1}K_{a2}}{[H^+]^2}\right)$$

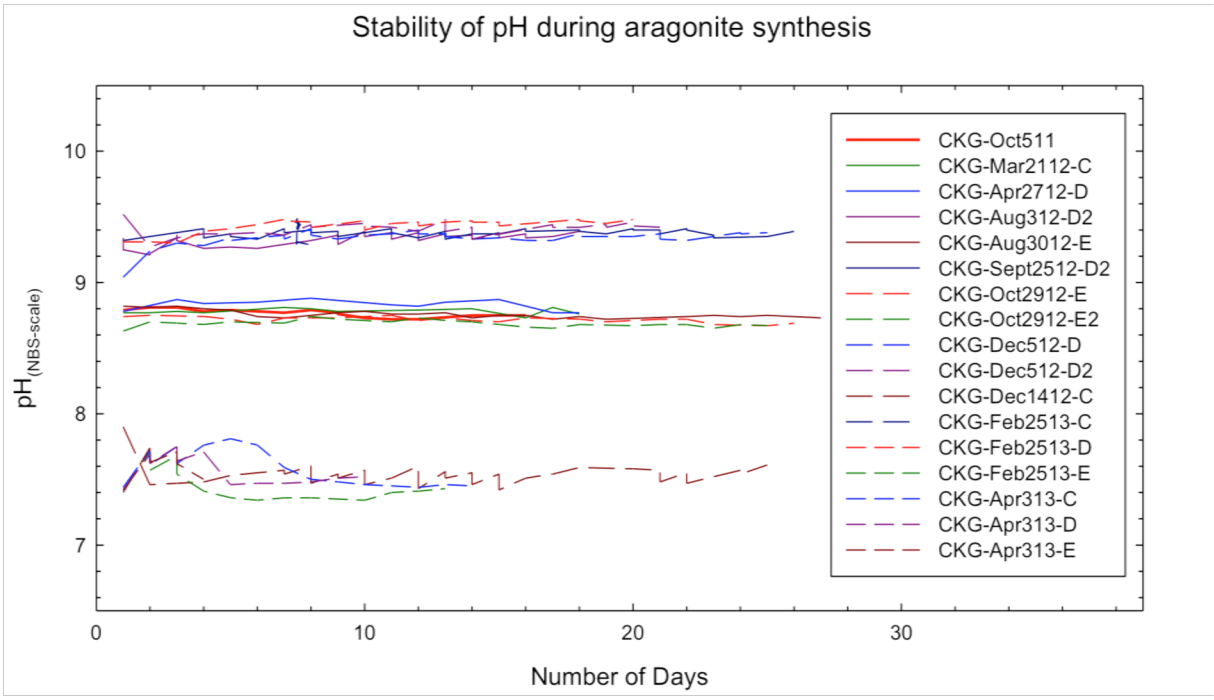

Figure A.2: Stability of pH throughout aragonite synthesis experiments

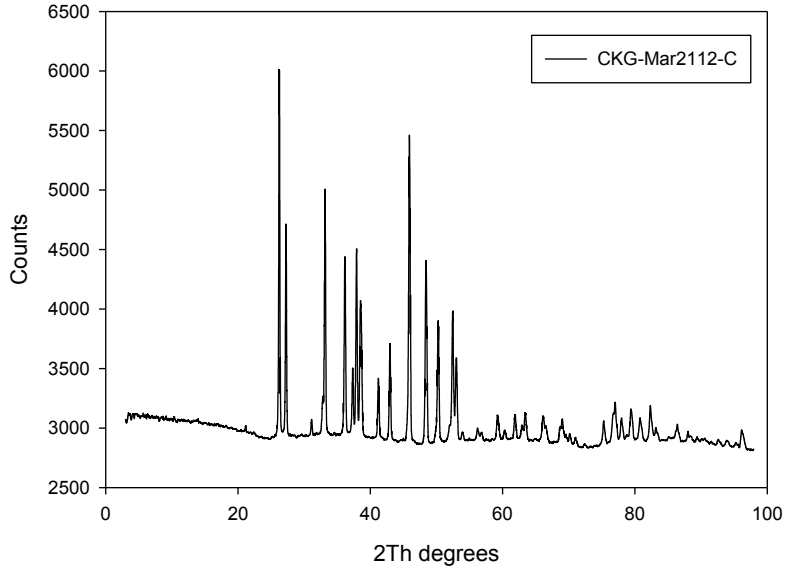

Figure A.3: XRD Results from CKG-Mar2112-C

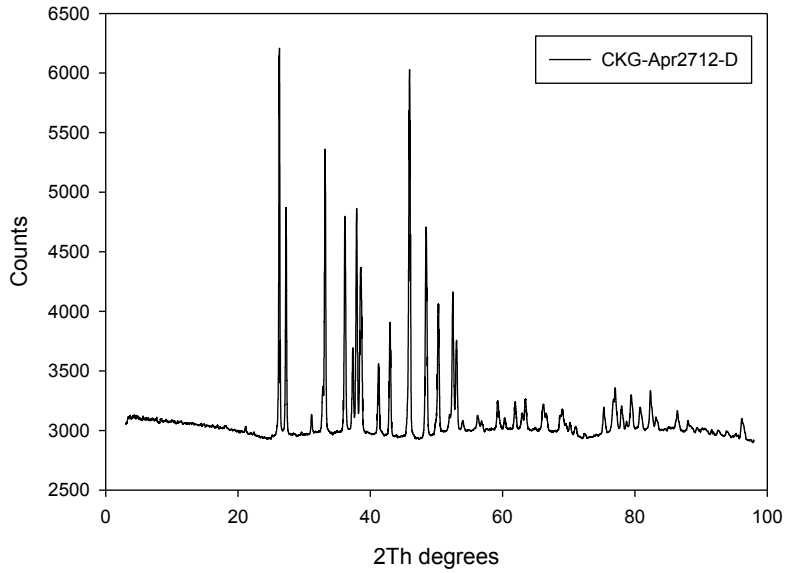

Figure A.4: XRD Results from CKG-Apr2712-D

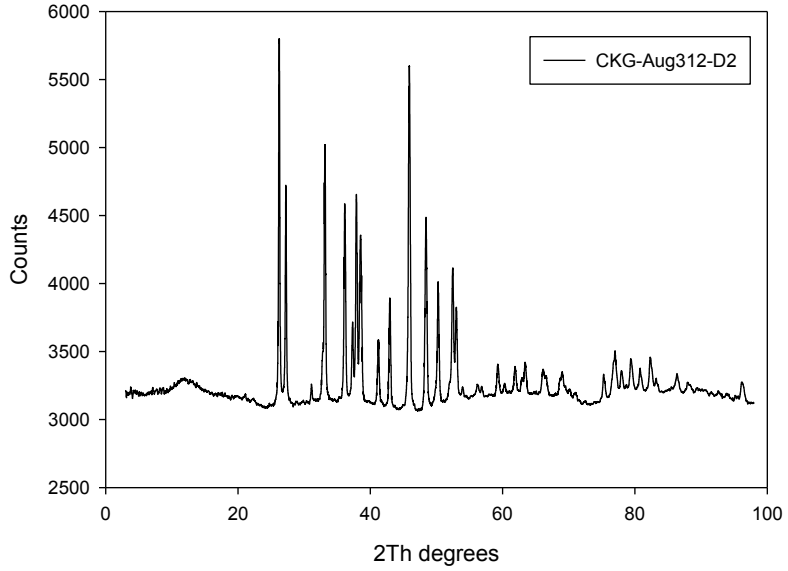

Figure A.5: XRD Results from CKG-Aug312-D2

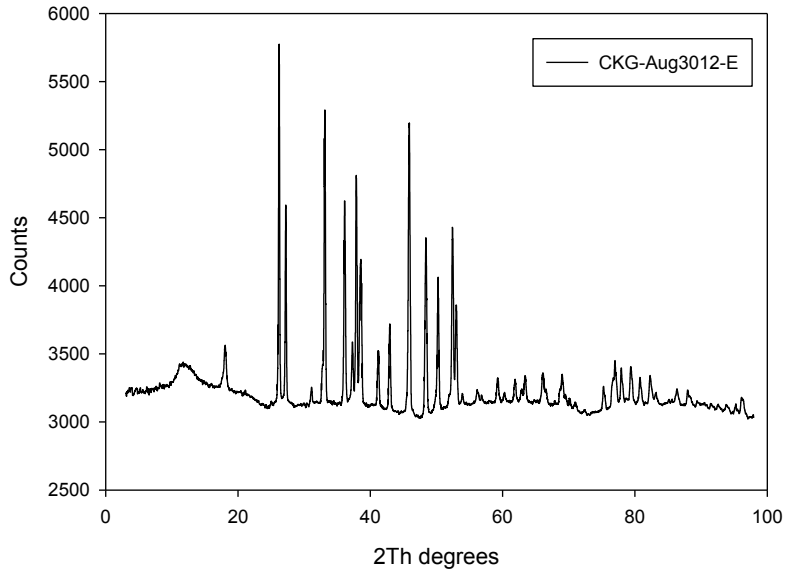

Figure A.6: XRD Results from CKG-Aug3012-E

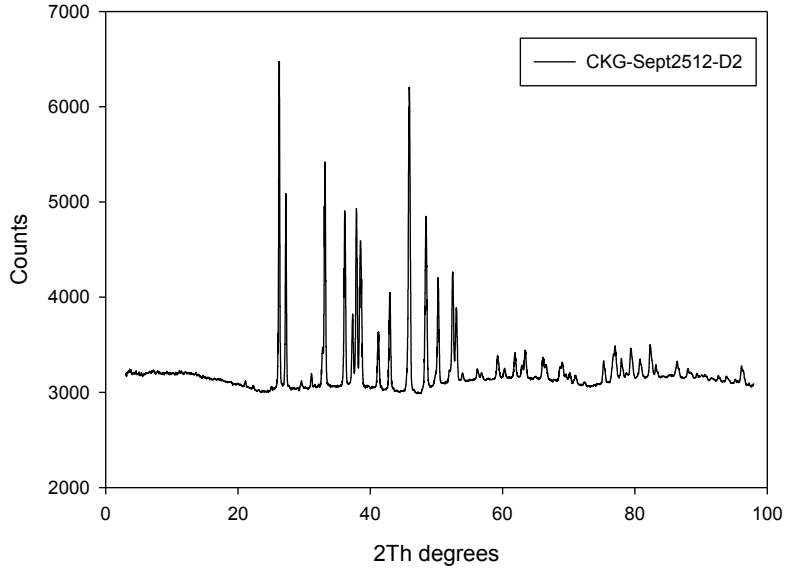

Figure A.7: XRD Results from CKG-Sept2512-D2

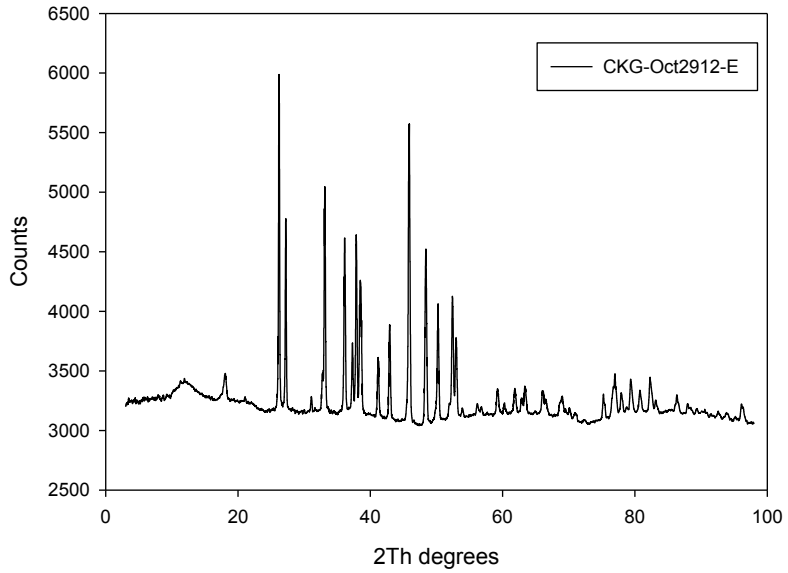

Figure A.8: XRD Results from CKG-Oct2912-E

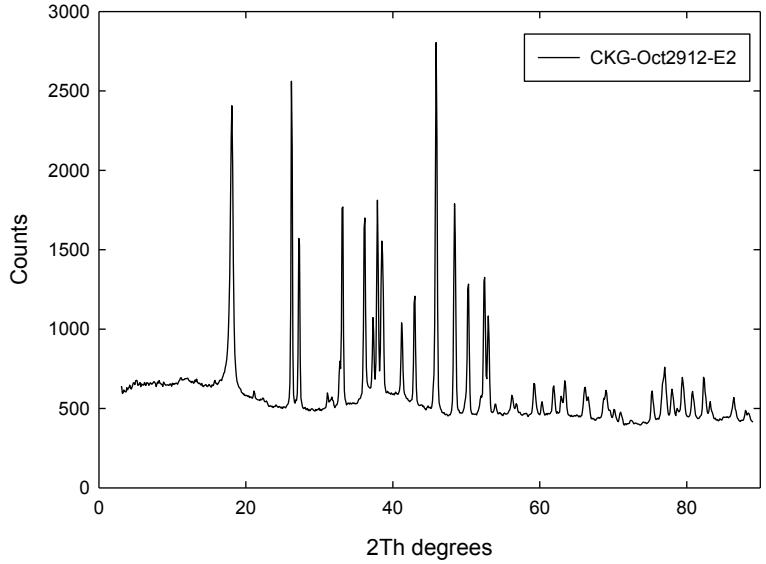

Figure A.9: XRD Results from CKG-Oct29-E2

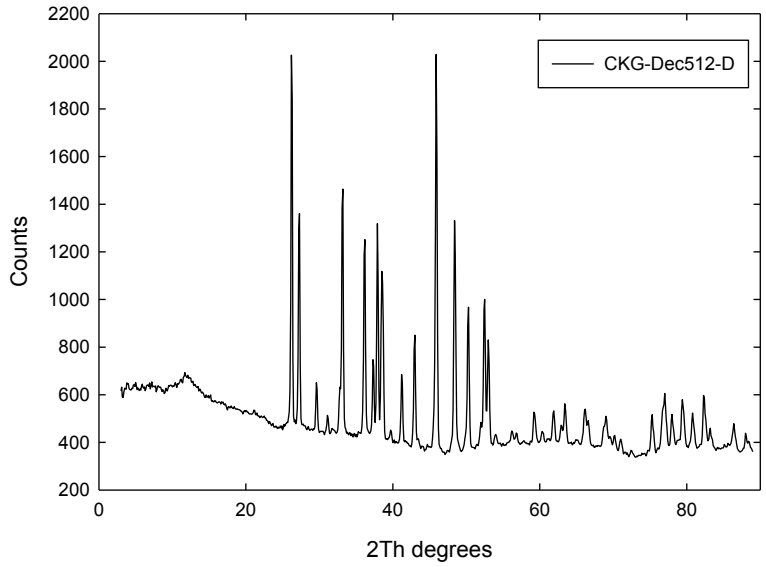

Figure A.10: XRD Results from CKG-Dec512-D

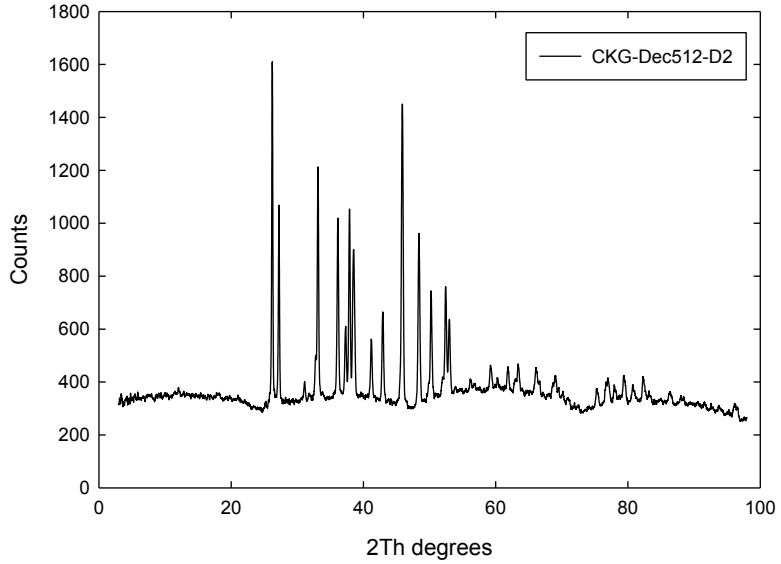

Figure A.11: XRD Results from CKG-Dec512-D2

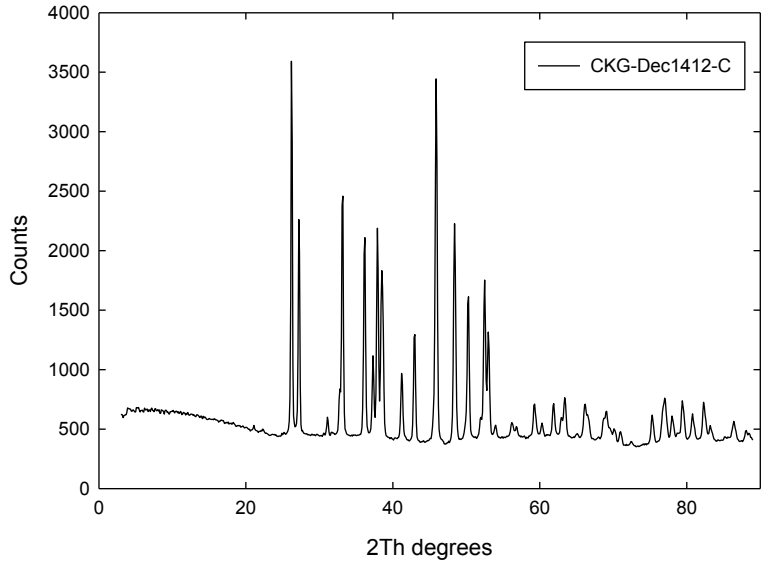

Figure A.12: XRD Results from CKG-Dec1412-C

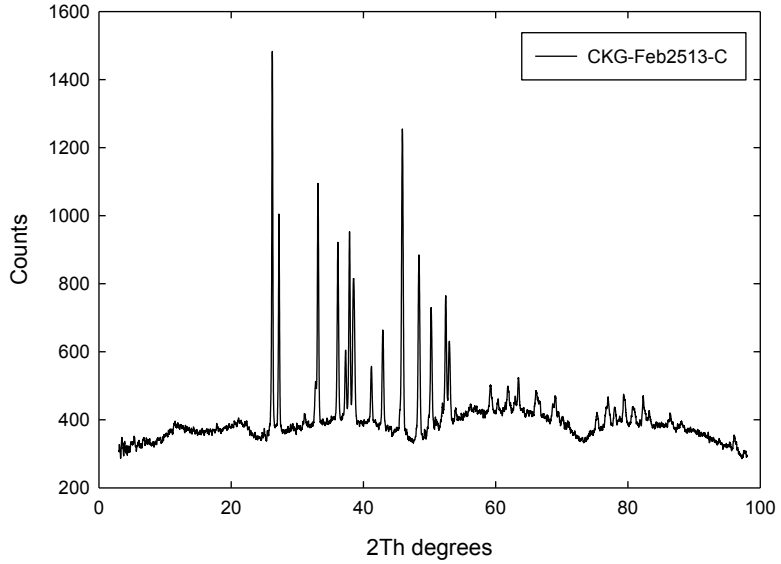

Figure A.13: XRD Results from CKG-Feb2512-C

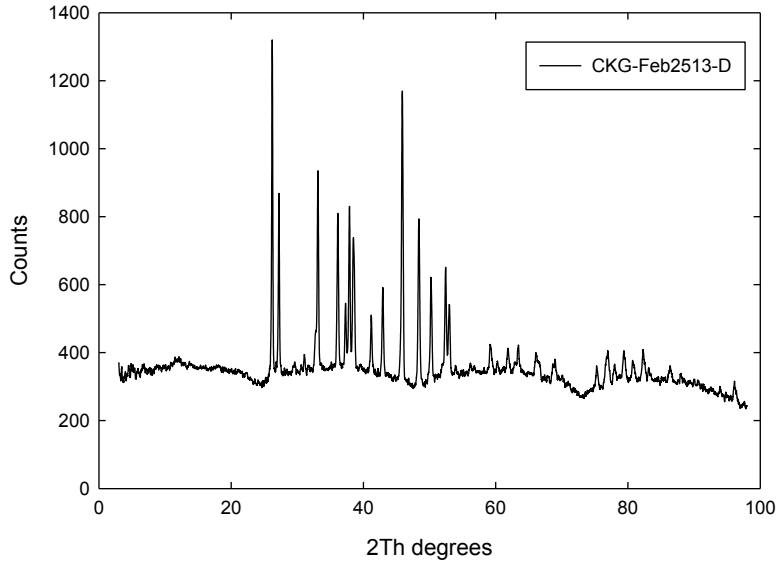

Figure A.14: XRD Results from CKG-Feb2513-D

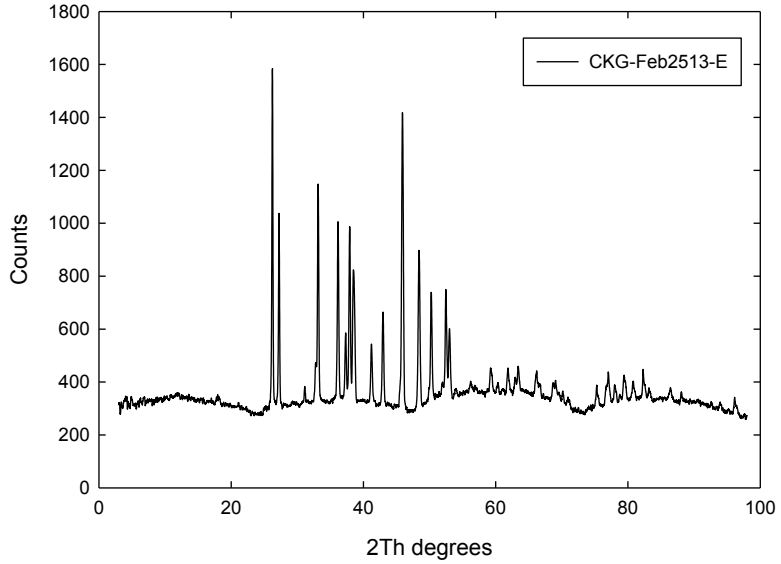

Figure A.15: XRD Results from CKG-Feb2512-E

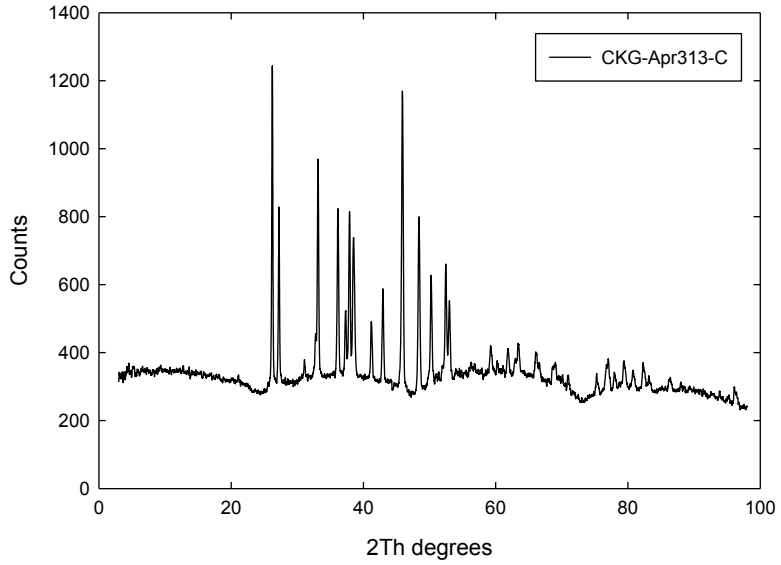

Figure A.16: XRD Results from CKG-Apr313-C

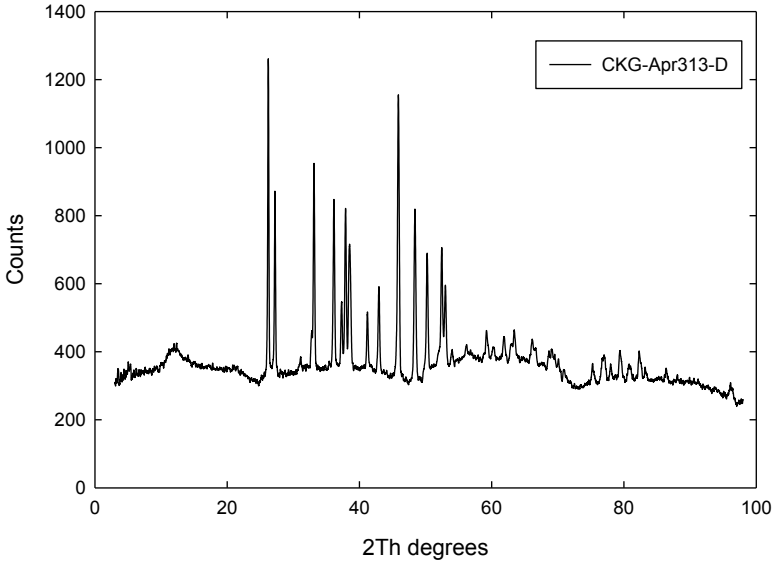

Figure A.17: XRD Results from CKG-Apr313-D

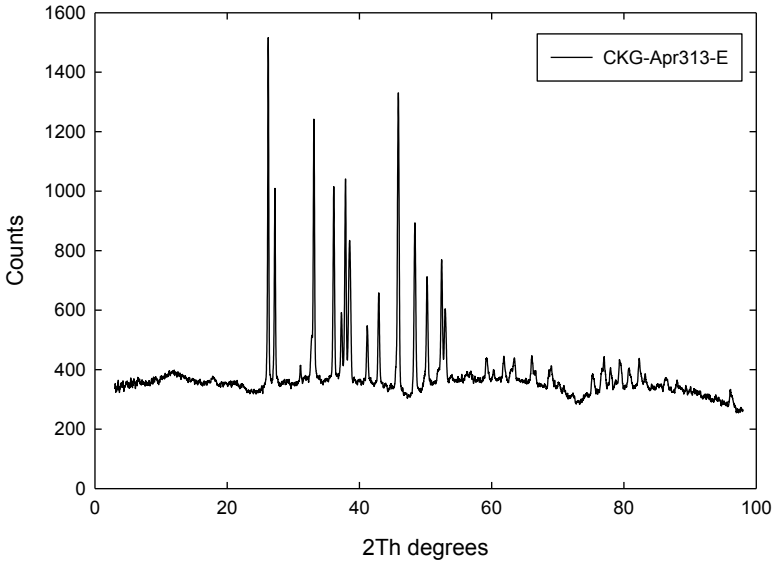

Figure A.18: XRD Results from CKG-Apr313-E